The Pennsylvania State University

The Graduate School

School of Forest Resources

EVALUATING THE EFFECTS OF FOREST LIMING IN APPALACHIAN WATERSHEDS: CHEMISTRY AND MULTI-ISOTOPE APPROACHES

A Thesis in

Forest Resources

by

Hyeon Jeong Kim

Submitted in Partial Fulfillment
of the Requirements
for the Degree of

Doctor of Philosophy

May 2007

The thesis of Hyeon Jeong Kim was reviewed and approved* by the following:

William E. Sharpe
Professor of Forest Hydrology
Thesis Advisor
Chair of Committee

David R. DeWalle
Professor of Forest Hydrology

James A. Lynch
Professor of Forest Hydrology

Richard R. Parizek
Professor of Geology and Geo-Environmental Engineering

Charles H. Strauss
Professor of Forest Economics
Director of the School of Forest Resources

Signatures are on file in the Graduate School.

Abstract

An investigation was conducted to determine the short-term effects of liming on soils, soil solutions, and streamwater at acidified watersheds in the northeast United States, using an integrated set of hydrometric, hydrochemical, and multi-isotope measurements. Additionally, this research compared timing of liming response on chemistry with estimated residence time as of water in soil and on basins. Based on Before-After-Control-Impact (BACI) design, coarse-grained dolomitic limestone sand was applied at a rate of 5 t ha^{-1} over the Laurel and 90 Degree watersheds in fall 2003 and 2004 and over six soil plots (15.2 meter by 9.1 meter) within the same watersheds in summer 2005. The adjacent Merrill and Tick watersheds served as control watersheds.

Within four months after liming application, mineral A horizon soils showed improvement in nutrient conditions such as increased soil pH, exchangeable base cations, and base saturation. Using ^{18}O in water as a tracer, the mean residence time of soil water was estimated as about 2-4 months. In agreement with this estimated residence time, soil solution at 30 cm depth had increased pH, conductivity, acid neutralizing capacity, and concentrations of Ca and Mg, as well as Ca/Sr, Mg/Sr, and Ca/Al molar ratios.

At the watershed scale, two treated watersheds had improved drainage water quality, with increased pH, conductivity, acid neutralizing capacity, and concentrations of Ca and Mg, as well as decreased Al during the 23-month monitoring period following application. Using ^{18}O in water tracer, the estimated mean residence time of streamwater at the 90 Degree watershed was about one year, approximately the time lag chemical response

to treatment. At this watershed, strontium isotope in water results also indicated a pattern of decrease in streamwater $^{87}Sr/^{86}Sr$ ratio 16 months after liming.

This study showed that; 1) the estimated mean residence time of water at the study watershed generally agreed with the water quality results and the strontium isotope results; 2) the $^{87}Sr/^{86}Sr$ ratio was very useful as an isotopic solute tracer of liming; and 3) forest liming treatment rapidly improved soil nutrient conditions and drainage water quality on the treated watersheds.

Table of Contents

List of Tables

List of Figures

Acknowledgments

Research support for this study was provided in part by the Growing Greener Program, PA Department of Environmental Protection, Penn State Institutes of the Energy and the Environment, School of Forest Resources, and Center for Watershed Stewardship.

I would like to express my appreciation to my advisor Dr. William E. Sharpe for his guidance, patience, and encouragement throughout the course of this study. Appreciation is also extended to my committee member; Dr. David R. DeWalle, Dr. James A. Lynch, and Dr. Richard R. Parizek for their valuable inputs and suggestions.

I would like to thank Dr. Brian R. Stewart for conducting strontium isotope analysis and Bryan R. Swistock for organizing limestone sand application over the watersheds. I also would like to thank Lysle S. Sherwin and Dr. Charles A. Cole for their guidance during the course of Watershed Stewardship program. Thanks also go to Chad Voorhees, Kevin Horner, Shawn Rummel, Leonard McNeal, Lindsey Donaldson, Nesha Mizel, Anthony Buda, and Stephanie Clemens for their assistance and cooperation in setting the field instruments. Gratitude is also extended to my friend; ChangGook Youn, Sungmi Jin, Jae Yeol Kim, Soojin Oh for their support and friendship. Finally, I want to thank my family in South Korea for their support and encouragement during my study abroad.

Chapter 1. General Introduction

Acid deposition has been a problem for at least five decades, especially in the Northeast United States, Canada, and Western Europe (Clair and Hindar, 2005). More recently, it has become a problem in the developing world, particularly in parts of Asia and the Pacific region (Duan et al., 2001; Hayashi and Okazaki, 2001).

Acid deposition results from the transformation of sulfur dioxide and nitrogen oxides into sulphuric acid, ammonium nitrate, and nitric acid. In the United States, about two-thirds of all sulfur dioxide and one-fourth of all nitrogen oxide comes from electric power generated by burning fossil fuels (USEPA, 2000). The burning of fossil fuels (coal or oil) releases sulfur into the air; the sulfur combines with oxygen and creates sulfur dioxide. Nitrogen oxides in the air are primarily formed by automobile exhausts and combustion processes. Agriculture is also a major contributor to nitrogen oxide. In addition, a small amount of nitrogen oxide is created by lightning and soil microbes.

Precipitation with the highest acidity (lowest value of pH 4.3) was reported in the northeastern United States due to high concentrations of power plants and dense population (Kulp, 1990). In addition, winds bring storms and thus acid deposition from the Midwest (i.e., Illinois, Indiana, and Ohio) into the Northeast (Pennsylvania).

The negative effects of acid deposition on forests have long been observed. Because of loss of soil nutrients through leaching, forest soils lose their ability to buffer strong acid inputs by cation exchange and become aluminum buffered. Tree roots damaged by a higher concentration of aluminum in forest soil water can impede the uptake of essential nutrient base cations. In turn tree growth is impaired, vulnerability to drought conditions is heightened, and an early end to the tree's life becomes more likely. The

overall effect of such is general forest degradation. MacKenzie and El-Ashry (1989) indicated that the decline of acid-sensitive tree species in the eastern US such as spruce-fir, white and yellow pines, and sugar maples was due to acid deposition and other air pollutants. Red spruce trees experienced declines caused by acidic deposition at higher elevations in the eastern US (Johnson and Siccama, 1983; Driscoll et al., 2003). Lower levels of base cations in soils and foliage caused the decline of sugar maple trees in Pennsylvania (Sharpe and Sunderland, 1995). Investigations in Norway show that needle loss and discoloration in Norway spruce were due to acid deposition (Nellmann and Thomsen, 2001).

Nitrogen oxides are generally thought to play a lesser role in forest degradation. This is because nitric acid formed when nitrate oxides contact with water generally supplies useful fertilization to forests. However, recent research found that nitrogen oxides could cause "nitrogen saturation,"—a condition that occurs when forest soils no longer can assimilate nitrogen inputs (Melewski, 1998). When "nitrogen saturation" occurs in forests, the ability of soil to retain nitrate is exhausted, and nitrate and other nutrients leach into streams. "Nitrogen saturation" in forests has been reported in a number of regions including the northeastern US; Colorado; and California (Aber et al., 1989, 1998; USEPA, 1999; Lovett et al., 2000).

Precipitation falls over forests and flows through terrestrial ecosystems into streams. When precipitation brings higher levels of acid deposition with it and forest soils can buffer by base cation exchange. However, with low base cation concentrations in soils, forest soil lose the ability to buffer free acidity, streamwater becomes acidic. When this

happens, forest soils release aluminum into streams, which is very toxic to fish and other aquatic organisms.

The effects of acid deposition can be either chronic or episodic. Chronic acidification refers to a continuously high level of acidity in the water (Turner et al., 1990). Episodic acidification refers to more variable conditions in which the pH level of water decreases dramatically during short periods of time such as snowmelts and heavy rain storms (Wigington et al., 1990, 1996). Episodic acidification is especially detrimental to the stream environment. Because of the sudden and marked increases in acidity comes with higher concentrations of aluminum, episodic acidification can kill fish, with negative effects on fish populations (Carline et al., 1992; Heard et al., 1997).

Title IV of the 1990 Clean Air Act Amendments required that by January 1, 2000 emissions of sulfur dioxide be reduced by 10 million tons from 1980 levels, and nitrogen oxides be reduced by 2 million tons from 1980 levels. With these regulations in place, the National Acid Precipitation Assessment Program (NAPAP) reported that both emissions of sulfur dioxide and nitrogen oxides from power generation have degreased (NAPAP, 2005). However, the acid deposition reductions have not yet improved aquatic and forest ecosystem health.

The rock weathering process is the main mechanism for neutralizing acidity naturally. However, it is a slow process requiring centuries to be significant. Consequently, additions of more readily soluble lime as either calcite or dolomitic calcite have been used to mitigate the negative effects of acid deposition by accelerating Ca and Mg addition to forest ecosystems (Tomlinson and Tomlinson, 1990; Ingerslev, 1997; Frank and Stuanes,

2003; Hindar et al., 2003) and surface waters (Howell and Brown 1986; Brown et al., 1988; Adams and Evans, 1989; Westling and Hultberg, 1990). Two general methods of liming are available: one adds lime materials directly into surface streams; and the other which adds liming materials to the entire catchment. In-stream liming has been widely used because many streams subjected to it have shown an immediate increase in pH and acid neutralizing capacity (Hindar and Henriksen, 1992; Bjerknes and Tjomsland, 2001). However, this method only improves stream conditions from below the treated site to some distance downstream over the short term unless continuous additions are made.

On the other hand, watershed liming has a number of advantages: 1) it requires no maintenance, making it useful in remote areas and tributaries with important ecosystems (Clair and Hindar, 2005); 2) it spreads evenly over the watershed at a fixed rate of dose; 3) it causes less variation in water chemistry during high-flow conditions by assisting aluminum retention in soils (Hindar, 2005); 4) it increases base saturation and nutrients in soils, thus supporting forest growth; and 5) its effects are enduring so that treatments need not be repeated frequently. The benefits of watershed liming may be sustained for at least 15 years (Dalziel et al., 1994) or even as long as 20 years (Staaf et al., 1996). However, based on the MAGIC model simulation, Hindar et al. (2003) predicted that a one-time dolomite application with a rate of 3 t ha^{-1}over the watershed would last at least 50 years. Although application costs can be expensive, the long-term benefits to an entire forest ecosystem may well provide more than ample compensation. In Europe, liming has been widely researched and shown to counteract acid deposition so that liming application strategies are well developed (Hindar and Henriksen, 1992; Dickson and Brodin, 1995).

However, limited research on liming applications has been conducted in North America.

This study employs an integrated set of hydrometric, hydrochemical, and isotopic measurements to investigate the short-term effects of dolomitic limestone application on acidified soils, soil solutions, and streamwater located in the Mosquito Creek basin of north-central Pennsylvania.

The remainder of the thesis consists of four chapters. Chapter 2 discusses research on limestone treatment effects on soil chemistry, soil solution chemistry, and streamwater chemistry of two watersheds within the Mosquito Creek basin. Chapter 3 presents research on the estimation of mean residence time in soil water and streamwater at the two treated watersheds, using ^{18}O in water isotope as a tracer. Chapter 4 presents research conducted on the estimation of limestone treatment effects on soil water and streamwater at the treated 90 Degree watershed using a strontium isotope as a tracer for the solute source. Chapter 5 explores the results of these research approaches in a synthesized way, examining also the implications of this study.

1.1. References

Aber, J., McDowell, W., Nadelhoffer, K., Magill, A., Berntson, G., Kamakea, M., McNulty, S., Currie, W., Rustad, L., Fernandez, I., 1998. Nitrogen saturation in temperate forest ecosystems: Hypotheses revisited. BioScience 48, 921-934.

Aber, J.D., Nadelhoffer, K.J., Steudler, P., Melillo, J.M., 1989. Nitrogen saturation in Northern forest ecosystems: Excess nitrogen from fossil fuel combustion may stress the biosphere. BioScience 39, 378-386.

Adams, W.A., Evans, G.M., 1989. Effects of lime applications to parts of an upland catchment on soil properties and the chemistry of drainage waters. Journal of Soil Science 40, 585-597.

Bjerknes, V., Tjomsland, T., 2001. Flow and pH modeling to study the effects of liming in regulated, acid salmon rivers. Water, Air, and Soil Pollution 130, 1409-1414.

Brown, D.A.J., Howells, G., Dalziel, T.R.K., Stewart, B.R., 1988. Loch Fleet-A research watershed liming project. Water, Air, and Soil Pollution 41, 25-41.

Carline, R.F., DeWalle, D.R., Sharpe W.E., Dempsey B.A., Gagen, C.J., Swistock, B., 1992. Water chemistry and fish community responses to episodic stream acidification in Pennsylvania, USA. Environmental Pollution 78, 45-48.

Clair, T., Hindar, A., 2005. Liming for the mitigation of acid rain effects in freshwaters: A review of recent results. Environmental Review 13, 91-128.

Dalziel, T.R.K., Wilson, E.J., Proctor, M.V., 1994. The effectiveness of catchment liming in restoring acid waters at Loch Fleet, Galloway, Scotland. Forest Ecology and Management 68, 107-117.

Dickson, W., Brodin, Y.-W., 1995. Strategies and methods for freshwater liming. pp. 81-124. Chapter 4. *In* Henrikson L. and Brodin, Y.-W.(eds.) Liming of acidified surface waters. Springer-Verlag, Berlin.

Driscoll, C.T., Driscoll, K.M., Mitchell, M.J., Raynal, D.J., 2003. Effects of acidic deposition on forest and aquatic ecosystems in New York State. Environmental Pollution 123, 327-336.

Duan, L., Xie, S., Zhou, Z., Ye, X., Hao, J., 2001. Calculation and mapping of critical loads for S, N, and acidity in China. Water, Air, and Soil Pollution 130, 1199-1204.

Frank, J., Stuanes, A.O., 2003. Short-term effects of liming and vitality fertilization on forest soil and nutrient leaching in a Scots pine ecosystem in Norway. Forest Ecology and Management 176, 371-386.

Hayashi, K., Okazaki, M., 2001. Acid deposition and critical load map of Tokyo. Water, Air, and Soil Pollution 130, 1211-1216.

Heard, R.M., Sharpe, W.E., Carline, R.F., Kimmel, W.G., 1997. Episodic acidification and changes in fish diversity in Pennsylvania headwater streams. Transactions of the American Fisheries Society 126, 977-984.

Hindar, A., 2005. Whole-catchment application of dolomite to mitigate episodic acidification of streams induced by sea-salt deposition. Science of the Total Environment 343, 35-49.

Hindar, A., Henriksen, A., 1992. Acidification trends, liming strategy and effects of liming for Vikedalselva, a Norwegian salmon river. Vatten 48, 54-58.

Hindar, A., Wright, R.F., Nilsen, P., Larssen, T., Høgberget, R., 2003. Effects on stream water chemistry and forest vitality after whole-catchment application of dolomite to a forest ecosystem in southern Norway. Forest Ecology and Management 180, 509-525.

Howells, G., Brown, D.A.J., 1986. Loch fleet: Techniques for acidity mitigation. Water, Air, and Soil Pollution 31, 817-825.

Ingerslev, M., 1997. Effects of liming and fertilization on growth, soil chemistry and soil water chemistry in a Norway spruce plantation on a nutrient-poor soil in Denmark. Forest Ecology and Management 92, 55-66.

Johnson, A.H., Siccama, T.G., 1983. Acid deposition and forest decline. Environmental Science and Technology 17, 294A-305A.

Kulp, J.L., 1990. Acid Rain: Causes, effects, and control. Regulation 13, 41-50.

Lovett, G.M., Weathers, K.C., Sobczak, W.V., 2000. Nitrogen saturation and retention in forested watersheds of the Catskill Mountains, New York. Ecological Applications 10, 73-84.

MacKenzie, J.J., El-Ashry, M.T., 1989. Air pollution's toll on forests and crops. Yale University Press, New Haven, CT. 376 pp.

Melewski, B., 1998. Acid deposition. Testimony of the Adirondack council before the senate subcommittee on clean air, wetlands, private property and nuclear safety

committee on environment and public works.

NAPAP (National Acid Precipitation Assessment Program), 2005. report to congress: An integrated assessment, Washington, D.C.

Nellemann, C., Thomsen, M.G., 2001. Long-term changes in forest growth: Potential effects of nitrogen deposition and acidification. Water, Air, and Soil Pollution 128, 197-205.

Sharpe, W.E., Sunderland, T.L., 1995. Acid-base status of upper rooting zone in declining and nondeclining sugar maple (*Acer saccharum* Marsh) stands in Pennsylvania. pp.172-178. *In* Gottschal, K.W., Fosbroke, S.L.C. (eds.) Proceedings of the Tenth Central Hardwood Forest Conference. U. S. Department of Agriculture, Forest Service General Technical Report NE-197.

Staaf, H., Persson, T., Bertills, U., 1996. Skogsmarkskalkning. Resultat och slutsatser från Naturvårdsverkets försöksversamhet (Liming of forest soil. Results and conclusions of the research activity by the Swedish Environmental Protection Agency), Report 4559, 290 pp. (in Swedish).

Tomlinson, G.H., Tomlinson, F.L., 1990. Effects of acid deposition on the forests of Europe and North America. Boca Raton, Florida, USA. CRC Press.

Turner, R.S., Cook, R.B., Van Miegroet, H., Johnson, D.W., Elwood, J.W., Bricker, O.P., Lindberg, S.E., Hornberger, G.M., 1990. Watershed and lake processes affecting surface water acid-base chemistry, NAPAP Report 10, *I*n Acidic deposition: State of Science and Technology, Volume II, National Acid Deposition Assessment Program, 722 Jackson Place, NW Washington, D.C.

USEPA (United States Environmental Protection Agency), 1999. Progressive report on the EPA acid rain program.

USEPA (United States Environmental Protection Agency), 2000. Inventory of U.S. greenhouse gas emissions and sinks: 1990-1998. Washington, D.C.

Westling, O., Hultberg, H., 1990. Liming and fertilization of acid forest soil: short-term effects of runoff from small catchments. Water, Air, and Soil Pollution 54, 391-497.

Wigington, P.J., Jr., Davies, T.D., Tranter, M., Eshleman, K.N., 1990. Episodic acidification of surface waters due to acidic deposition, NAPAP Report 12, *I*n Acidic deposition: State of Science and Technology, Vol. II. National Acid Deposition Assessment Program, Washington, D.C. 200 pp.

Wigington, P.J., Jr., DeWalle, D.R., Kretser, P.S., Murdoch, P.S., Simonin, H.A., Van Sickle,

J., McDowell, M.K., Peck, D.V., Barchet, W.R., 1996. Episodic acidification of small streams in the Northeastern United States: Episodic response project, Ecological Application 6, 374-388.

Chapter 2. Changes in Chemistry of Soils, Soil Solution, and Streamwater: Effects of Liming on Acidified Watersheds

ABSTRACT

Acid deposition, which causes damage to fish and aquatic organisms, forests, and streams and lakes, has been a problem for at least five decades in northeast United States. The purpose of this research was to test limestone sand treatment effects on the chemistry of soils, soil solutions, and streamwater based on two paired Before-After-Control-Impact (BACI) design studies. Coarse-grained dolomitic limestone sand was applied at a rate of 5 t ha^{-1} over the Laurel and 90 Degree watersheds in fall 2003 and 2004 and over six soil plots (15.2 meter by 9.1 meter) within the same watersheds in summer 2005. Adjacent Merrill and Tick watersheds were used as the controls. After treatment, A horizon soils showed significant increased soil pH, exchangeable calcium and magnesium, and base saturation. With the addition of limestone sand, pH, conductivity, Ca/Al molar ratio, and concentrations of calcium, magnesium, and acid neutralizing capacity in soil solution at A horizon (30 cm soil depth) also increased over those of the controls. Analysis of monthly streamwater chemistry indicated increased pH, conductivity, calcium, magnesium, acid neutralizing capacity and decreased aluminum within 23 months after limestone sand treatment. Limestone sand application improved soil nutrient conditions and drainage water quality.

2.1. Introduction

Acid deposition has created forest degradation problems for three decades in eastern North America (Driscoll et al., 2003). Acidified forest soils lose their ability to neutralize strong acid inputs due to loss of soil nutrients, resulting in increased

concentrations of aluminum in soil water (Geary and Driscoll, 1996). The higher concentration of aluminum not only impedes the uptake of base cations in soil water from tree roots, it is also toxic to fish and other aquatic organisms in streams. Haines and Baker (1986), for example, have reported a decline in fish populations due to acidification in eastern United States.

In the eastern US, acid-sensitive tree species have declined in a way that suggests acid deposition has played a role. Red spruce has experienced winter weather injury, and its growth rate in this region has decreased (DeHayes, 1992; DeHayes et al., 1999). Further, acid deposition has been blamed for the decline in red spruce at high elevations in the eastern US (Johnson and Siccama, 1983; Driscoll et al., 2003). Moreover, the decline in sugar maple trees in Pennsylvania has been attributed to low levels of base cations in soil and foliage (Sharpe and Sutherland, 1995; Horsley et al., 2000; Drohan et al., 2002; Bailey et al., 2004).

Because of the slow rock weathering process that neutralizes acidity naturally, more readily soluble lime has been used in nutrient-poor forest ecosystems. As a result of numerous studies on liming to counteract acid deposition in Europe (i.e., Denmark (Ingerslev, 1997), Norway (Hindar et al., 2003), Sweden (Andersson and Persson, 1988)), liming application strategies are well developed (Hindar and Henriksen, 1992; Dickson and Brodin, 1995). However, limited research on forest liming has been conducted in North America.

The objective of this research, therefore, was to investigate the short-term effects of dolomitic limestone treatment on soil, soil solution, and streamwater chemistry in the

Mosquito Creek basin, Pennsylvania, USA.

2.2. Methods

2.2.1. Study Area

2.2.1.1. Location

The Mosquito Creek basin is a tributary of the West Branch of the Susquehanna River located in Clearfield, Elk, and Cameron counties in northcentral Pennsylvania (Figure 2.1). Located in the Allegheny Plateau physiographic province, the Mosquito Creek basin has a drainage area of 23,000 hectares (230 km^2). Elevations within the Mosquito Creek basin vary from 260 m to 688 m. Local people use the Mosquito Creek basin for a variety of social, economic and cultural purposes, including fishing, hunting, and camping. The basin has been and continues to be severely impacted by acid deposition, which has greatly reduced trout and other aquatic populations.

Located on Gifford Run in the Mosquito Creek basin at $41^o11'N$ / $78^o17'W$, the four watersheds were selected to study the effectiveness of dolomitic limestone sand treatments in the amelioration of acidity (Figure 2.2). All four watersheds, Laurel, 90 Degree, Merrill, and Tick, are located adjacent to each other; they measure about 176, 136, 221 and 129 hectares, respectively, in area. Laurel and 90 Degree watersheds were treated with limestone sand at a rate of five tons per hectare in the fall of 2003 and 2004; the Merrill and Tick watersheds were assigned roles as control watersheds. Soil plot (15.2 meter by 9.1 meter) were established at lower, middle, and upper elevations of the Laurel, 90 Degree, and Merrill watersheds for the evaluation of limestone sand effects on soil water

chemistry.

2.2.1.2. Climate

The Mosquito Creek basin experiences a continental climate. Average total annual precipitation, based on 1971-2000 records from the climate station at Clarence (elevation 424 m, 41°03'N / 77°57'W) was 1056 mm (Table 2.1). Precipitation is fairly evenly distributed throughout the year, with the highest precipitation occurring in June, July and September, and the lowest in December, January and February. Although the runoff from melting snow in spring is not a main water supply for the Mosquito Creek community, a high proportion of annual precipitation does come in the form of snow.

2.2.1.3. Soils and bedrock

The soil information of the Mosquito Creek watersheds is shown in Figure 2.3 and described in Table 2.2. The watersheds are primarily Hazleton, Clymer and Cookport series, very stony loams (U.S. Department of Agriculture, Natural Resources Conservation Service, 2005). The most common soils at lower elevations of watersheds are the Hazelton series with Clymer and Cookport series, very stony soils at higher elevations.

Information regarding the bedrock of the Mosquito Creek watersheds is shown in Figure 2.4 and Table 2.3. The bedrock of Mosquito Creek watersheds is mainly dominated by the Pottsville Formation (Department of Conservation and Natural Resources, Pennsylvania Bureau of Topographic and Geologic Survey, 2001). The Burgoon Sandstone occupies the lower elevations near the outlet of each watershed. The higher elevations of

Tick and Merrill watersheds are underlain by the Allegheny Formation. The dominant lithology at the Mosquito Creek watersheds was sandstone, which characteristically has a low buffering capacity and is typically acidic.

2.2.1.4. Forest cover

The Mosquito Creek basin is located within the Moshannon State Forest in Clearfield, Elk and Cameron counties, Pennsylvania. The land is mainly dominated by deciduous forest with a small section of coniferous forest in the Tick watershed. The dominant tree species in the study watersheds are red oak (*Quercus rubra*), red maple (*Acer rubrum*), and white oak (*Quercus alba*), which are about 80-100 years old. Small amounts of black oak (*Quercus velutina*), chestnut oak (*Quercus montana*), sassafras (*Sassafras albidum*), and black cherry (*Prunus serotina*) are also present in the study watersheds. The shrub species, mountain laurel (*Kalmia latifolia*) is also present in the watershed. The herbaceous vegetation of the watershed consists of a combination of bracken fern (*Pteridium aquilinum*), hay-scented fern (*Dennstaedtia punctilobula*), blueberry (*Vaccinium spp.*), teaberry (*Gaultheria procumbens*), and huckleberry (*Gaylussacia spp.*).

2.2.2. Data Collection

2.2.2.1. Precipitation and throughfall

Daily total precipitation, daily minimum and maximum temperatures during the study period were obtained from the nearest National Weather Service (NWS) climate station at Clarence, Pennsylvania (elevation 423.7 m, 41^{o}03'N 77^{o}57'W).

Within the study watersheds, throughfall samples were collected on an event-basis and obtained for 17 rain events from April to October 2005 (Figure 2.2). A throughfall collector was installed under the forest canopy using a plastic funnel and a bottle in summer 2004. A small pit was excavated to place the collecting bottle, and covered with plywood for protection. The plastic funnel was protected with a cheese cloth, and the hose connecting the funnel to the collection bottle was looped to prevent evaporation of the sample prior to collection. Adjacent to the throughfall collector, a standard tipping-bucket rain gage coupled to a battery-operated event recorder was installed to measure the throughfall intensity and volume of a rain event (17 rain events in total) from April to October 2005. In order to minimize microbial reactions in unfiltered samples, throughfall samples were placed in a cooler with an ice pack immediately after sampling.

2.2.2.2. Soil and soil solution

Soil samples from soil plots were collected before limestone sand application in June 3, 2005, and after limestone sand application on October 6, 2005. At each plot (15.2 meter by 9.1 meter), three mineral A horizon soil samples (54 mineral A horizon samples in total) were immediately placed in small zipperlock bags after collection.

Soil solution samples were collected on an event-basis and obtained for 10 rain events before limestone sand application and 8 rain events after liming in 2005. Soil solution samples were collected by lysimeters from soil plots located at the lower, middle, and upper elevations of the Laurel, 90 Degree, and Merrill watersheds (Figure 2.2). Soil solution samples were collected at both 30 cm and 80 cm soil depths using both tension and

zero-tension lysimeters (Figure 2.5). Two tension lysimeters and one zero-tension lysimeter were installed at each plot. A tension lysimeter and a zero-tension lysimeter were installed at 30 cm soil depth. Another tension lysimeter was installed at 80 cm soil depth (bottom of the unsaturated zone) during the summer of 2004. Soil solution samples from tension lysimeters were collected by applying a suction to create a -60 k Pa vacuum within 36 hours before rainfall began and at the termination of each episodic storm event. Soil solution samples from zero-tension lysimeters were collected within 36 hours prior to the beginning of rainfall and at the termination of each storm event. In order to minimize microbial reactions in unfiltered samples, soil solution samples were placed in a cooler with an ice pack immediately after sampling.

Tension lysimeters were constructed following methods by Mitchell et al. (2001). A tension lysimeter consisted of a 3.8 cm inner diameter PVC pipe with a cap at one end and a ceramic porous cup (pore size 2.5 μm) at the other. They were purchased from Soil Moisture Equipment Corporation. A power auger was used to drill a hole to the appropriate depth for each tension lysimeter. A slurry was made with water and soil from the bottom of the hole, and was packed around the ceramic porous cup. The soil from the lysimeter hole was replaced to restore its original order and then compacted to avoid overland flow along the outside of lysimeter tube (Swistock et al., 1990). To protect it from wild animals, each tension lysimeter was covered with an 8.9 cm inner diameter PVC pipe with a lid on it, and then fixed with a stake.

To collect soil solution at 30 cm depth by zero-tension lysimeter, a pit was excavated by hand to an approximate soil depth of 70 cm. Zero-tension lysimeters were

constructed with 847 cm^2 polyethylene trays filled with polypropylene beads. An 8 mm hole formed an outlet on the corner of tray; a spout was formed in the hole and tubing attached to it and connected to a collecting bottle. The outlet was covered with cheese cloths to prevent the spout from becoming clogged with soil and to facilitate drainage of soil solution into the collecting bottle (Swistock et al., 1990). The zero-tension lysimeter was installed horizontally in the side wall of the soil pit. Pits were covered with a sheet of plywood to prevent animal damage.

2.2.2.3. Streamwater

Monthly streamwater samples during baseflow conditions were collected in clean polyethylene bottles by grab sampling at each watershed gauging station (Figure 2.2). The 250 ml polyethylene bottles were rinsed with streamwater three times before collection. Monthly streamwater samples were immediately placed in a cooler with an ice pack to minimize microbial reactions in unfiltered samples. Samples were returned to the laboratory and stored in a refrigerator at 4 ^oC until analysis.

2.2.3. Limestone Sand Application

2.2.3.1. Watershed application

The coarse-grained dolomitic limestone sand was purchased from the New Enterprise Stone and Lime Co. in Tyrone, PA. Dolomitic limestone sand was applied by The Penn State Regenerator (a rubber tired skidder with attached wet lime spreader) at a rate of 5 t ha^{-1} over the Laurel and 90 Degree watersheds. A total of 507 t of coarse-grained

dolomitic limestone sand was spread over 76 percent of the 90 Degree watershed between October 16 and November 10, 2003. A total of 420 t of limestone sand was spread over the Laurel watershed; 228 t in November, 2003, and 192 t in September and October, 2004. Fifty one percent of the Laurel watershed was treated. The particle size distribution of limestone sand applied over the Laurel and 90 Degree watersheds is shown in Table 2.4.

2.2.3.2. Soil plot application

For the soil plot study, the six plots (15.2 meter by 9.1 meter) located within the Laurel and 90 Degree watersheds did not receive the watershed basis limestone sand treatment in 2003 and 2004, based on the results from response of soil chemistry to liming in fall 2004. As a result, additional limestone sand treatment over the soil plots was required to study the response of soil and soil solution chemistry to liming. The six soil plots located within the Laurel and 90 Degree watersheds were treated with hand applied limestone sand at a rate of 5 t ha^{-1} on June 8, 2005. The particle size distribution of limestone sand applied over the six soil plots is shown in Table 2.4.

2.2.4. Data Analysis

2.2.4.1. Limestone sand chemical analysis

The chemical elements in the limestone sand were analyzed by a Leeman Labs PS3000UV inductively coupled plasma emission spectrophotometer (ICP) at the Materials Characterization Laboratory (Materials Research Institute, The Pennsylvania State University, University Park). The results of the limestone sand chemical analysis are shown

in Table 2.5 for both watersheds and soil plot application.

2.2.4.2. Soil chemistry analysis

All soil samples (3 samples per soil plot and 54 samples in total) were sent to the Agricultural Analytical Services Laboratory (The Pennsylvania State University, University Park) within 6 hours of collection. Mineral A horizon soil samples were analyzed for pH, P, exchangeable cations (Acidity, K, Mg, Ca, Cation Exchange Capacity), and % saturation of the CEC (K, Mg, and Ca). Soil pH was measured using 1:1 soil water pH (Eckert and Sims, 1995). To establish pH buffering capacity, acidity was measured using the Mehlich Buffer pH method (Mehlich, 1976). Exchange base cations (K, Mg, and Ca) were extracted using Mehlich 3 extractant (Wolf and Beegle, 1995). The CEC, a measure of the quantity of soils that can retain positively charged ions (cations) by electrostatic forces, was determined by summation of exchangeable cations (Ross, 1995).

2.2.4.3. Throughfall, soil solution, and streamwater chemical analysis

Throughfall collected from the site, soil solution samples collected from both tension lysimeters and zero-tension lysimeters, and monthly streamwater grab samples were analyzed at the Penn State Institutes of the Environment Laboratory at The Pennsylvania State University. All samples were stored at 4 ^{o}C until analysis and analyzed according to *Standard Methods for the Examination of Water and Wastewater*, 20th Edition (Eaton et al., 1998). All water samples were analyzed for pH, calcium, magnesium, total dissolved aluminum, acid neutralizing capacity, and conductivity. The pH and conductivity

of water samples were determined by using unfiltered samples with the Beckman 360 pH meter and an YSI 3200 conductivity instrument, respectively. The concentrations of calcium and magnesium in samples were analyzed with the Perkin-Elmer 5100 flame atomic absorption spectrometer with 0.45 μm filtered water samples. The concentration of total dissolved aluminum in water samples was analyzed with the Perkin-Elmer 5100 furnace atomic absorption spectrometer with a 0.1μm filtered sample. The concentration of acid neutralizing capacity in water samples was analyzed on unfiltered samples with Radiometer Triburrette.

2.2.4.4. Statistical data analysis

The study design Before-After-Control-Impact (BACI) was used for data analysis (Green, 1979; Skalski and Robson, 1992; McDonald et al., 2000). McDonald et al. (2000) note that the BACI design-- because it includes both time and control sites--reduces the possibility that unmeasured covariates are influencing observed effects.

Soil and soil solution analysis

Mineral A horizon soil samples, 27 samples in total, were obtained. Soil solution samples collected from lower, middle, and upper slopes in the watershed were averaged in order to represent soil solution characteristics on a watershed basis and to allow analysis where there were missing values. Based on the BACI study design, soil and soil solution samples were analyzed with Analysis of Variance (Minitab, 2003). The following general linear model was used as a formula:

Sample Data= Year+ Site+ Year*Site+ error (1)

where Sample Data indicates the appropriate soil and soil solution chemistry parameter; Year indicates 1 versus 2 (1 indicates before limestone sand application and 2 indicates after limestone sand application); and Site indicates location of watershed.

In order to test significant limestone sand treatment effects on mineral A horizon soils and soil solution, the interaction between Year and Site (Year*Site) was tested with pairwise comparison using the Tukey method (Minitab, 2003).

Streamwater analysis

In order to investigate streamwater chemistry parameters as they change over time incorporated the data from each month, Analysis of Covariance (Minitab, 2003) was used, under which time is considered a covariate in the general linear model. The analysis incorporated the time component as a covariate, which allowed for removal of any of the effects of the variability in month and to determine the significance of the treatments over time. The general linear model is as follows:

Sample Data = TreatCont + Time + Time*Time + Time*Time*Time
+ Time*TreatCont + error (2)

where Sample Data indicates the water chemistry parameter, log transformed; Treat indicates the watershed receiving limestone sand treatment; Cont indicates the control watershed; TreatCont is the term for treatment versus control; Time indicates the monthly date of sample collection; Time*Time is a quadratic term for Time to help model the curvature in the data; Time*Time*Time is a cubic term for Time which again helps model the curvature in the data; and Time*TreatCont represents the interaction between the treated versus control watershed and Time.

Because there are two distinct time periods, before and after limestone sand treatment, the dates were split into two groups, analysis was run separately for before and after limestone sand application. The data were tested for normality using normal probability plots of the residual and residual versus fitted values as well as the Tukey test with pairwise comparison.

2.3. Results

2.3.1. Climatic Perspective

Average total annual precipitation was 1056 mm, based on 1971-2000 climate records from the National Climate Data Center (NCDC) climate station (elevation 423.7 m, 41^{o}03'N / 77^{o}57'W) at Clarence. The study covered the period from July 2003 to October 2005 (Figure 2.6 and Table 2.6). Average total annual precipitation in 2003, 2004, and 2005 was 1503 mm, 1511 mm, and 1043 mm, respectively. Weather in year 2003 and 2004 was much wetter than the long-term average, whereas weather in year 2005 was drier than the

long-term average. The highest monthly total precipitation during the study period was 281 mm in September 2004, as a result of Hurricane Ivan. Daily mean air temperature showed quite similar patterns throughout the 2003, 2004, and 2005 calendar year. Daily mean air temperature ranged from -6.97 ^{o}C in January to 19.40 ^{o}C in August, with an annual average of 7.51 ^{o}C, for the study period.

Throughfall on the watersheds during the soil plot study period from April 4 to October 9, 2005 was acidic (Figure 2.7). The average pH of throughfall was 4.91, ranging from 4.25 to 6.08. The pH of throughfall, varied with time. Before limestone sand application, the average pH of throughfall was slightly higher than that after treatment.

The concentrations of calcium and magnesium in throughfall were similar over time (Figure 2.8). Before liming application, base cation deposition was slightly lower over the watersheds than during the post-treatment period. The calcium concentration of 9 events before treatment ranged from 8.73 μmol/L to 34.18 μmol/L, with an average of 19.52 μmol/L. After treatment, calcium concentration of 8 events ranged from 5.99 μmol/L to 41.17 μmol/L, with an average of 23.67 μmol/L. The mean magnesium concentrations of the before and after liming events were 10.19 μmol/L and 11.88 μmol/L, respectively. The aluminum concentration of throughfall before liming was higher than that in throughfall after liming (Figure 2.9). The mean concentration of aluminum in throughfall before liming was 1.89 μmol/L, ranging from 0.93 μmol/L to 3.71 μmol/L. The mean concentration of aluminum in throughfall after liming period was 1.52 μmol/L, ranging from 0.30 μmol/L to 3.89 μmol/L.

2.3.2. Soil Chemistry Treatment Effects

Soil plays a major role in determining the health of a forest ecosystem, therefore, it is important to understand its chemical composition as affected by treatment. Mineral A horizon soil samples were collected both just before dolomitic limestone sand application and right before termination of soil solution monitoring. About four months separated the two sampling dates. Figure 2.10 shows mean exchangeable calcium and magnesium in the mineral A horizon before and after liming application. With the addition of dolomitic limestone, calcium and magnesium concentrations in soils were expected to increase. As expected, mean exchangeable calcium and magnesium in the mineral A horizon increased with lime application, whereas mean exchangeable calcium and magnesium in the mineral A horizon in control plots decreased between the two sample dates. Detailed chemical characteristics in mineral A horizon both prior to and post dolomitic limestone sand application at Mosquito Creek watersheds are shown in Table 2.7.

Prior to application, the mineral A horizon was generally acidic at all sampling plots. Average soil pH of 9 soil plots was 3.64 ranging from 3.30 to 4.0. The mineral A horizon chemistry changed more or less after treatment. Exchangeable acidity decreased significantly ($\alpha \leq 0.05$) from 23.23 meq/100g to 18.97 meq/100g in soil plots at the Laurel watershed and from 27.17 meq/100g to 18.77 meq/100g in soil plots at the 90 Degree watersheds with treatments. Although exchangeable acidity in unlimed Merrill plots decreased from 27.70 meq/100g to 22.97 meq/100g, the mean difference between the two sampling dates was not statistically significant ($\alpha \leq 0.05$). Mean exchangeable calcium in the mineral A horizon increased, but the increase was not statistically significant ($\alpha \leq 0.05$).

However, the mean exchangeable magnesium in the mineral A horizon showed statistically significant responses to limestone treatment and increased as follows: from 0.48 meq/100g to 1.4 meq/100g in the Laurel soil plots, and from 0.56 meq/100g to 2.59 meq/100g in the 90 Degree soil plots. The cation exchange capacity (CEC) is the total amount of basic and acidic cations that a soil can hold. The mean CEC increased for both the Laurel and 90 Degree soil plots, although the difference before and after treatment was not statistically significant in the Laurel plots. In unlimed Merrill soil plots, the mean CEC in the mineral A horizon decreased between two sampling dates. Percent base saturation is defined as percentage of basic cations on soil exchange sites. Base saturation increased from 13.52% (before liming) to 17.9% (after liming) in the Laurel soil plots and from 17.02% (before liming) to 26.57% (after liming) in the 90 Degree soil plots, but these differences were not statistically significant. However, percent base saturation in unlimed Merrill watersheds decreased significantly ($\alpha \leq 0.05$) from 13.80% to 8.44%.

2.3.3. Soil Solution Chemistry Treatment Effects

The summer of 2005 was very dry, thus less soil solution was available for collection. Soil solution samples were collected on an event-basis rather than a fixed-schedule basis. The reason for this was to evaluate percolating soil water and not water held in the soil under tension between rainfall events. Soil solution samples were collected within 36 hours after a rain event. Drought and transpirational soil water loss resulted in many lysimeters without adequate sample for analysis. Soil solution was collected for 10 rainfall events from April to June before the addition of dolomitic limestone sand. Data

were also collected for 8 rainfall events from June to October after application of dolomitic limestone sand.

2.3.3.1. Soil solution chemistry at 30 cm soil depth collected by tension lysimeter

The detailed mean soil solution chemical characteristics collected by tension lysimeters at 30 cm depth in 2005 are shown in Table 2.8. The pH of soil solution increased with the addition of limestone sand at both the Laurel and 90 Degree watersheds (Figure 2.11). Mean pH of soil solution collected by tension lysimeter at 30 cm depth increased from 4.99 (prior to liming) to 5.24 (post liming) at the Laurel watershed, and from 5.20 (prior to liming) to 5.60 (post liming) at the 90 Degree watershed. The unlimed Merrill watershed pH increased only 0.01 pH units.

With the addition of dolomitic limestone sand, soil solutions were expected to show an increase in base cations. With the addition of limestone sand, concentrations of calcium and magnesium in soil solution, as collected by tension lysimeters, increased at 30 cm depth (Figures 2.12 and 2.13). The mean calcium concentration in the soil solution collected by tension lysimeters at 30 cm soil depth at Laurel and 90 Degree watersheds increased significantly ($\alpha \leq 0.05$) from 19.11 µmol/L to 33.37 µmol/L and from 25.17 µmol/L to 44.66 µmol/L, respectively (Table 2.8). The unlimed Merrill watershed had a slight increase in mean calcium concentration in soil solution from 25.45 µmol/L to 27.34 µmol/L. Magnesium concentrations in soil solution collected by tension lysimeters at 30 cm depth showed similar results. Mean magnesium concentration in soil solution doubled on the Laurel and 90 Degree watersheds. The Merrill watershed showed only a 0.83 µmol/L

increase in mean magnesium concentration.

With the addition of dolomitic limestone sand, mean aluminum concentration in soil solution at the Laurel and 90 Degree watersheds decreased by about 2 μmol/L whereas, mean aluminum concentration in soil solution at the Merrill watershed increased about 3.6 μmol/L (Table 2.8, Figure 2.14). With the addition of lime, the mean conductivity in soil solution at 30 cm depth increased at the Laurel and 90 Degree watersheds (Figure 2.15), while conductivity decreased on the Merrill watershed.

A large increase in acid neutralizing capacity (ANC) in soil solution at 30 cm depth was observed on both the treated and control watersheds (Figure 2.16). The mean concentration of ANC in soil solution increased significantly ($\alpha \leq 0.05$) from -1.56 μeq/L to 23. 47 μeq/L on the Laurel watershed and from 10.72 μeq/L to 55.80 μeq/L on the 90 Degree watershed. The Merrill watershed ANC increased from 4.74 μeq/L to 13.12 μeq/L. ANC increases on the Laurel and 90 Degree watersheds were more than fifteen and four times higher, respectively, than their mean concentration prior to liming application. Calcium/aluminum (Ca/Al) molar ratio of soil solution at 30 cm depth on Laurel and 90 Degree watersheds increased with the addition of limestone sand (Figure 2.17), but decreased significantly ($\alpha \leq 0.05$) on the unlimed Merrill watershed.

2.3.3.2. Soil solution chemistry at 80 cm soil depth collected by tension lysimeter

The detailed mean soil solution chemical characteristics at 80 cm depth in 2005 collected by tension lysimeters are shown in Table 2.9. There were no statistically significant treatment effects on pH in soil solution, however, the mean pH in soil solutions

at 80 cm depth increased more on treated watersheds (Table 2.9, Figure 2.18).

Mean calcium concentration of soil solution at the Laurel watershed increased significantly ($\alpha \leq 0.05$) with the addition of limestone sand (Figure 2.19). A slight increase occurred at both the 90 Degree watershed with liming and the Merrill watershed without liming. However, magnesium concentrations in soil solution and conductivity appeared to be increased by treatment (Figure 2.20). The mean concentration of magnesium at the Laurel and 90 Degree watersheds increased from 27.40 µmol/L to 38.81 µmol/L and from 23.70 µmol/L to 34.56 µmol/L, respectively. However, mean concentrations of magnesium at the Merrill watershed increased by only 1.31 µmol/L from 16.54 µmol/L to 17.85 µmol/L.

The aluminum concentration in soil solution at 80 cm depth appeared to be unaffected by the limestone sand application (Figure 2.21). Both the 90 Degree and Merrill watersheds showed decreases in aluminum concentration after liming; the Laurel watershed showed a slight increase. Conductivity increased slightly in the Laurel and 90 Degree watersheds and decreased in the Merrill watershed (Figure 2.22).

The mean concentration of ANC in the soil solution collected at all watersheds increased before and after liming periods (Figure 2.23). However, there were some limestone sand treatment effects based on maximum concentrations of ANC in soil solution at 80 cm depth. The maximum concentration of ANC in soil solution at the Laurel and 90 Degree watersheds increased from the 27.20 µeq/L (before liming) to the 149.0 µeq/L (after liming) and from 28.54 µeq/L (before liming) to 185.7 µeq/L (after liming), respectively. The maximum concentration of ANC in the soil solution at the Merrill watershed after

liming was 14.00 μeq/L decreased from 15.84 μeq/L before liming.

The Ca/Al molar ratio of soil solution at 80 cm depth increased on both treated and control watersheds after liming. The mean Ca/Al molar ratio of soil solution at the Laurel and 90 Degree watersheds increased more than twice over with the addition of limestone sand, whereas the unlimed Merrill watershed showed increased only 1.4 times (Figure 2.24).

2.3.3.3. Soil solution chemistry at 30 cm depth collected by zero-tension lysimeter

The detailed mean soil solution chemical characteristics at 30 cm depth in year 2005 collected by zero-tension lysimeters are shown in Table 2.10. With an addition of limestone sand, the mean pH of soil solution at 30 cm depth increased on both the Laurel and 90 Degree watersheds (Figure 2.25). The 90 Degree watershed showed a great increase in mean pH from 5.02 to 5.95 with a maximum of 7.1 immediately after treatment. However, the mean pH value at the Merrill watershed during post treatment was 4.87, a decrease from 5.02.

The calcium and magnesium concentrations in soil solution increased at all watersheds (Figures 2.26 and 2.27). Mean calcium concentration in soil solution at the Laurel watershed increased significantly ($\alpha \leq 0.05$) from 13.22 μmol/L to 270 μmol/L. At the 90 Degree watershed increased from 12.48 μmol/L to 99.1 μmol/L. The maximum concentrations of calcium and magnesium in soil solution at 30 cm depth at the Laurel watershed were 640 μmol/L and 831 μmol/L, respectively, about 3 and half months after liming application. However, mean calcium and magnesium concentrations in the soil solution at the unlimed Merrill watershed increased slightly (less than 15 μmol/L).

Treatment effects on aluminum concentrations in soil solution at 30 cm depth were variable (Figure 2.28). The mean and maximum concentrations of aluminum in soil solution at both the Laurel and Merrill watersheds increased compared to their values before liming. However, the mean aluminum concentration in soil solution at 30 cm depth at the 90 Degree watershed decreased.

With the addition of limestone sand, mean conductivity increased significantly ($\alpha \leq 0.05$) from 29.6 μS/cm to 241.3 μS/cm at the Laurel watershed (Table 2.10, Figure 2.29). Likewise, it increased from 30.31 μS/cm to 81.9 μS/cm at the 90 Degree watershed. Maximum conductivity in soil solution at the Laurel and 90 Degree watersheds were 471.7 μS/cm and 114.5 μS/cm in September 30, respectively. Mean conductivity at the unlimed Merrill watershed increased by only about 10μS/cm after the liming period at compared with its value before the liming period.

It seems only the 90 Degree watershed increased with mean ANC in soil solution with the addition of limestone sand (Figure 2.30). Although the maximum ANC concentration was observed at the Laurel watershed on September 30, this value was quite different from the remaining post-treatment data. Before liming, the mean concentration of ANC in soil solution at the 90 Degree watershed was 23.0 μeq/L, ranging from -6.11 μeq/L to 77 μeq/L. After liming, the mean concentration of ANC in soil solution was 472 μeq/L, ranging from 35 μeq/L to 1271 μeq/L. The maximum concentration in soil solution at the 90 Degree watershed was measured immediately after the limestone sand treatment. Lack of sampling resulted in only one observation of ANC for the Merrill watershed before treatment.

The mean Ca/Al molar ratio of soil solution at the Laurel and 90 Degree watersheds increased dramatically, by more than six times, with the addition of limestone sand (Figure 2.31). However, the unlimed Merrill watershed showed a Ca/Al molar ratio did not appear to increase, but only two observations were available prior to treatment.

2.3.4. Streamwater Chemistry Treatment Effects

2.3.4.1. The pH

Streams with a pH above 6 are considered desirable for a variety of fish species and aquatic organisms (Earle and Callaghan, 1998). Prior to liming, the streamwater in the four of the watersheds was chronically acidic (Figure 2.32). The monthly pH in streamwater at the Laurel watershed was higher compared to the other watersheds before limestone treatment. The mean pH of streamwater at the Laurel watershed prior to liming was 5.89, ranging from 5.32 to 6.29 (Table 2.11). The pH of streamwater at the Laurel watershed did not change much during the post-treatment period; the mean pH of streamwater decreased from 5.89 (before liming) to 5.88 (after liming), however, the mean pH in streamwater at the 90 Degree watershed increased from 5.58 before liming to 5.90 after liming, with the highest pH of 7.29 recorded in October 2005. The pH of streamwater on control watersheds was expected to be the same or decrease without liming, however, the monthly mean pH of streamwater on the Merrill watershed increased throughout the study period. Before liming, the mean pH of Merrill streamwater was 5.37; which increased to 5.61 during the post-treatment period and the maximum pH increased from 5.56 to 6.5. On the other hand, the mean monthly pH of streamwater on the Tick watershed increased

only slightly summer 2005 from 4.89 (pre-liming) to 4.96 (post-liming). Statistical analysis showed no significant difference in mean pH between the treated and untreated watersheds and their interaction with time before the liming period (Table 2.11). However, after the liming period there was a significant difference in mean pH between the limed and unlimed watersheds, as well as a significant difference with time at the 0.05 significance level.

2.3.4.2. The concentration of calcium

The pattern of monthly calcium concentration in control watersheds was steady and similar in range throughout the study period (Figure 2.33). The monthly calcium concentration in streamwater at the Merrill watershed ranged from 20.21 μmol/L to 42.91 μmol/L, with an average of 32.41 μmol/L. Calcium on the Tick watershed ranged from 20.21 μmol/L to 31.94 μmol/L, with an average of 25.48 μmol/L (Table 2.11). Patterns of increasing calcium concentration in streamwater were observed on the treated watersheds. With the addition of limestone sand, the monthly mean calcium concentration in streamwater at the 90 Degree watershed increased from 45.11 μmol/L (before liming) to 49.85 μmol/L (after liming). With a maximum value of 114.77 μmol/L in September, 2005, which was two times higher than the maximum concentration prior to liming. Although mean calcium concentrations in streamwater at the Laurel watershed decreased slightly from 43.17 μmol/L (before liming) to 42.96 μmol/L (after liming), the maximum concentration increased from 52.40 μmol/L (before liming) to 74.85 μmol/L (after liming). During the post-treatment period, there was a significant difference in the mean calcium concentration in streamwater between the limed and unlimed watersheds and with time,

with a p-value of 0.000 at the 0.05 significance level (Table 2.11).

2.3.4.3. The concentration of magnesium

Magnesium concentration data in streamwater were not available prior to liming so limestone sand treatment effects for before and after liming could not be estimated. Magnesium concentrations in streamwater from the treated watersheds relative to streamwater from the control watersheds were analyzed for differences after application. The monthly magnesium concentrations in streamwater were quite similar in range for all watersheds until May 2005, then Mg concentrations on the treated watersheds increased peaking in September 2005 (Figure 2.34). In contrast, monthly magnesium concentrations for streamwater on the Merrill and Tick watersheds increased only slightly. The mean monthly magnesium concentrations were highest for the 90 Degree watershed. Monthly magnesium concentrations in streamwater on the 90 Degree watershed ranged from 28.80 µmol/L to 85.99 µmol/L, with mean of 44.44 µmol/L. The mean monthly magnesium concentration in streamwater on the Tick watershed was 26.40 µmol/L, and ranged from 22.63 µmol/L to 30.86 µmol/L (Table 2.11). Statistical analysis showed a significant difference in the mean monthly magnesium concentrations between the treated and control watersheds and with time at the 0.05 significance level.

2.3.4.4. The concentration of aluminum

Streams with aluminum concentrations below 2 µmol/L are considered less likely to be impaired by acid deposition (EMEP, 2005). The highest monthly aluminum

concentrations in streamwater for both the before and after liming periods were observed at the Tick watershed (Figure 2.35). These concentrations were 6.12 μmol/L before liming and 9.64 μmol/L after liming. Aluminum on the Merrill watershed increased by twice its maximum value (2.85 μmol/L) before liming to 5.93 μmol/L after liming. With the addition of limestone sand, the mean aluminum concentrations in streamwater at the Laurel watershed increased from 1.18 μmol/L before liming to 1.37 μmol/L after liming, where its maximum concentration increased more than two times from 2.22 μmol/L before liming to 5.56 μmol/L after liming (Table 2.11). The mean aluminum concentrations in streamwater at the 90 Degree watershed decreased from 2.73 μmol/L before liming to 2.34 μmol/L after liming, where its maximum concentration increased from 4.26 μmol/L before liming to 5.93 μmol/L after liming. However, monthly aluminum concentrations in streamwater at the Laurel and 90 Degree watershed generally showed a pattern of decreases. Statistical analysis showed no significant difference in the mean monthly aluminum concentrations between the treatment and control subwatersheds and their interaction with time both before and after liming periods at the 0.05 significance level.

2.3.4.5. Conductivity

Prior to limestone sand application, monthly conductivity in streamwater at the Laurel watershed ranged from 23.80 μS/cm to 31.00 μS/cm, with a mean of 26.54 μS/cm. On the 90 Degree watershed, conductivity ranged from 23.80 μS/cm to 32.10 μS/cm, with an average of 27.04 μS/cm (Table 2.11). Conductivity increased slightly on the Laurel watershed and significantly on the 90 Degree watershed after August 2005 (Figure 2.36).

Conductivity values in monthly streamwater on the control watersheds were similar for the before and after liming periods, as expected. Differences in conductivity were not significant between the treatment and control watersheds before liming (Table 2.11). However, after liming, mean conductivity was significantly different between the treatment and control watersheds and these differences were also significant with time ($\alpha \leq 0.001$).

2.3.4.6. The concentration of acid neutralizing capacity

Acid neutralizing capacity (ANC) was used to estimate the ability of water to neutralize acidic compounds. Streams with ANC values below 0 μeq/L, between 0 μeq/L and 50 μeq/L, and above 50 μeq/L are generally considered to be chronically acidic, susceptible to episodic acidification, and relatively not sensitive to acid deposition problems, respectively (Driscoll et al., 2001). An ANC of 50 μeq/L or more is considered critical for aquatic organisms. Prior to dolomitic limestone sand application, the mean monthly ANCs on the Laurel and 90 Degree watersheds were 23.12 μeq/L and 0.85 μeq/L, respectively (Table 2.11), while the mean monthly ANCs for the Merrill and Tick watersheds were -2.21 μeq/L and -17.08 μeq/L, respectively, indicating chronically acidic streamwater. ANCs on the treated watersheds were well above 50 μeq/L the second summer following treatment and remained so for the duration of the study (Figure 2.37). In contrast, ANCs for the controls were always well below 50 μeq/L with slight increases near the end of the study period. Statistical analysis revealed no significant difference in mean ANC between the treatment and control watersheds prior to treatment (Table 2.11). However, after liming there was a significant difference in mean ANCs between the treatment and

control watersheds ($\alpha \leq 0.001$).

2.4. Discussion

2.4.1. Soil Chemistry

Forest liming is generally thought to counteract soil acidification caused by atmospheric deposition. In our experiment, liming over the forest floor increased exchangeable calcium and magnesium. The mean exchangeable magnesium increased nearly threefold on the Laurel watershed and more than fourfold on the 90 Degree watershed after liming. On the Merrill control watershed (the only control for the soil and soil solution experiment) mean exchangeable calcium and magnesium decreased from before to after liming period. Exchangeable calcium increased slightly after liming on the Laurel and 90 Degree watersheds, however, exchangeable calcium decreased by almost twofold on the unlimed control. Magnesium appeared to move more rapidly than calcium into the A horizon. The statistically significant decrease in mean exchangeable acidity at the treated soil plots indicates that limestone sand application played a role in its reaction in the mineral A horizon. Mean exchangeable acidity on the control decreased but the change was not statistically significant.

Mean available phosphorus in the A horizon decreased after liming, but increased on the control before and after treatment. This decrease in available phosphorus in the treated soil plots may be explained by the formation of insoluble calcium phosphates (Brady, 1974) or increased plant uptake. The increase of phosphorus in control plots could indicate a decrease in vegetation uptake of phosphate or it may be an artifact of the

extraction method which extracts a fraction of non available phosphorus. Exchangeable potassium also decreased in the A horizon of both the treated and control soil plots.

2.4.2. Soil Solution Chemistry

Understanding nutrient content in soil solution is necessary to sustain forest ecosystem health because soil solution provides a direct source of nutrients for plant uptake as well as food for forest macroinvertebrates. In addition, subsurface flow is considered the dominant mechanism of generating storm flow in forest watersheds in humid temperate regions (Whipkey, 1965; Weyman, 1970; Mosley, 1979; Pearce, 1990); consequently, soil solution from the terrestrial ecosystem is expected to eventually reach streams during storm events. Therefore, understanding the chemistry of soil solutions may be helpful in predicting the chemistry of streamwater.

Overall, dolomitic limestone sand application over the forest floor increased pH and concentrations of calcium, magnesium, and the acid neutralizing capacity of soil solution collected at 30 cm depth by both tension and zero-tension lysimeters. Slight increases were also noted on the control. In general, these increases were apparent four months after treatment. Two things may account for the rapidity of this effect; first, soil macropores may have served as conduits for infiltrating precipitation (Beven and Germann, 1982; Mosley, 1982; Jardine et al., 1989) and; second, the hydrophobic nature of organic material in the forest floor created by the dry conditions prevalent in summer 2005 may have enhanced macropore transport (Marshner et al., 1992; Geary and Driscoll, 1996). The noticeable increases of pH, Ca, Mg, and ANC in soil solution at 30 cm soil depth were

observed in the first rain event after limestone sand application, nine days following liming, from both tension and zero tension lysimeters. Marshner et al. (1992) reported similar results. The rapid responses of solute concentration in soil solution after liming are supported in another liming study conducted in Denmark by Ingerslev (1997) who reported that peaks in ionic concentrations in soil solution following liming were observed within 8 months.

The calcium/aluminum (Ca/Al) molar ratio of the soil solution has been used as an indicator for assessing the potential impacts of acidic deposition to forest ecosystems. Soil solution with Ca/Al molar ratios ≤1.0 were reported to result in stress to trees from aluminum stress at 50% (Cronan and Grigal, 1995). Before liming, the mean Ca/Al ratio of soil solution collected by tension lysimeters at both 30 cm and 80 cm soil depths was greater than 1 for all three watersheds. This indicates no risk of forest damage by aluminum stress. However, the mean Ca/Al molar ratios of soil solution collected by zero-tension lysimeters at 30 cm depth at the Laurel and 90 Degree watersheds were 0.69 and 0.71, respectively. This indicates a 50% risk of forest damage from aluminum stress (Cronan and Grigal, 1995). However, with the addition of dolomitic limestone, the Ca/Al molar ratio increased by more than 6 times on the Laurel watershed and by more than 9 times on the 90 Degree watershed to Ca/Al ratios well in excess of 1.0. On the control soil plots, mean Ca/Al ratio increased slightly, from 1.55 to 1.77. Liming application is, therefore, indicated as likely to help prevent forest ecosystem aluminum stress.

Soil solutions collected by tension lysimeters are expected to have higher ionic concentrations than those collected by zero-tension lysimeters (Shuford et al, 1977;

Swistock et al., 1990). Before liming, calcium and magnesium concentrations in soil solution collected by tension lysimeters were higher than those same ion concentrations in soil solution collected by zero-tension lysimeters at 30 cm depth. This result was expected based on previous work (Cozzarelli et al., 1987; Joslin et al., 1987; Swistock et al., 1990). However, increased solute concentrations in soil solutions collected by zero-tension lysimeters in response to liming were expected, because soil solution was collected immediately after rainfall events when rapidly moving percolating water was most likely to reach the zero-tension lysimeters before the tension lysimeters.

The observed increases in pH and increases in concentrations of calcium, magnesium, and acid neutralizing capacity in soil solution at 30 cm depth when compared to 80 cm depth was also expected by a result of the increased distance from the soil surface which was the fate of the limestone sand application. After the addition of limestone sand, the conductivity of soil solution at 30 cm depth was also greater than that at 80 cm depth on the treated watersheds, as was expected.

2.4.3. Streamwater Chemistry

A stream is the final place to which water from the terrestrial environment flows through the ecosystem and arrives at the outlet of the watershed. Therefore, the chemistry of streamwater reflects the overall biogeochemical status of the watershed as a whole. The ultimate goal of mitigating stream acidity by terrestrial liming and concomitant enhancement of the cold water fishery in Mosquito Creek was achieved. Overall, increases in pH and increases in concentrations of calcium, magnesium, and acid neutralizing

capacity in streamwater were evident within 23 months after the liming application.

This lag time could be a consequence of the mean residence time of water in the watershed. Preliminary work with oxygen-18 as a tracer of baseflow water (see Chapter 3) indicates general agreement between the observed water quality improvements and the residence time for precipitation on the treated watersheds.

General water quality indicators used to measure recovery from acid deposition include pH $\geq$ 6.0, Al $\leq$ 2 μmol/L, and ANC $\geq$ 50 μeq/L. From June 2005 to end of the study period, the mean pHs of streamwater at treated and control watersheds were 6.6 and 5.6, respectively. The mean concentrations of aluminum in streamwater for treated and control watersheds were 0.95 μmol/L and 2.31μmol/L, respectively, and its ANC's for treated and control watersheds were 132 μeq/L and 5.2 μeq/L, respectively. These indicators are further evidence that forest liming reversed the effects of acid deposition on the treated watersheds.

2.5. Conclusion

Application of dolomitic limestone sand to large areas of two forested watersheds in the Mosquito Creek basin resulted in significant ANC increases in soil solution and streamwater. Concomitant increases in Ca and Mg, decreases in Al and increased pH were also observed. Forest liming was effective in remediating streamwater acidity as a consequence of acid deposition.

2.6. References

Andersson, F., Persson, T., 1988. Liming as a measure to improve soil and tree condition in areas affected by air pollution. National Swedish Environmental Protection Board, Report No. 3518, Solna, Sweden, 131pp.

Bailey, S.W., Horsley, S.B., Long, R.P., Hallett, R.A., 2004. Influence of edaphic factors on sugar maple nutrition and health on the Allegheny plateau. Soil Science Society of America Journal 68, 243-252.

Beven, K., Germann, P., 1982. Macropores and water flow in soils. Water Resources Research 18, 1311-1325.

Brady, N.C., 1974. The nature and properties of soils. 10th ed. MacMillan, New York.

Cozzarelli, I.M., Herman, J.S., Parnell, R.A., 1987. The mobilization of aluminum in a natural soil system: effects of hydrologic pathways. Water Resources Research 23, 859-874.

Cronan, C. S., Grigal, D.F., 1995. Use of calcium/aluminum ratios as indicators of stress in forest ecosystems. Journal of Environmental Quality 24, 209-226.

Department of Conservation and Natural Resources, Pennsylvania Bureau of Topographic and Geologic Survey, 2001. Bedrock Geology of Pennsylvania. Harrisburg, Pennsylvania.

DeHayes, D.H., 1992. Winter injury and developmental cold tolerance in red spruce. pp. 296-337. *In* Eagar, C., Adams, M.B. (eds.) The Ecology and Decline of Red Spruce in the Eastern United States. Springer-Verlag. New York.

DeHayes, D.H., Schaberg, P.G., Hawley, G.J., Strimbeck, G.R., 1999. Acid rain impacts on calcium nutrition and forest health. BioScience 49, 789-800.

Dickson, W., Brodin, Y.-W., 1995. Strategies and methods for freshwater liming. pp.81-124. Chapter 4. *In* Henrikson, L., Brodin, Y.-W. (eds.) Liming of acidified surface waters. Springer-Verlag, Berlin.

Driscoll, C.T., Driscoll, K.M., Mitchell, M.J., Raynal, D.J., 2003. Effects of acidic deposition on forest and aquatic ecosystems in New York State. Environmental Pollution 123, 327-336.

Driscoll, C.T., Lawrence, G.B., Bulger, A.J., Butler, T.J., Cronan, C.S., Eager, C., Lambert,

K.F., Likens, G.E., Stoddard, J.L., Weathers, K.C., 2001. Acidic deposition in the Northeastern US: Sources and inputs, ecosystem effects, and management strategies. BioScience 51, 180–198.

Drohan, P.J., Stout, S.L., Petersen, G.W., 2002. Sugar maple (*Acer saccharum* Marsh.) decline during 1979-1989 in northern Pennsylvania. Forest Ecology and Management 170, 1-17.

Earle, J., Callaghan, T., 1998. Effects of mine drainage on aquatic life, water uses, and man-made structure. Chapter 4. pp.1-10. *In* Coal Mine Drainage Prediction and Pollution prevention in Pennsylvania. Pennsylvania Department of Environmental Protection, Harrisburg, PA, 10 pp.

Eaton, A.D., Clesceri, L.S., Greenberg, A.E., 1998. Standard Methods for the Examination of Water and Wastewater, 20th edition, American Public Health Association (APHA), American Water Works Association (AWWA), Water Environment Federation (WEF). 1200 pp.

Eckert, D., Sims, J.T., 1995. Recommended soil pH and lime requirement tests. pp. 11-16. *In* Sims, J.T., Wolf, A. (eds.) Recommended soil testing procedures for the Northeastern United States. Northeast Regional Bulletin #493. Agricultural Experiment Station, University of Delaware, Newark, DE.

EMEP (Environmental Monitoring, Evaluation, and Protection Program), 2005. Assessment of extent to which intensively studied lakes are representative of the Adirondack Mountain region. New York State Energy Research and Development Authority. Project update, August 2005, New York.

Geary, R.J., Driscoll, C.T., 1996. Forest soil solutions: Acid/base chemistry and response to calcite treatment. Biogeochemistry 32, 195-220.

Green, R.H., 1979. Sampling Design and Statistical Methods for Environmental Biologists, Wiley, New York.

Haines, T.A., Baker, J.P., 1986. Evidence of fish population response to acidification in the Eastern United States. Water, Air, and Soil Pollution 31, 659-629.

Hindar, A., Henriksen, A., 1992. Acidification trends, liming strategy and effects of liming for Vikedalselva, a Norwegian salmon river. Vatten 48, 54-58.

Hindar, A., Wright. R.F., Nilsen, P., Larssen, T., Høgberget, R., 2003. Effects on stream water chemistry and forest vitality after whole-catchment application of dolomite to a forest ecosystem in southern Norway. Forest Ecology and Management 180, 509-525.

Hosley, S.B., Long, R.P., Bailey, S.W., Hallett, R.A., Hall, T.J., 2000. Factors associated with the decline-disease of sugar maple on the Allegheny Plateau. Canadian Journal of Forest Research 30, 1365-1378.

Ingerslev, M. 1997. Effects of liming and fertilization on growth, soil chemistry and soil water chemistry in a Norway spruce plantation on a nutrient-poor soil in Denmark. Forest Ecology and Management 92, 55-66.

Jardine, P.M., Wilson, G.V., Luxmore, R.J., McCarthy, J.F., 1989. Transport of inorganic and natural organic tracers through an isolated pedon in a forest watershed. Soil Science Society of America Journal 53, 317-323.

Johnson, A.H., Siccama, T.G., 1983. Acid deposition and forest decline. Environmental Science and Technology 17, 294A-305A.

Joslin, J.D., Mays, P.A., Wolfe, M.H., Kelly, J.M., Garber, R.W., Brewer, P.F., 1987. Chemistry of tension lysimeter water and lateral flow in spruce and hardwood stands. Journal of Environmental Quality 16, 152-160.

Marshner, B., Stahr, K., Renger, M.Z., 1992. Lime effects on pine forest floor leachate chemistry and element fluxes. Journal of Environmental Quality 21, 410-419.

McDonald, T., Erickson, W.P., McDonald, L.L., 2000. Analysis of count data from Before-After Control-Impact Studies. Journal of Agricultural, Biological, and Environmental Statistics 5, 262-279.

Mehlich, A., 1976. New buffer pH method for rapid estimation of exchangeable acidity and lime requirement of soils. Communications in Soil Science and Plant Analysis 7, 637-652.

Minitab, 2003. Minitab for Windows, (Release 14.1). Minitab Inc., State College, PA.

Mitchell, M.J., McGee, G.., McHale, P., Weathers, K.C., 2001. Experimental design and instrumentation for analyzing solute concentrations and fluxes for quantifying biogeochemical processes in watersheds. The 4th International Conference on Long Term Ecological Research (LTER) in East Asian and Pacific Region Lake Hovsgol, Mongolia.

Mosley, M.P., 1979. Streamflow generation in a forested watershed, New Zealand. Water Resources Research 15, 795-806.

Mosley, M.P., 1982. Subsurface flow velocities through selected forest soils, South Island, New Zealand. Journal of Hydrology 55, 65-92.

Pearce, A.J., 1990. Streamflow generation processes. An Austral view. Water Resources Research 26, 3037-3047.

Ross, D., 1995. Recommended soil tests for determining soil cation exchange capacity. pp. 62-69. *In* Sims, J.T., Wolf, A. (eds.) Recommended soil testing procedures for the Northeastern United States. Northeast Regional Bulletin #493. Agricultural Experiment Station, University of Delaware, Newark, DE.

Sharpe, W.E., Sunderland, T.L., 1995. Acid-base status of upper rooting zone in declining and nondeclining sugar maple (*Acer saccharum* Marsh) stands in Pennsylvania. Pp. 172-178. *In* Gottschal, K.W., Fosbroke, S.L.C. (eds.) Proceedings of the Tenth Central Hardwood Forest Conference. U. S. Department of Agriculture, Forest Service General Technical Report NE-197.

Shuford, J.W., Fritton, D.D., Baker, D.E., 1977. Nitrate-nitrogen and chloride movement through undisturbed field soil. Journal of Environmental Quality 6, 255-259.

Skalski, J.R., Robson, D.S., 1992. Techniques for Wildlife Investigations, Design and Analysis of Capture Data, New York: Academic.

Swistock, B.R., Yamona, J.J., DeWalle, D.R., Sharpe, W.E., 1990. Comparison of soil water chemistry and sample size requirements for pan vs. tension lysimeters. Water, Air, and Soil Pollution 50, 387-396.

U.S. Department of Agriculture, Natural Resources Conservation Service, 2005. Soil Survey Geographic (SSURGO) database for Clearfield County, Pennsylvania. Fort Worth, Texas.

Weyman, D.R., 1970. Throughflow on hillslopes and its relation to the stream hydrograph. Bulletin of the International Association of Scientific Hydrology 15, 25-33.

Whipkey, R.Z., 1965. Subsurface stormflow on forested slopes. Bulletin of the International Association of Scientific Hydrology 10, 74-85.

Wolf, A.M., Beegle, D.B., 1995. Recommended soil tests for macronutrients: phosphorus, potassium, calcium, and magnesium. pp. 25-34. *In* Sims, J.T., Wolf, A. (eds.) Recommended soil testing procedures for the Northeastern United States. Northeast Regional Bulletin #493. Agricultural Experiment Station, University of Delaware, Newark, DE.

Table 2.1. Total monthly precipitation of climate normal (1971-2000) at the Clarence NCDC climate station (elevation 423.7m, 41°03'N / 77°57'W).

Month	**Precipitation (mm)**
January	71.4
February	67.6
March	86.1
April	80.8
May	91.9
June	117.1
July	110.5
August	91.2
September	101.6
October	80.0
November	85.6
December	72.4
Total	1056.1

Table 2.2. Soil information of the Mosquito Creek study watersheds (modified from U.S. Department of Agriculture, Natural Resources Conservation Services, 2005).

Mapping Unit	Soil Description	Erodibility
ClB	Clymer channery loam, 3 to 8 percent slopes	Potentially highly erodible land
CmB	Clymer very stony loam, 0 to 8 percent slopes	Potentially highly erodible land
CmC	Clymer very stony loam, 8 to 15 percent slopes	Potentially highly erodible land
CoB	Cookport channery loam, 3 to 8 percent slopes	Potentially highly erodible land
CoC	Cookport channery loam, 8 to 15 percent slopes	Highly erodible land
CxB	Cookport very stony loam, 0 to 8 percent slopes	Potentially highly erodible land
CxD	Cookport very stony loam, 8 to 25 percent slopes	Highly erodible land
DxB	Dekalb very stony loam, 0 to 8 percent slopes	Potentially highly erodible land
HbD	Hazleton very stony loam, 8 to 25 percent slopes	Highly erodible land
HbF	Hazleton very stony loam, 25 to 80 percent slopes	Highly erodible land
HcB	Hazleton-Clymer channery loams, 3 to 8 percent slopes	Potentially highly erodible land
HcC	Hazleton-Clymer channery loams, 8 to 15 percent slopes	Potentially highly erodible land
HdB	Hazleton-Clymer very stony loams, 0 to 8 percent slopes	Potentially highly erodible land
Ru	Rubble land-Dystrochrepts complex	Potentially highly erodible land

Table 2.3. Bedrock information of the Mosquito Creek study watersheds (modified from Department of Conservation and Natural Resources, Pennsylvania Bureau of Topographic Geologic Survey, 2001).

Name	Age	LITH1	LITH2	LITH3
Allegheny Formation	Pennsylvanian	Sandstone	Shale	Limestone; Clay; Coal
Pottsville Formation	Pennsylvanian	Sandstone	Conglomerate	Shale; siltstone; claystone; limestone; coal
Burgoon Sandstone	Mississippian	Sandstone	Conglomerate	Shale; coal
Huntley Mountain Formation	Mississippian and Devonian	Sandstone	Siltstone	Shale

where 1) Name is the geologic unit in the explanation of the 1980 state geologic map (Berg and others, 1980), 2) Age is at the level of a geologic period which indicates the geologic age, 3) LITH1 is the dominant lithology, volumetrically, in the rock unit, 4) LITH2 is the second most dominant lithology, volumetrically, in the rock unit, and 5) LITH3 is other major lithologies, volumetrically, in the rock unit.

Table 2.4. Particle-size distribution of coarse-grained limestone sands on the entire watershed application in fall 2003 and 2004 and soil plot application in summer 2005.

Particle size fraction	Limestone sand (% total weight)	
	Watershed application	Plot application
	2003 and 2004	2005
> 4.75 mm	3.19	3.43
> 3.35 mm	10.06	13.66
> 2 mm	25.61	25.83
>1.0 mm	21.62	23.98
> 500 μm	14.83	13.68
> 250 μm	9.20	6.42
>125 μm	6.25	4.27
> 88 μm	0.48	1.04
> 63 μm	5.51	3.85
< 63 μm	3.25	3.84
Total	100.00	100.00

Table 2.5. Spectrochemical analysis of the limestone sand over the watershed application in fall 2003 and 2004 and soil plot application in summer 2005.

	Limestone sand (% total weight)	
	Watershed application	**Plot application**
	2003 and 2004	**2005**
Loss on Ignition	41.70	40.70
CaO	26.00	27.40
MgO	16.40	18.00
SiO_2	8.04	9.76
Al_2O_3	1.25	1.53
K_2O	0.89	1.00
Fe_2O_3	0.54	0.68
MnO	0.02	<0.05
BaO	0.01	0.01
TiO_2	0.06	0.07
Na_2O	< 0.005	< 0.05
SrO	< 0.005	< 0.05
Total	94.9	99.2

Table 2.6. Total monthly precipitation and daily average temperature during the study period (2003-2005) at the Clarence NCDC climate station (elevation 423.7 m, 41°03'N / 77°57'W).

	Precipitation (mm)			Daily average temperature (°C)		
Month	**2003**	**2004**	**2005**	**2003**	**2004**	**2005**
January	67.3	98.0	152.9	-8.5	-7.8	-4.6
February	95.5	69.6	82.8	-6.2	-6.0	-2.8
March	72.1	90.9	84.8	0.6	2.1	-2.2
April	77.0	125.0	60.2	5.9	7.1	7.3
May	137.2	177.3	42.9	12.6	16.3	9.8
June	106.9	93.0	54.6	15.4	16.6	18.8
July	204.5	231.9	45.2	17.4	19.1	20.7
August	156.7	93.7	82.6	19.5	18.8	19.9
September	229.4	280.7	50.8	14.5	16.4	16.7
October	89.4	91.9	158.0	7.5	8.9	10.1
November	129.5	71.1	160.5	5.8	4.8	4.5
December	137.7	87.4	68.1	-2.1	-1.8	-4.9

Table 2.7. Chemical characteristics of the mineral A horizon both prior to and post dolomitic limestone sand application at the Mosquito Creek watersheds in 2005. Standard deviations from the mean are shown in parentheses and an asterisk indicates significant difference after liming at $\alpha \leq 0.05$ compared to before liming.

		Treatment				**Control**	
		Laurel		**90 Degree**		**Merrill**	
Parameter		Before	After	Before	After	Before	After
	pH	3.69 (0.20)	3.91 (0.30)	3.69 (0.19)	4.28 (0.58)*	3.54 (0.18)	3.46 (0.13)
		p= 0.567		p = 0.002		p= 0.979	
	P	30.89 (7.62)	26.44 (6.23)	26 (5.74)	22.22 (7.97)	27.11 (6.57)	37.78 (9.02)
		p=0.813		p=0.640		p=0.085	
	% Base Saturation	13.52 (3.48)	17.9 (6.95)	17.02 (4.49)	26.57 (12.49)	13.80 (1.65)	8.44 (3.01)*
		p=0.647		p=0.255		p=0.019	
exchangeable cations (meq/100g)	Acidity	23.23 (2.87)	18.97 (3.36)*	27.17 (3.09)	18.77 (3.17)*	27.70 (3.51)	22.97 (2.38)
		p=0.034		p=0.000		p=0.088	
	K	0.433 (0.12)	0.322 (0.10)	0.33 (0.13)	0.23 (0.07)	0.30 (0.07)	0.23 (0.07)
		p=0.392		p=0.233		p=0.535	
	Mg	0.48 (0.12)	1.4 (0.85)*	0.56 (0.14)	2.59 (1.66)*	0.47 (0.05)	0.29 (0.11)
		p=0.000		p=0.000		p=0.117	
	Ca	1.46 (0.54)	1.62 (0.77)	2.23 (0.85)	2.99 (1.81)	1.64 (0.32)	0.88 (0.42)*
		p=0.998		p=0.986		p=0.030	
	CEC	17.34 (0.70)	18.08 (1.96)	18.11 (1.00)	20.61 (3.03)*	17.43 (0.33)	16.41 (0.56)
		p=0.926		p=0.030		p=0.607	
% saturation of the CEC	K	2.41 (0.61)	1.77 (0.41)	1.86 (0.60)	1.23 (0.28)*	1.74 (0.36)	1.52 (0.44)
		p=0.185		p=0.044		p=0.851	
	Mg	2.72 (0.66)	7.28 (3.78)*	2.99 (0.75)	11.82 (6.00)*	2.74 (0.29)	1.70 (0.56)*
		p=0.000		p=0.000		p=0.052	
	Ca	8.29 (2.82)	8.62 (3.25)	12.18 (3.73)	13.64 (6.58)	9.41 (1.76)	5.31 (2.46)*
		p=1.000		p=1.000		p=0.018	

Table 2.8. Mean soil solution chemistry at 30 cm depth collected by tension lysimeters on treatment and control plots before and after dolomitic limestone application in 2005. Standard deviations from the mean are shown in parentheses and an asterisk indicates significant difference after liming at $\alpha \leq 0.05$ compared to before liming.

	Treatment				**Control**	
	Laurel		**90 Degree**		**Merrill**	
Parameter	Before	After	Before	After	Before	After
pH	4.99 (0.22)	5.24 (0.26)	5.20 (0.15)	5.60 (0.20)*	5.22 (0.11)	5.23 (0.12)
	p= 0.168		p = 0.003		p= 1.000	
Calcium (µmol/L)	19.11 (6.09)	33.37 (9.06)*	25.17 (4.72)	44.66 (11.35)*	25.45 (2.64)	27.34 (4.78)
	p= 0.009		p = 0.000		p= 0.992	
Aluminum (µmol/L)	16.17 (9.22)	13.77 (8.74)	15.67 (4.03)	13.61 (4.77)	4.751 (0.991)	8.35 (2.76)
	p=0.978		p=0.970		p=0.782	
Magnesium (µmol/L)	15.51 (4.22)	28.59 (7.99)	23.12 (4.48)	59.97 (20.70)*	18.39 (2.26)	19.22 (3.64)
	p= 0.180		p = 0.000		p= 1.000	
Conductivity (µS/cm)	25.41 (3.38)	29.18 (2.92)	23.37 (1.49)	32.04 (7.27)*	24.71 (1.89)	24.47 (3.30)
	p= 0.549		p = 0.000		p= 1.000	
ANC (µeq/L)	-1.56 (8.35)	23.47 (17.12)*	10.72 (4.51)	55.80 (27.20)*	4.74 (7.18)	13.12 (4.94)
	p= 0.014		p = 0.000		p= 0.665	
Ca/Al	1.78 (1.33)	2.97 (1.63)	1.74 (0.72)	3.51 (1.14)	5.66 (1.76)	3.58 (1.32) *
	p= 0.653		p = 0.079		p= 0.0313	

Table 2.9. Mean soil solution chemistry at 80 cm depth collected by tension lysimeters on treatment and control plots before and after dolomitic limestone application in 2005. Standard deviations from the mean are shown in parentheses and an asterisk indicates significant difference after liming at $\alpha \leq 0.05$ compared to before liming.

	Treatment				**Control**	
	Laurel		**90 Degree**		**Merrill**	
Parameter	Before	After	Before	After	Before	After
pH	5.29 (0.55)	5.56 (0.56)	5.03 (0.17)	5.28 (0.32)	5.01 (0.12)	5.16 (0.29)
	p= 0.718		p = 0.694		p= 0.953	
Calcium (μmol/L)	14.60 (6.06)	30.15 (16.33)*	23.83 (5.67)	27.45 (7.79)	19.49 (1.69)	23.73 (3.09)
	p=0.002		p=0.902		p=0.824	
Aluminum (μmol/L)	15.12 (7.15)	16.59 (12.46)	10.78 (3.26)	6.08 (1.79)	6.74 (9.24)	3.94 (1.76)
	p=0.998		p=0.696		p=0.953	
Magnesium (μmol/L)	27.40 (6.26)	38.81 (7.58)	23.70 (4.88)	34.56 (19.94)	16.54 (2.05)	17.85 (3.87)
	p=0.407		p=0.421		p=0.998	
Conductivity (μS/cm)	26.28 (2.16)	27.55 (3.86)	31.52 (4.08)	31.93 (11.12)	26.59 (2.98)	23.87 (1.43)
	p=0.997		p=1.000		p=0.874	
ANC (μeq/L)	10.03 (15.20)	58.1 (49.0)*	0.09 (12.55)	35.7 (60.9)	-8.43 (15.25)	1.94 (11.22)
	p=0.051		p=0.181		p=0.984	
Ca/Al	1.39 (1.13)	3.86 (4.00)	2.33 (0.72)	4.88 (2.11)	5.23 (2.62)	7.39 (3.75)
	p=0.407		p=0.282		p=0.461	

Table 2.10. Mean soil solution chemistry at 30 cm depth collected by zero-tension lysimeters on treatment and control plots before and after dolomitic limestone application in 2005. Standard deviations from the mean are shown in parentheses and an asterisk indicates significant difference after liming at $\alpha \leq 0.05$ compared to before liming.

	Treatment				**Control**	
	Laurel		**90 Degree**		**Merrill**	
Parameter	Before	After	Before	After	Before	After
pH	4.72 (0.24)	4.97 (0.30)	5.02 (0.13)	5.95 (0.69)*	5.02 (0.11)	4.87 (0.23)
	p= 0.891		p = 0.007		p= 0.996	
Calcium (μmol/L)	13.22 (4.78)	270 (280)*	12.48 (2.74)	99.1 (50.6)	8.86 (2.65)	17.47 (5.12)
	p=0.007		p=0.736		p=1.000	
Aluminum (μmol/L)	23.79 (14.15)	56.63 (19.28)	22.40 (12.03)	17.32 (6.61)*	6.41 (3.93)	13.22 (7.45)
	p=0.229		p=0.007		p=1.000	
Magnesium (μmol/L)	12.58 (5.06)	269 (377)	7.20 (1.49)	108.4 (53.30)	4.11 (1.75)	8.23 (2.42)
	p=0.240		p=0.904		p=1.000	
Conductivity (μS/cm)	29.66 (8.90)	241.3 (179.8)*	30.31 (3.75)	81.9 (30.3)	22.43 (12.83)	32.50 (5.74)
	p=0.002		p=0.884		p=1.000	
ANC (μeq/L)	-17.36 (14.22)	136 (342)	23.0 (46.8)	472 (471)	-28.79	15.68 (8.68)
	p=0.964		p=0.321		p=1.000	
Ca/Al	0.69 (0.36)	4.35 (4.23)	0.71 (0.37)	6.74 (4.69)*	1.55 (0.54)	1.77 (1.02)
	p=0.229		p=0.007		p=1.000	

Table 2.11. The chemical characteristics of streamwater draining the four watersheds both before and after liming. The SD indicates standard deviation, T indicates time, and an asterisk indicates a significant difference in means between treated and controlled watersheds at $\alpha \leq 0.05$.

		Before				**After**			
		Treatment		**Control**		**Treatment**		**Control**	
parameter		Laurel	90 Degree	Merrill	Tick	Laurel	90 Degree	Merrill	Tick
pH	mean	5.89	5.58	5.37	4.89	5.88	5.9	5.61	4.97
	SD	0.38	0.39	0.13	0.13	0.49	0.65	0.35	0.20
	treatment vs. control	p=0.295				p=0.045*			
	T* treatment vs. control	p=0.297				p=0.041*			
Calcium (µmol/L)	mean	43.17	45.11	32.73	28.59	42.96	49.85	32.34	24.80
	SD	9.80	5.28	5.22	1.96	12.82	23.32	5.51	2.59
	treatment vs. control	p=0.254				p=0.000*			
	T* treatment vs. control	p=0.251				p=0.000*			
Magnesium (µmol/L)	mean	-	-	-	-	39.50	44.44	30.95	26.40
	SD	-	-	-	-	10.66	19.95	5.77	2.32
	treatment vs. control	-				p=0.000*			
	T* treatment vs. control	-				p=0.000*			
Aluminum (µmol/L)	mean	1.18	2.73	2.31	4.15	1.37	2.34	2.09	3.45
	SD	0.71	1.29	0.48	1.76	1.44	1.52	1.58	1.91
	treatment vs. control	p=0.960				p=0.866			
	T* treatment vs. control	p=0.961				p=0.854			
Conductivity (µS/cm)	mean	26.54	27.04	21.68	24.70	25.91	28.53	21.78	23.19
	SD	3.37	3.18	3.51	2.20	4.69	7.67	2.69	1.86
	treatment vs. control	p=0.776				p=0.000*			
	T* treatment vs. control	p=0.779				p=0.000*			
Acid neutralizing capacity (µeq/L)	mean	23.12	0.85	-2.21	-17.08	39.90	36.90	1.98	-12.10
	SD	11.99	8.52	2.12	2.55	48.40	74.70	9.77	7.42
	treatment vs. control	p=0.679				p=0.000*			
	T* treatment vs. control	p=0.682				p=0.000*			

Figure 2.1. Mosquito Creek basin in northcentral Pennsylvania with location of Clarence weather station.

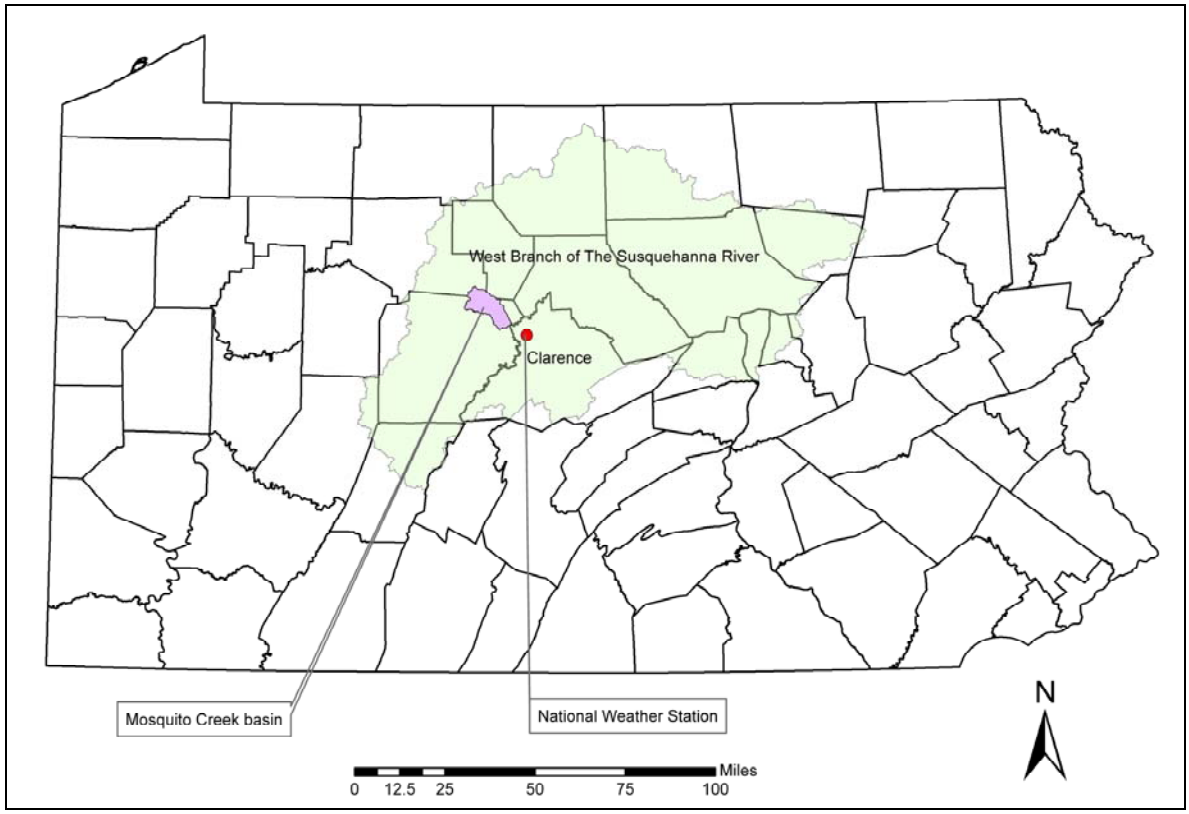

Figure 2.2. Locations of field data collection at the Mosquito Creek watersheds.

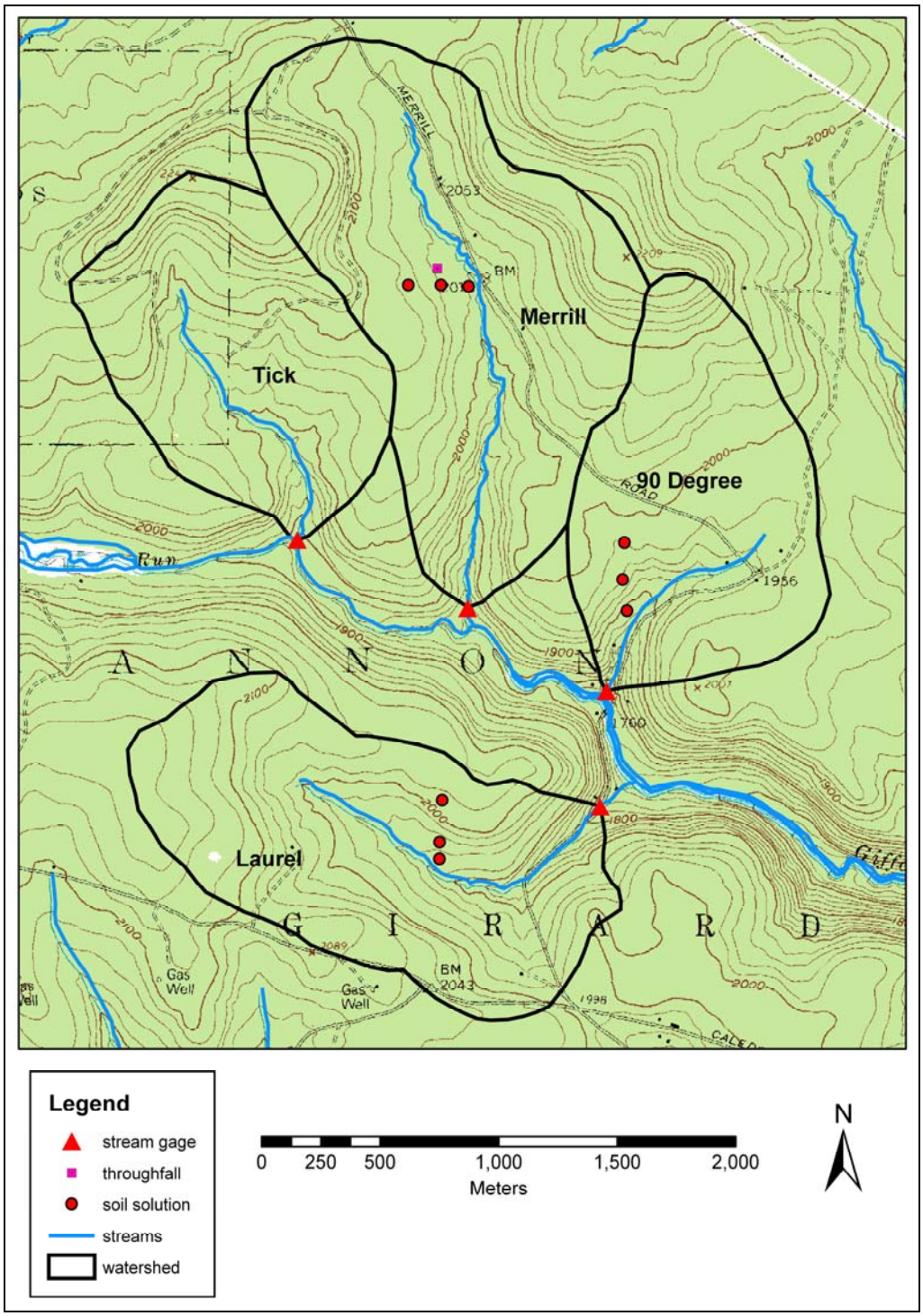

Figure 2.3. The characteristics of soil distribution at the Mosquito Creek watersheds (modified from U.S. Department of Agriculture, Natural Resources Conservation Services, 2005).

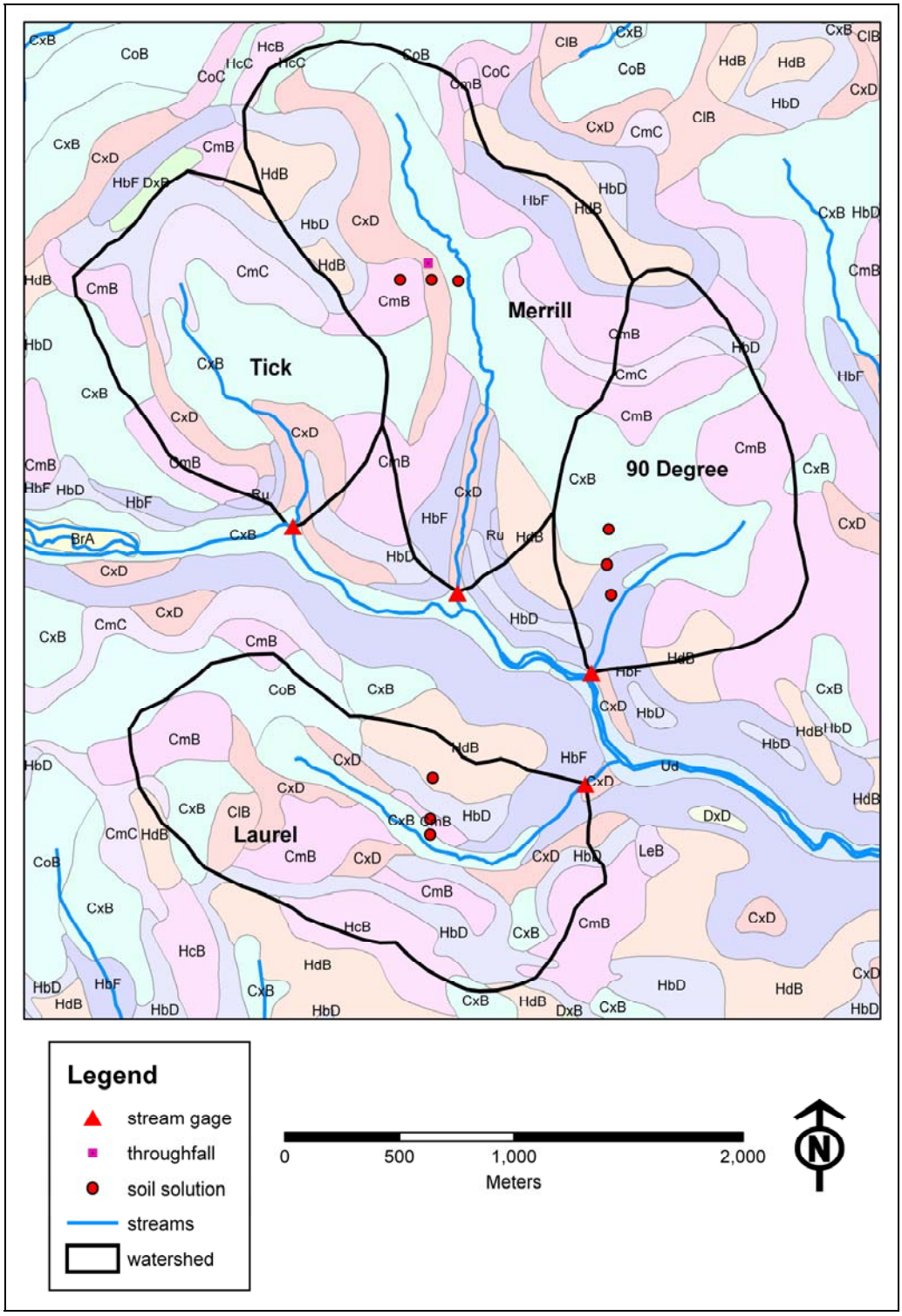

Figure 2.4. The characteristics of bedrock distribution at the Mosquito Creek watersheds (modified from Department of Conservation and Natural Resources, Pennsylvania Bureau of Topographic and Geologic Survey, 2001).

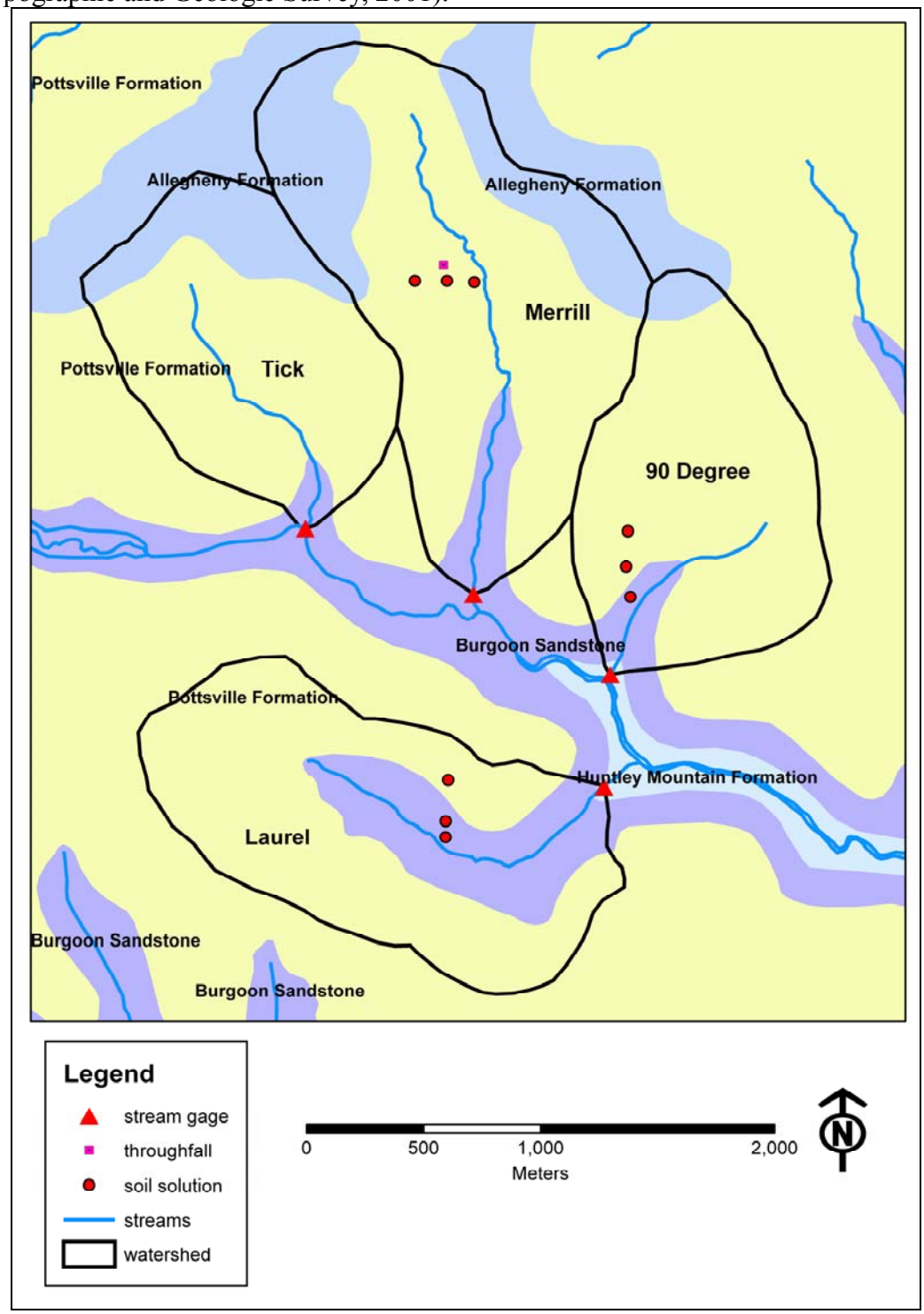

Figure 2.5. Design of soil solution sampling at the each soil plot.

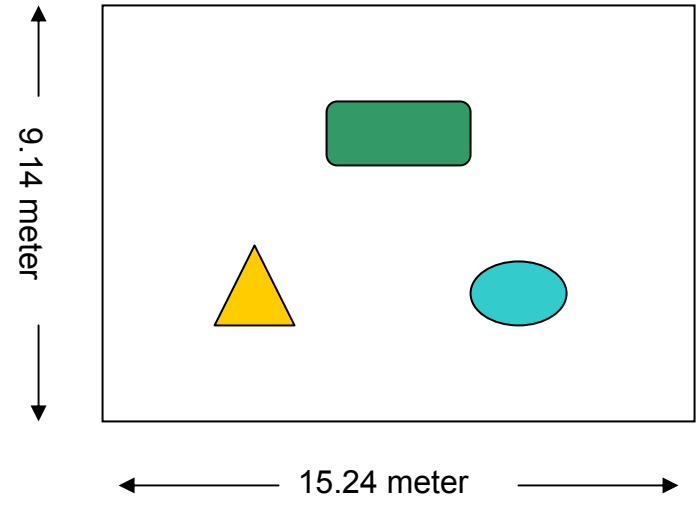

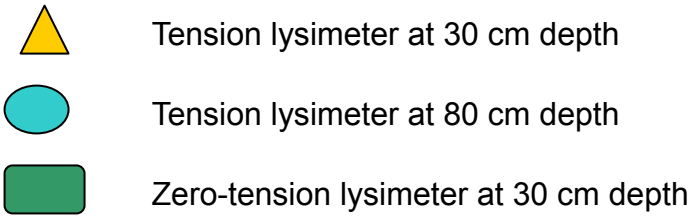

Figure 2.6. Monthly average, minimum, and maximum temperature and total monthly precipitation during the study period (July 2003-October 2005) at the Clarence NCDC climate station (elevation 423.7 m, 41°03'N / 77°57'W).

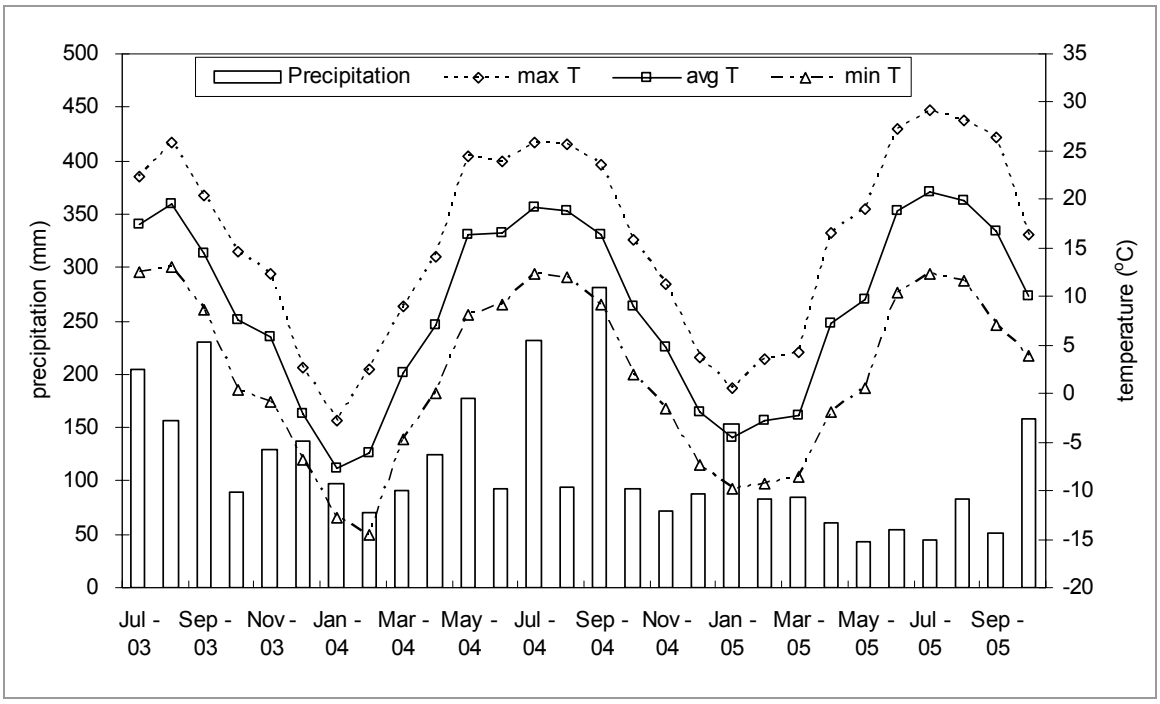

Figure 2.7. The pH of throughfall at the Mosquito Creek watersheds from April to October 2005.

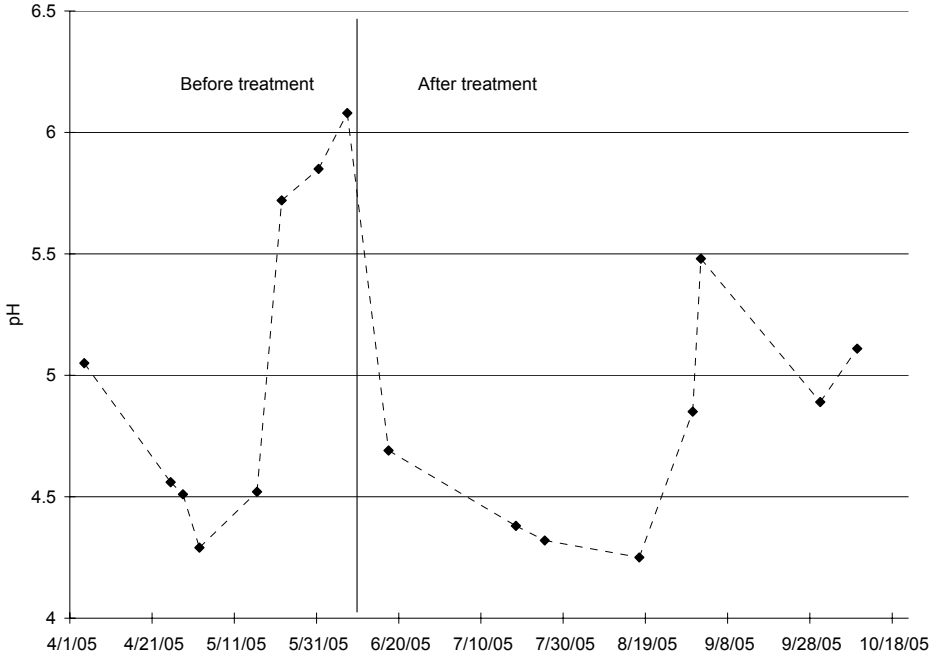

Figure 2.8. The calcium and magnesium concentrations in throughfall at the Mosquito Creek watersheds from April to October 2005.

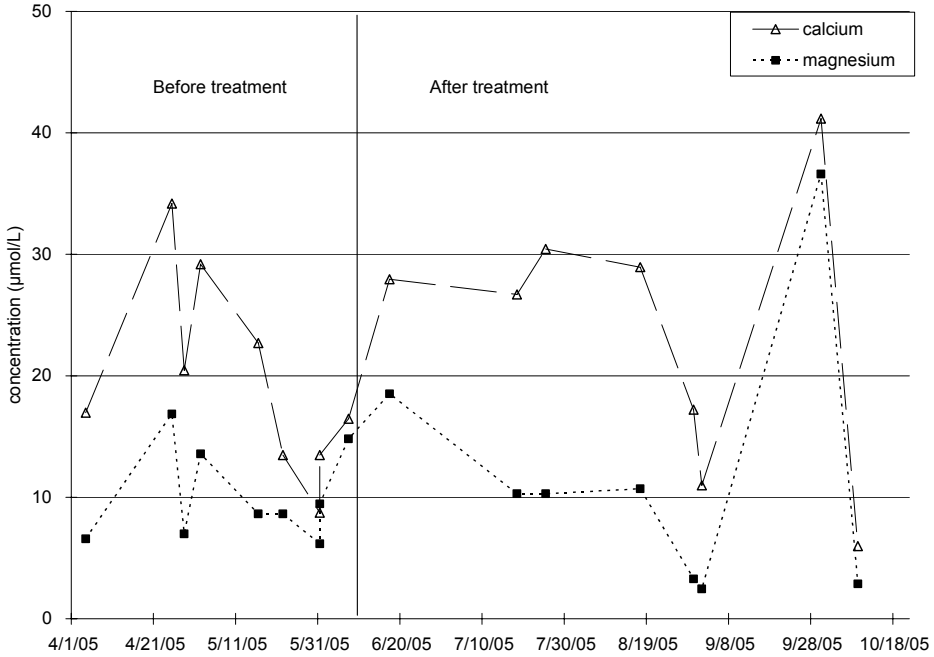

Figure 2.9. The aluminum concentration in throughfall at the Mosquito Creek watersheds from April to October 2005.

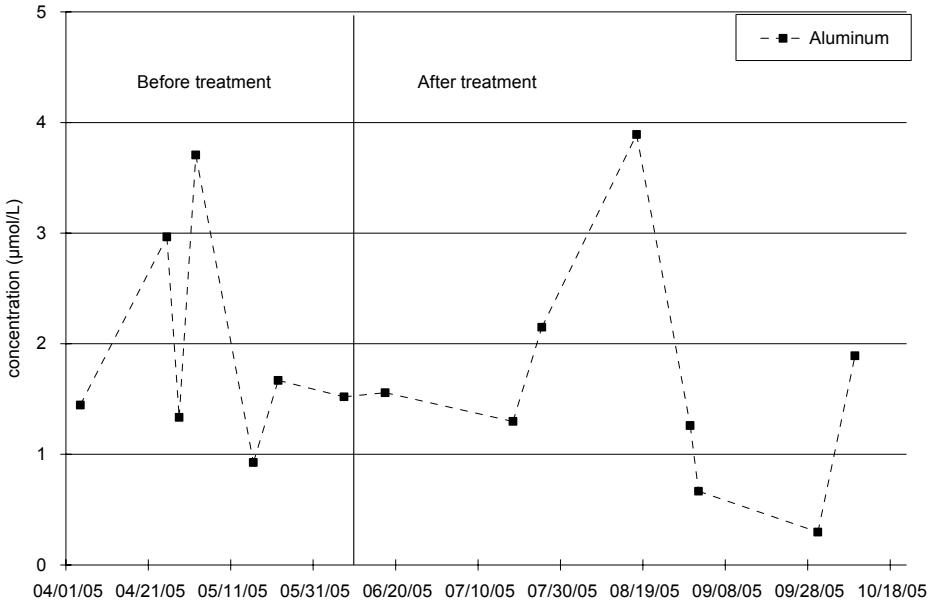

Figure 2.10. Mean exchangeable calcium and magnesium in the mineral A horizon before and after limestone sand application at the Mosquito Creek watershed in 2005

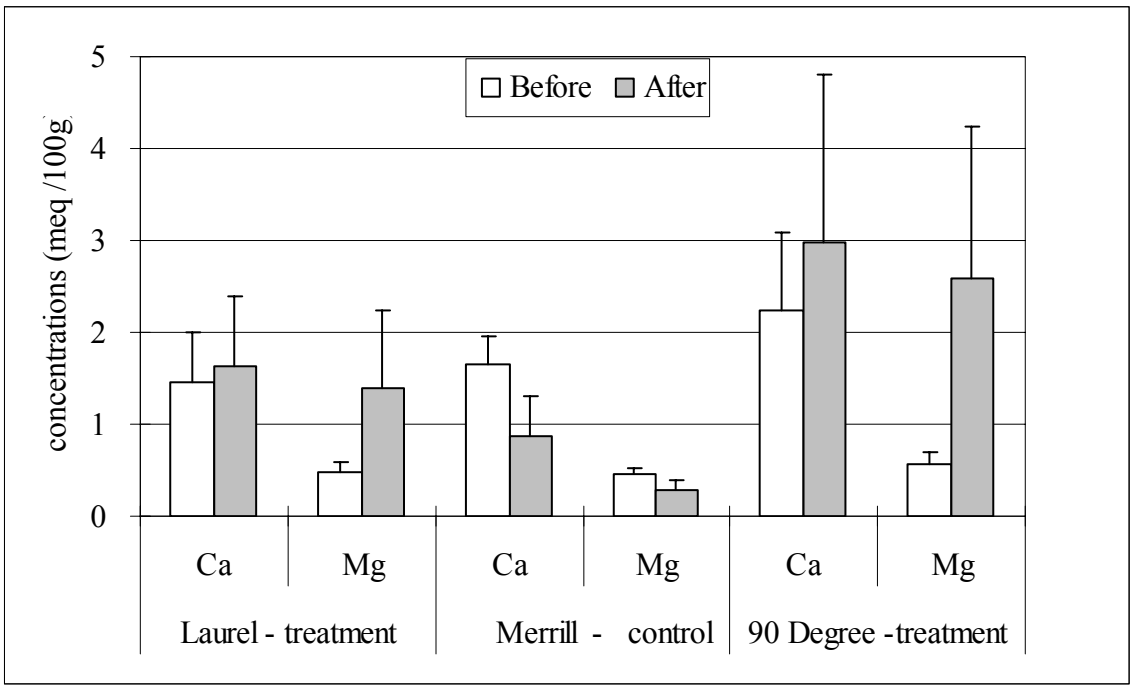

Figure 2.11. Mean pH in soil solution collected by tension lysimeter at 30 cm depth in 2005.

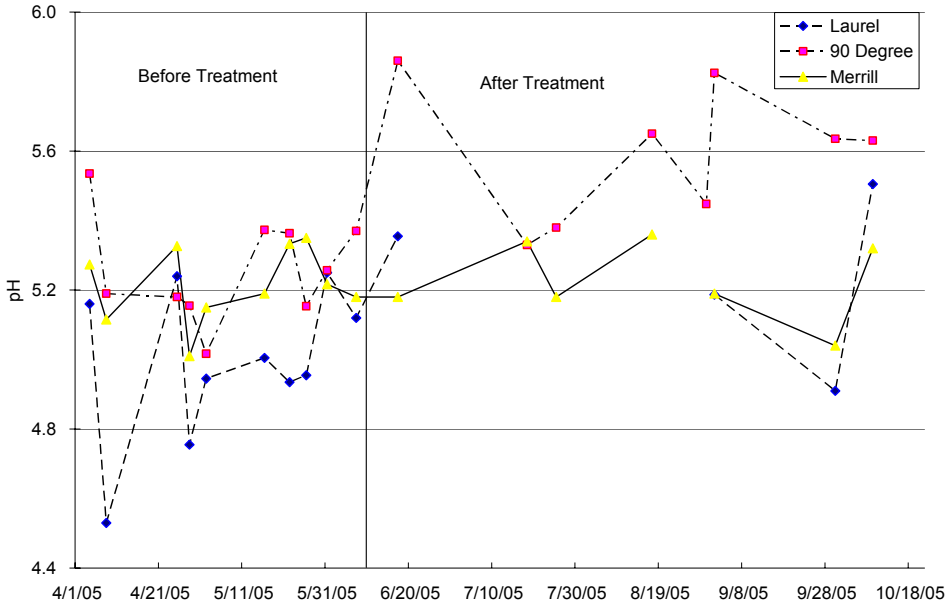

Figure 2.12. Mean calcium concentration in soil solution collected by tension lysimeter at 30 cm depth in 2005.

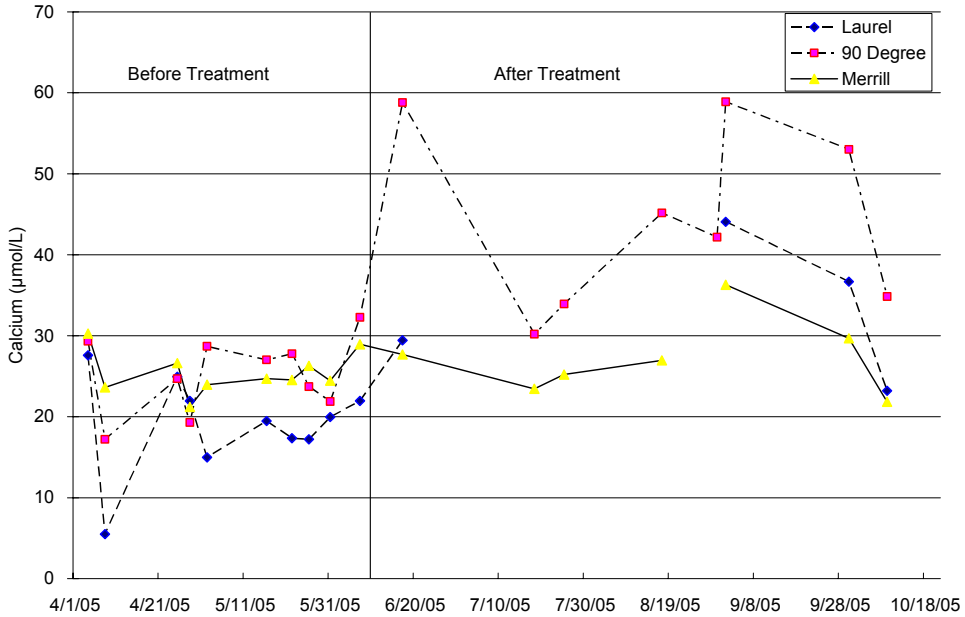

Figure 2.13. Mean magnesium concentration in soil solution collected by tension lysimeter at 30 cm depth in 2005.

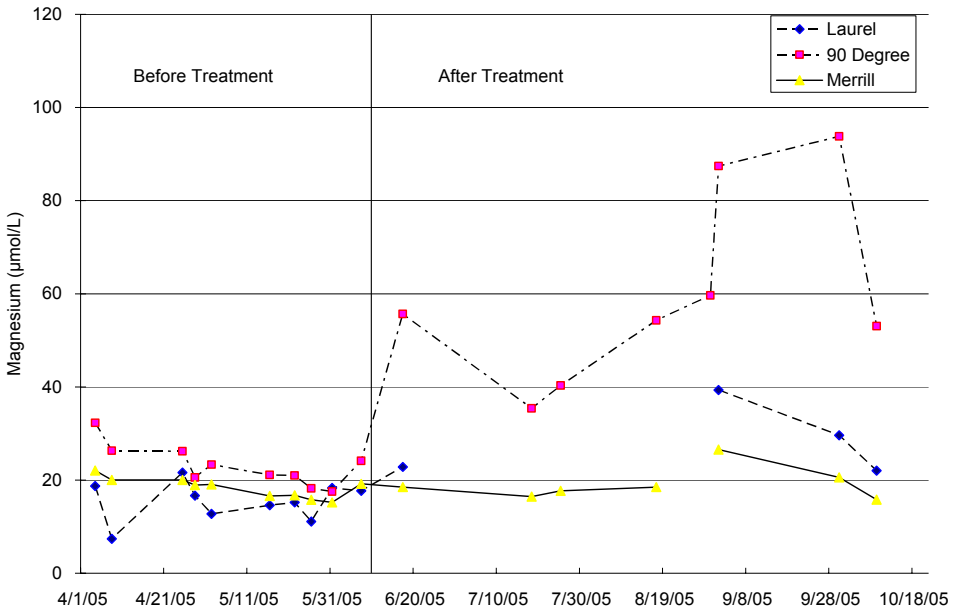

Figure 2.14. Mean aluminum concentration in soil solution collected by tension lysimeter at 30 cm depth in 2005.

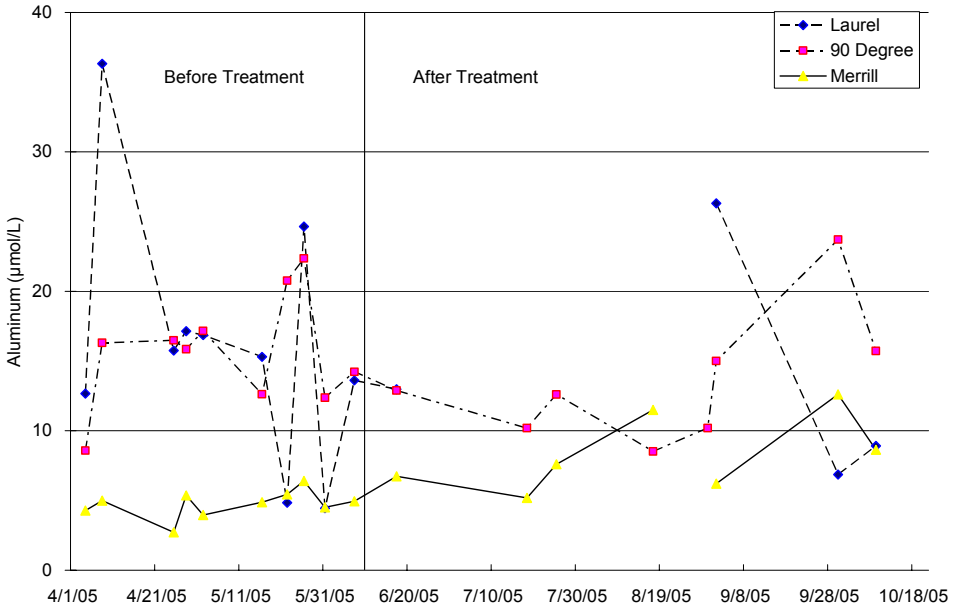

Figure 2.15. Mean conductivity in soil solution collected by tension lysimeter at 30 cm depth in 2005.

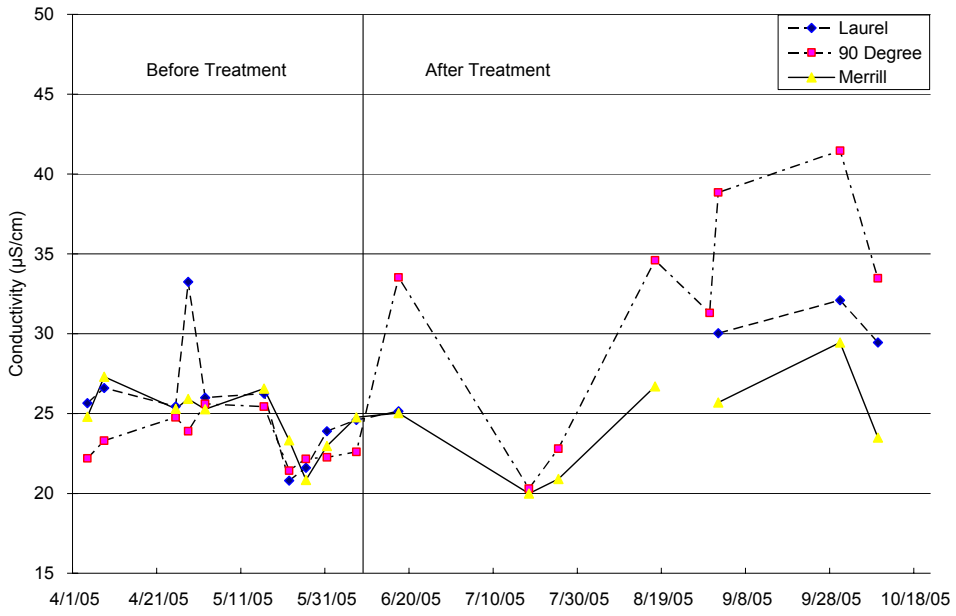

Figure 2.16. Mean ANC in soil solution collected by tension lysimeter at 30 cm depth in 2005.

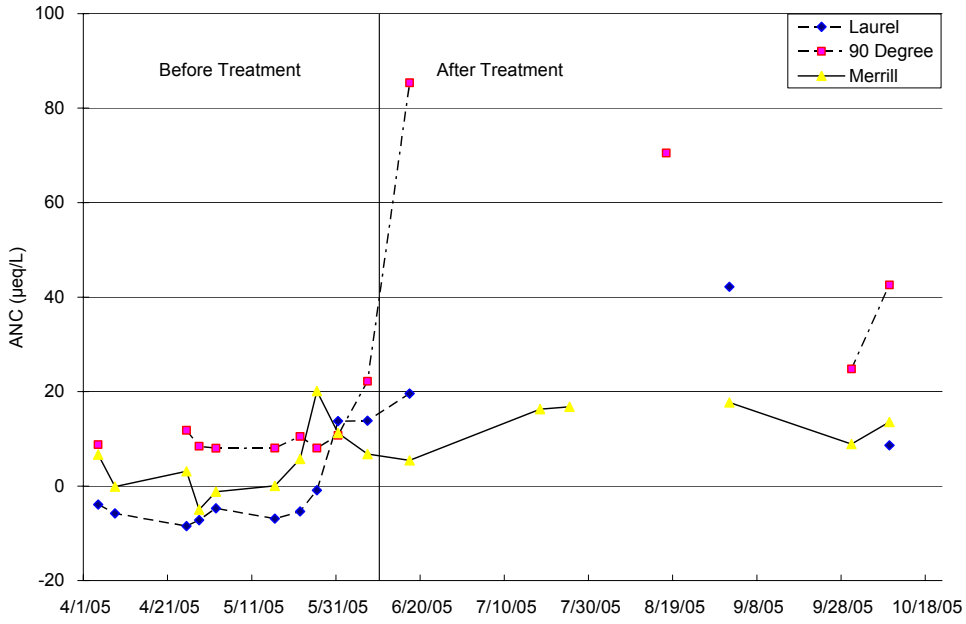

Figure 2.17. Mean calcium/aluminum molar ratio in soil solution collected by tension lysimeter at 30 cm depth in 2005.

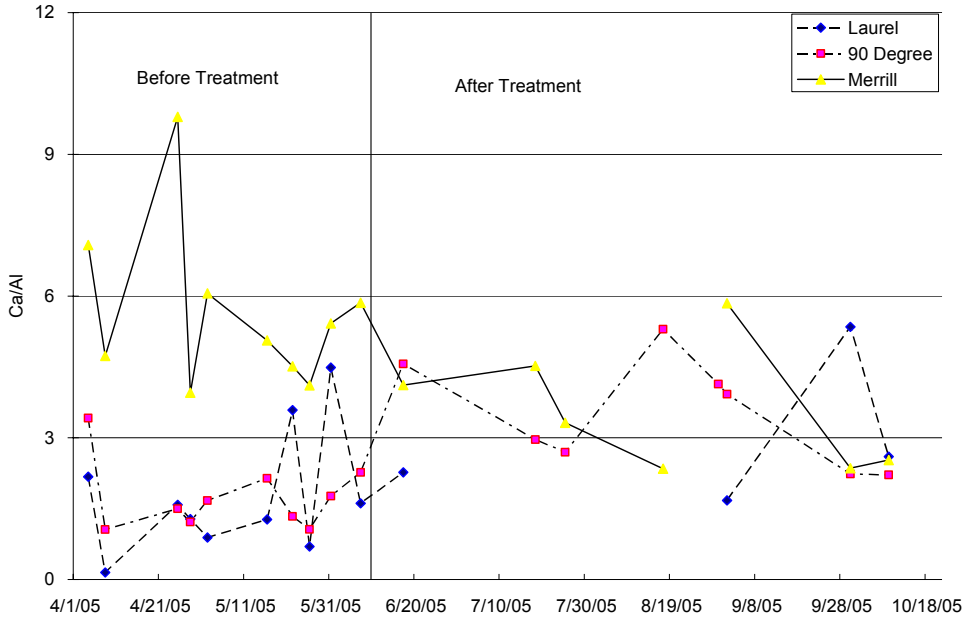

Figure 2.18. Mean pH in soil solution collected by tension lysimeter at 80 cm depth in 2005.

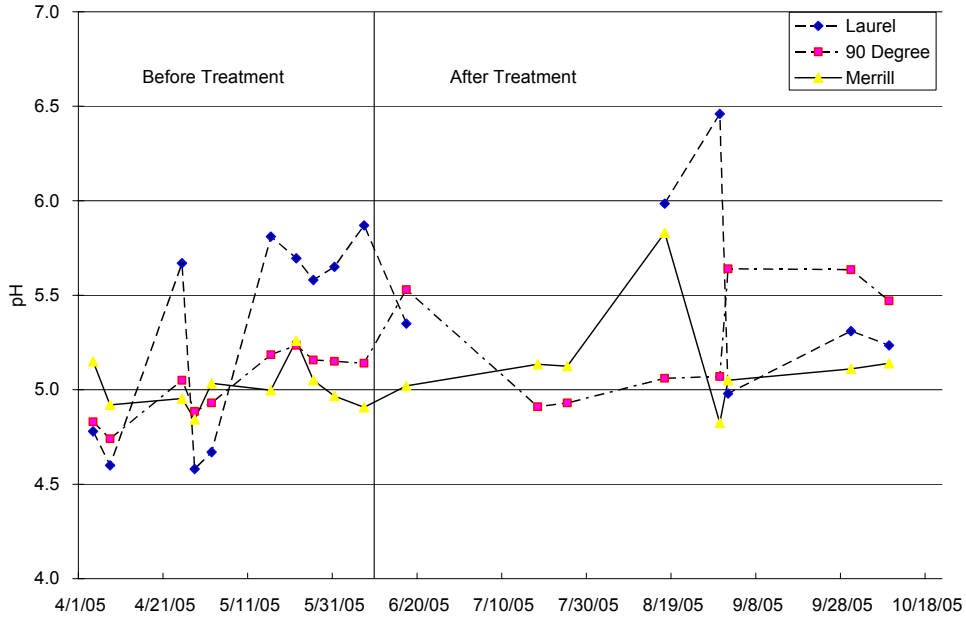

Figure 2.19. Mean calcium concentration of soil solution collected by tension lysimeter at 80 cm depth in 2005.

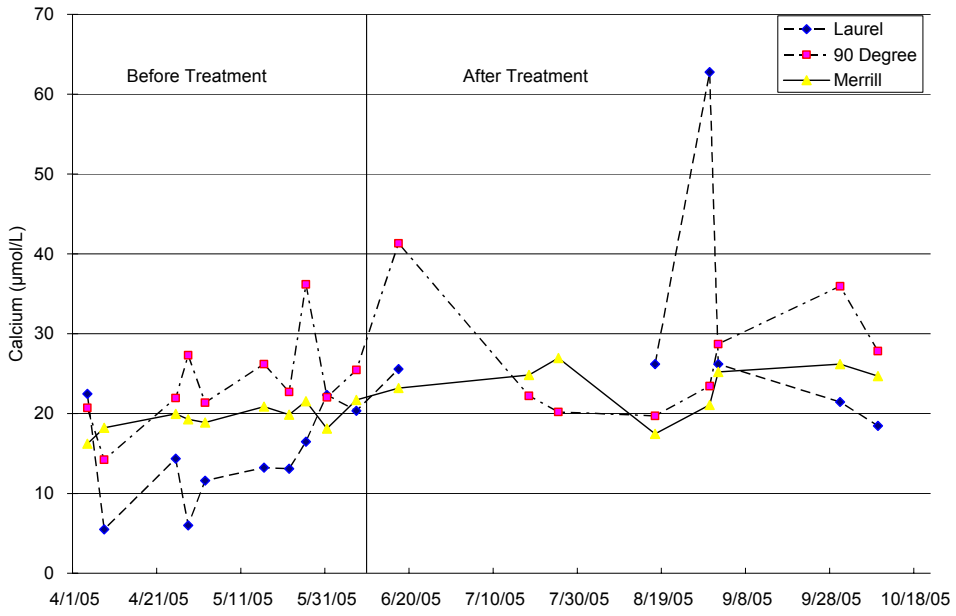

Figure 2.20. Mean magnesium concentration in soil solution collected by tension lysimeter at 80 cm depth in 2005.

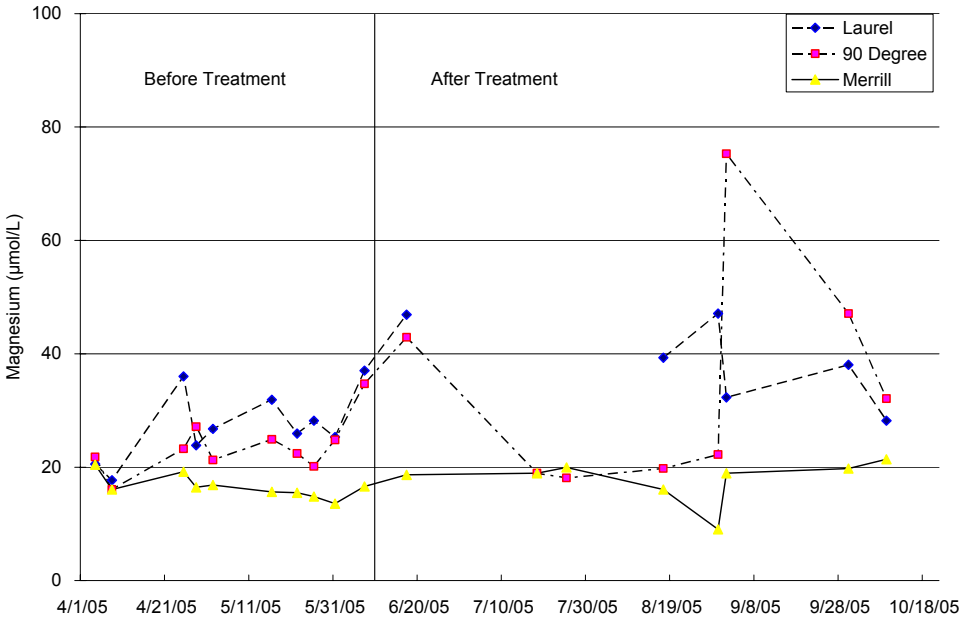

Figure 2.21. Mean aluminum concentration in soil solution collected by tension lysimeter at 80 cm depth in 2005.

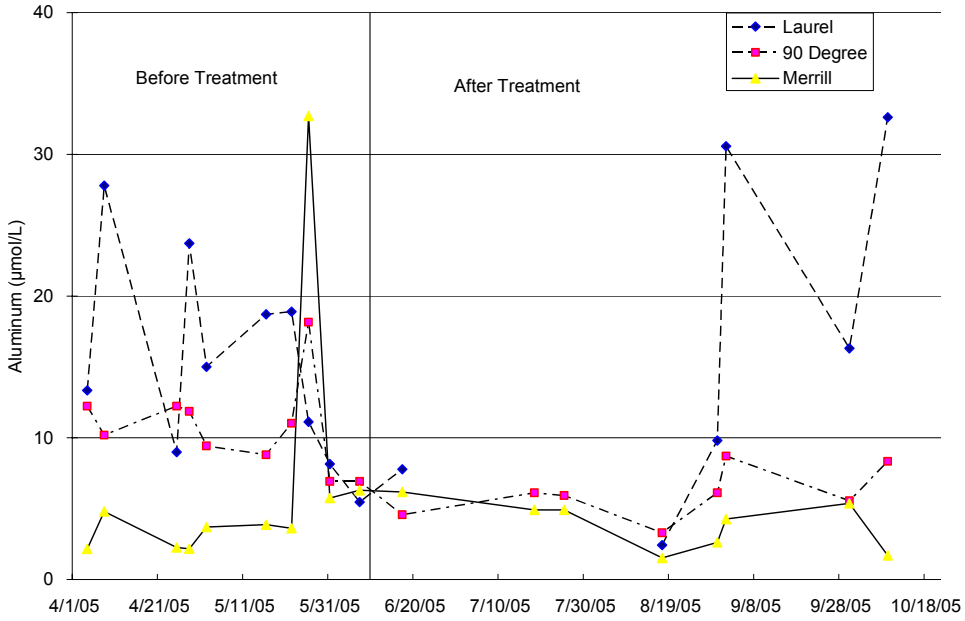

Figure 2.22. Mean conductivity in soil solution collected by tension lysimeter at 80 cm depth in 2005.

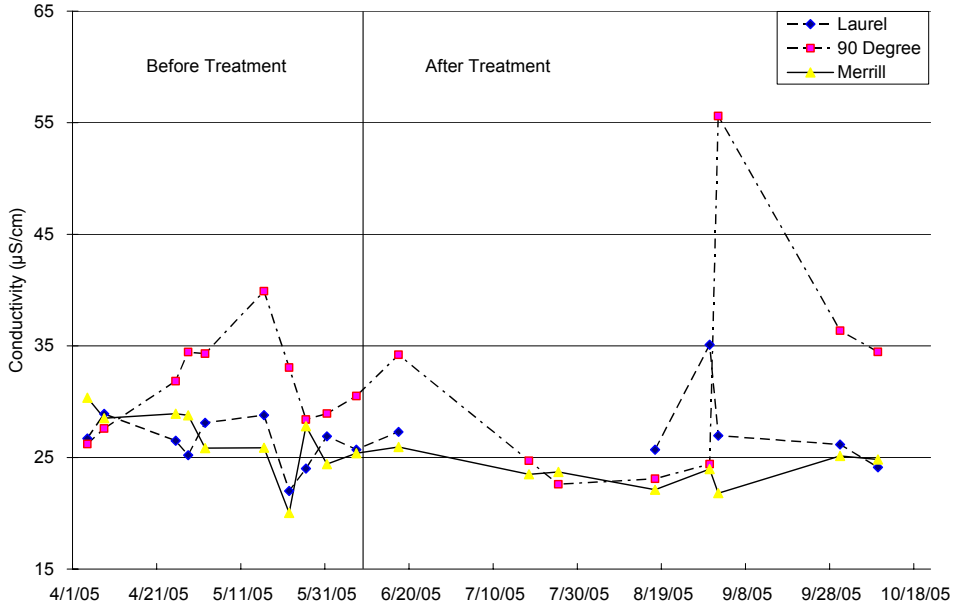

Figure 2.23. Mean ANC in soil solution collected by tension lysimeter at 80 cm depth in 2005.

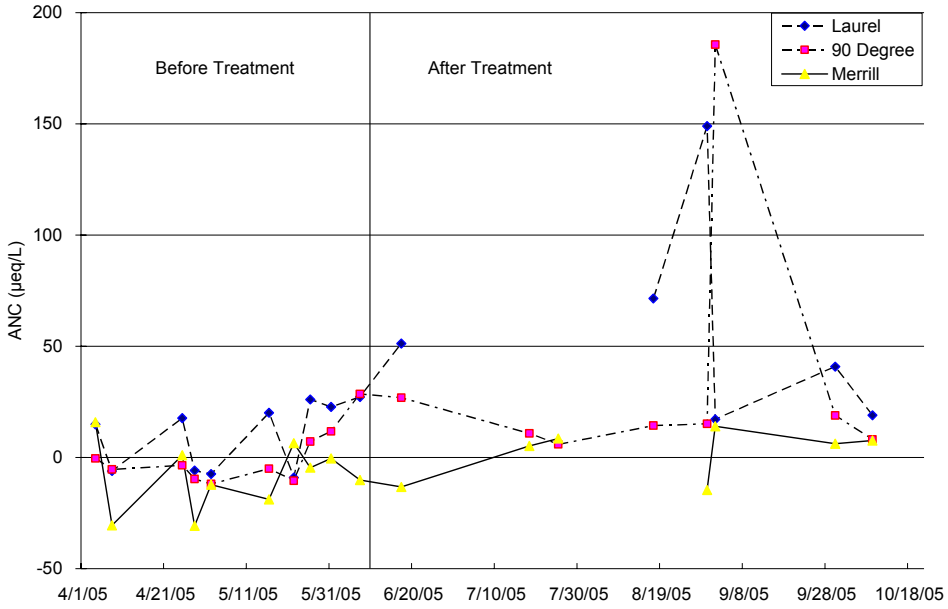

Figure 2.24. Mean calcium/aluminum molar ratio in soil solution collected by tension lysimeter at 80 cm depth in 2005.

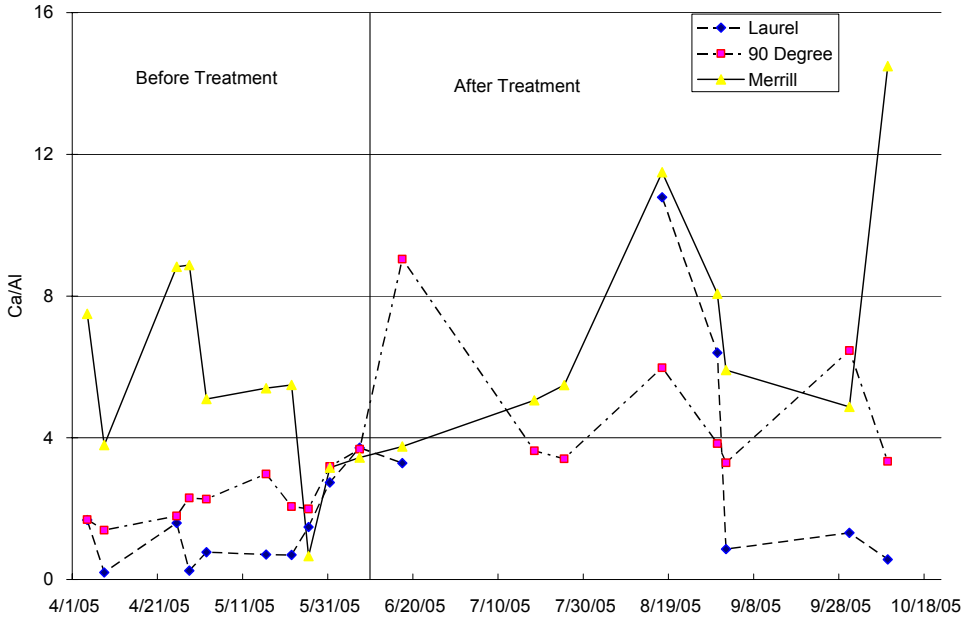

Figure 2.25. Mean pH in soil solution collected by zero-tension lysimeter at 30 cm depth in 2005.

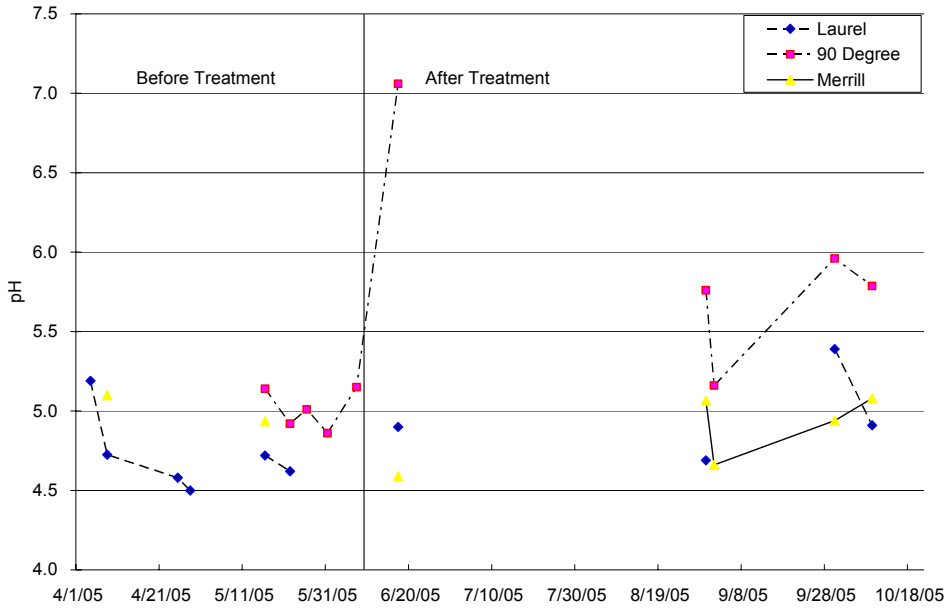

Figure 2.26. Mean calcium concentration in soil solution collected by zero-tension lysimeter at 30 cm depth in 2005.

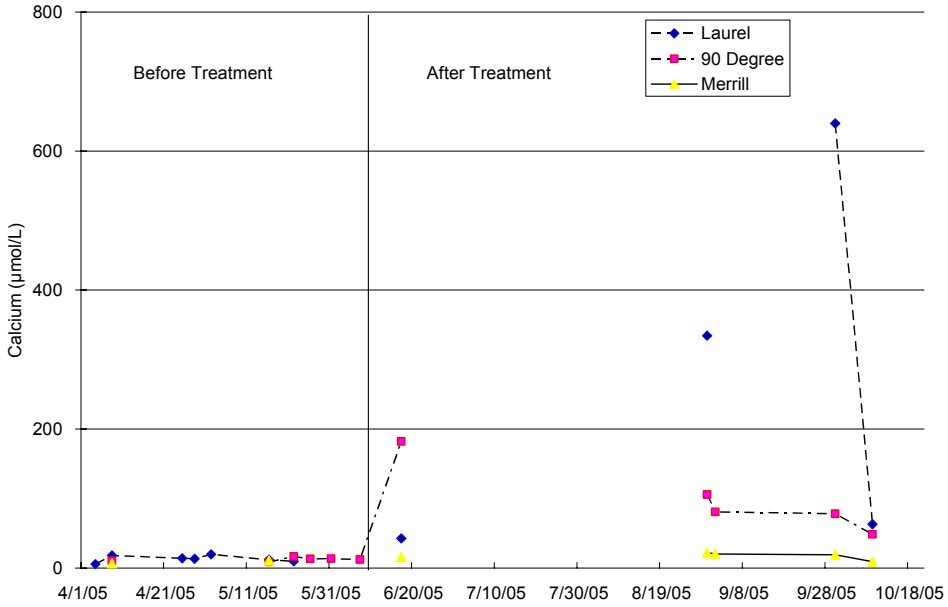

Figure 2.27. Mean magnesium concentration in soil solution collected by zero-tension lysimeter at 30 cm depth in 2005.

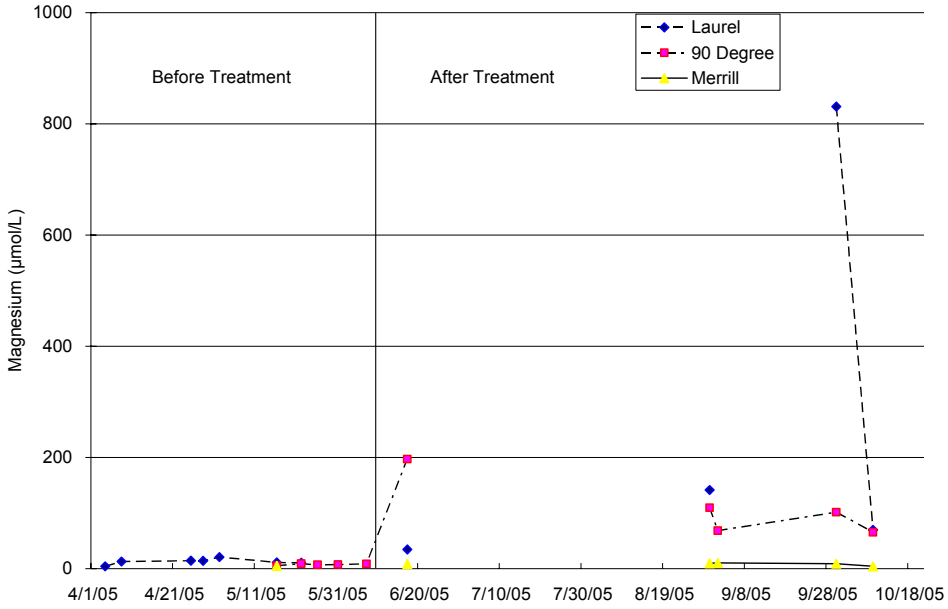

Figure 2.28. Mean aluminum concentration in soil solution collected by zero-tension lysimeter at 30 cm depth in 2005.

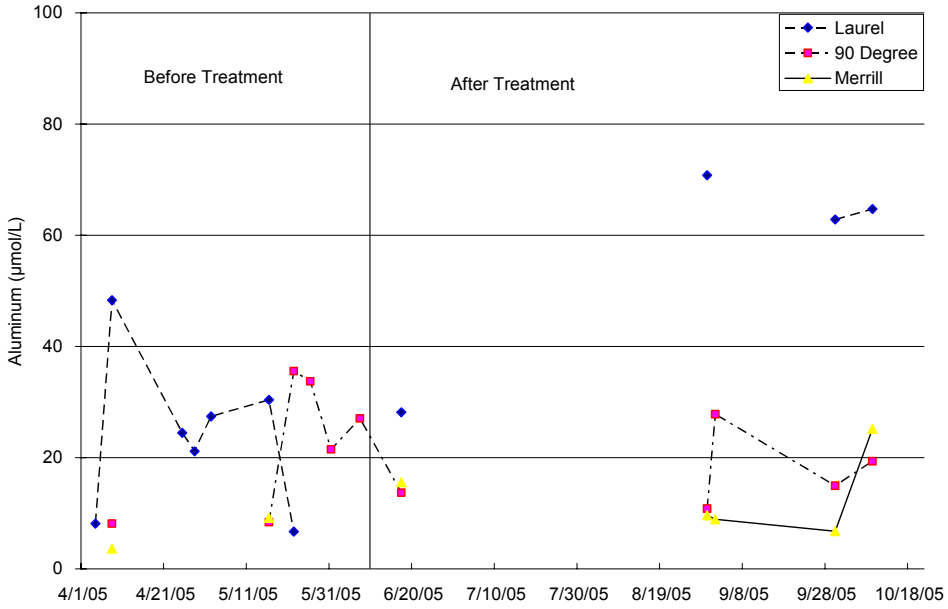

Figure 2.29. Mean conductivity in soil solution collected by zero-tension lysimeter at 30 cm depth in 2005.

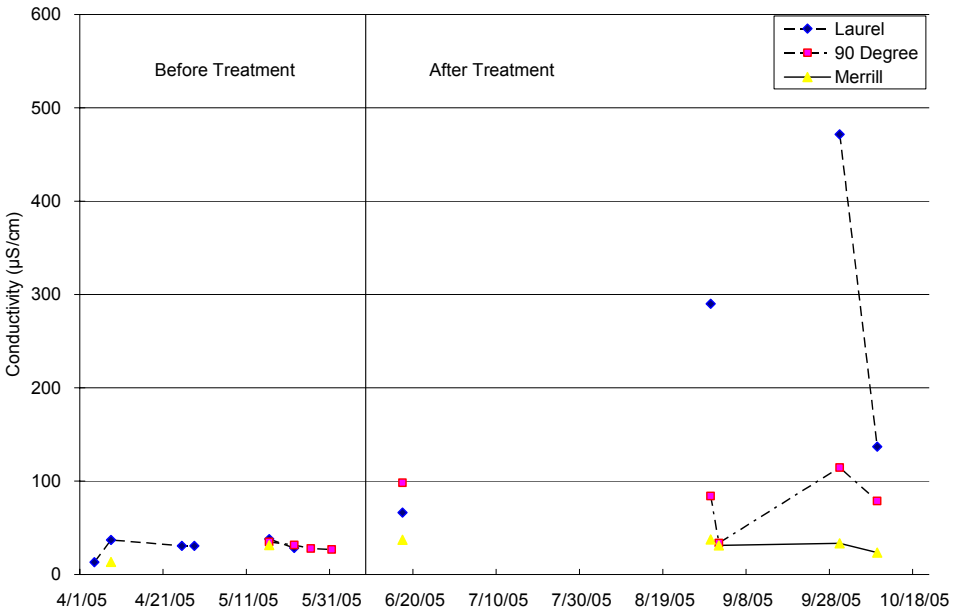

Figure 2.30. Mean ANC in soil solution collected by zero-tension lysimeter at 30 cm depth in 2005.

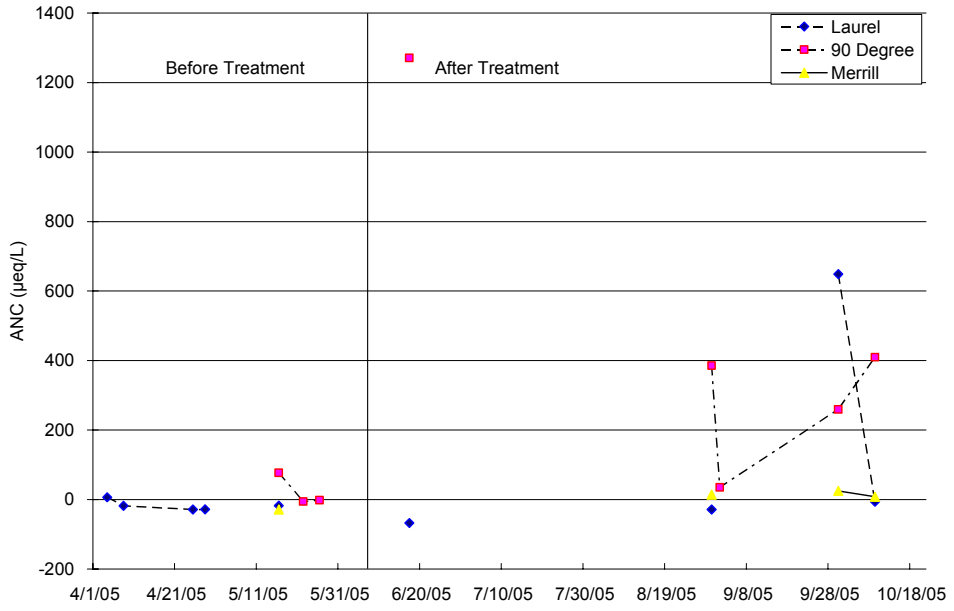

Figure 2.31. Mean calcium/aluminum molar ratio in soil solution collected by zero-tension lysimeter at 30 cm depth in 2005.

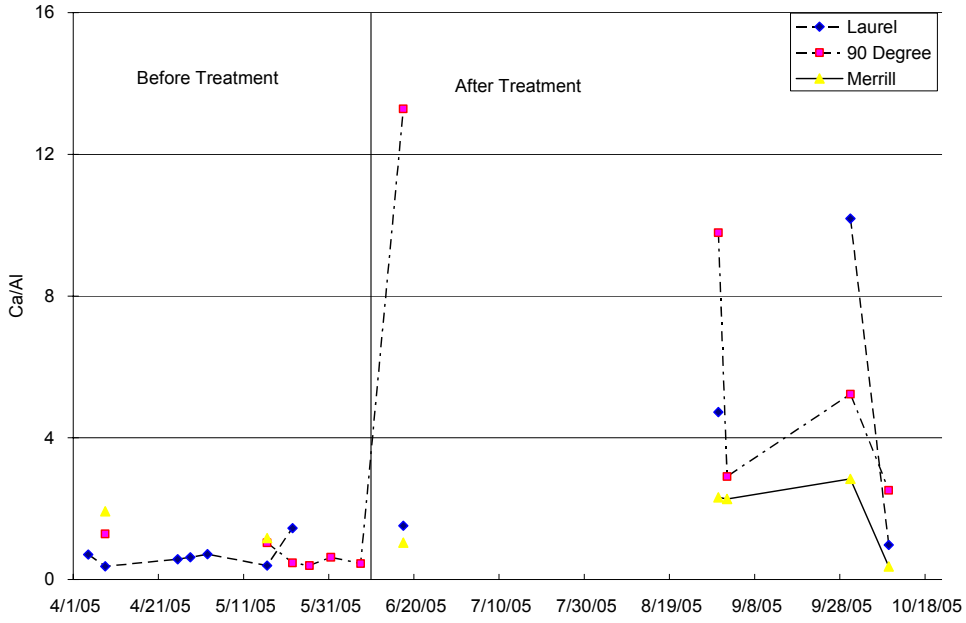

Figure 2.32. The pH of monthly streamwater at the Mosquito Creek watersheds during the study period (July 2003-October 2005).

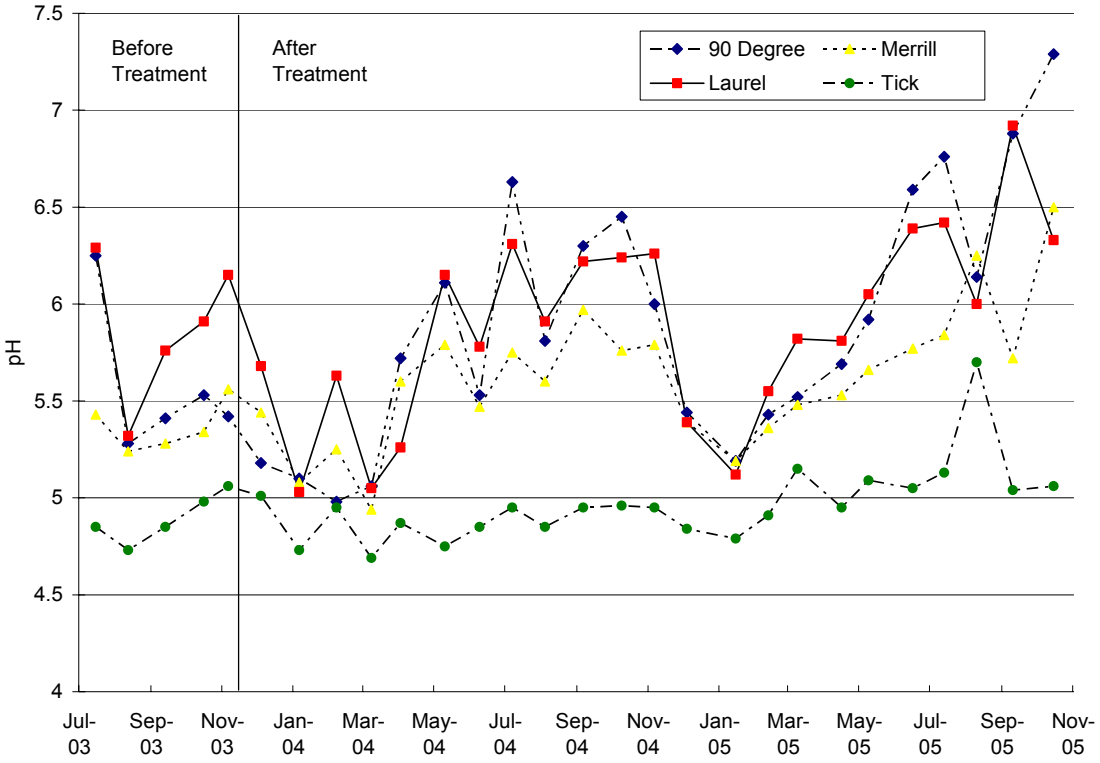

Figure 2.33. The calcium concentration of monthly streamwater at the Mosquito Creek watersheds during the study period (July 2003-October 2005).

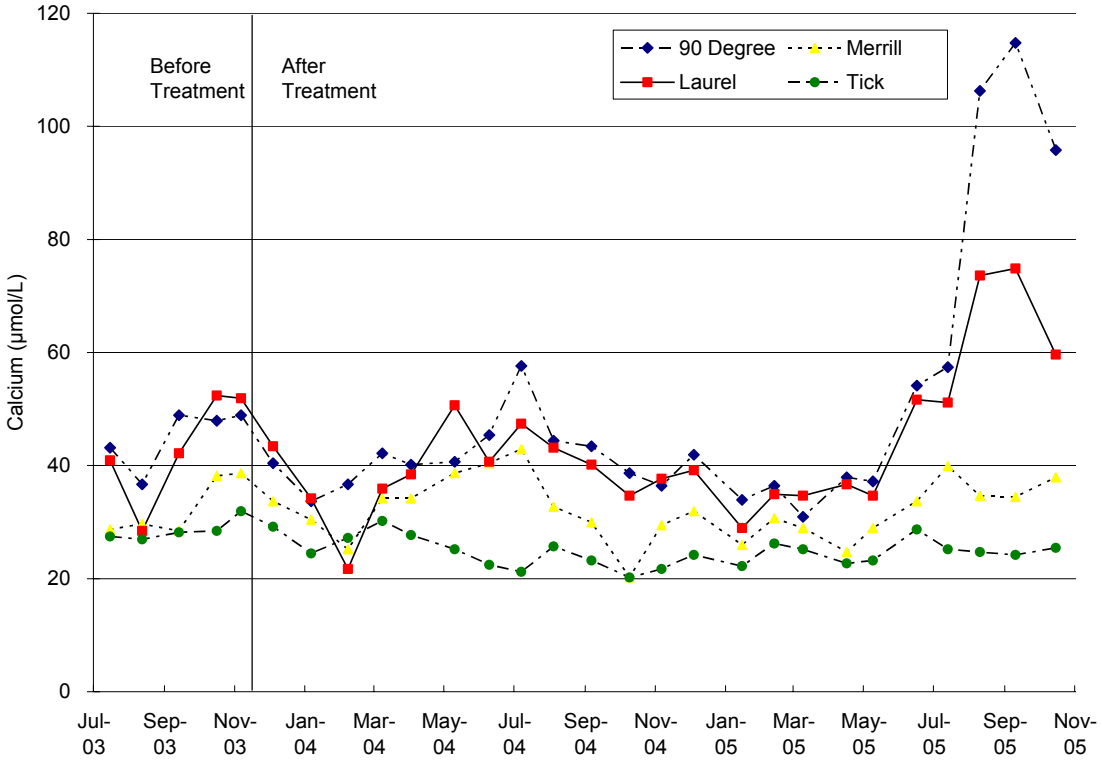

Figure 2.34. The magnesium concentration in monthly streamwater at the Mosquito Creek watersheds during the post-liming period (October 2004-October 2005).

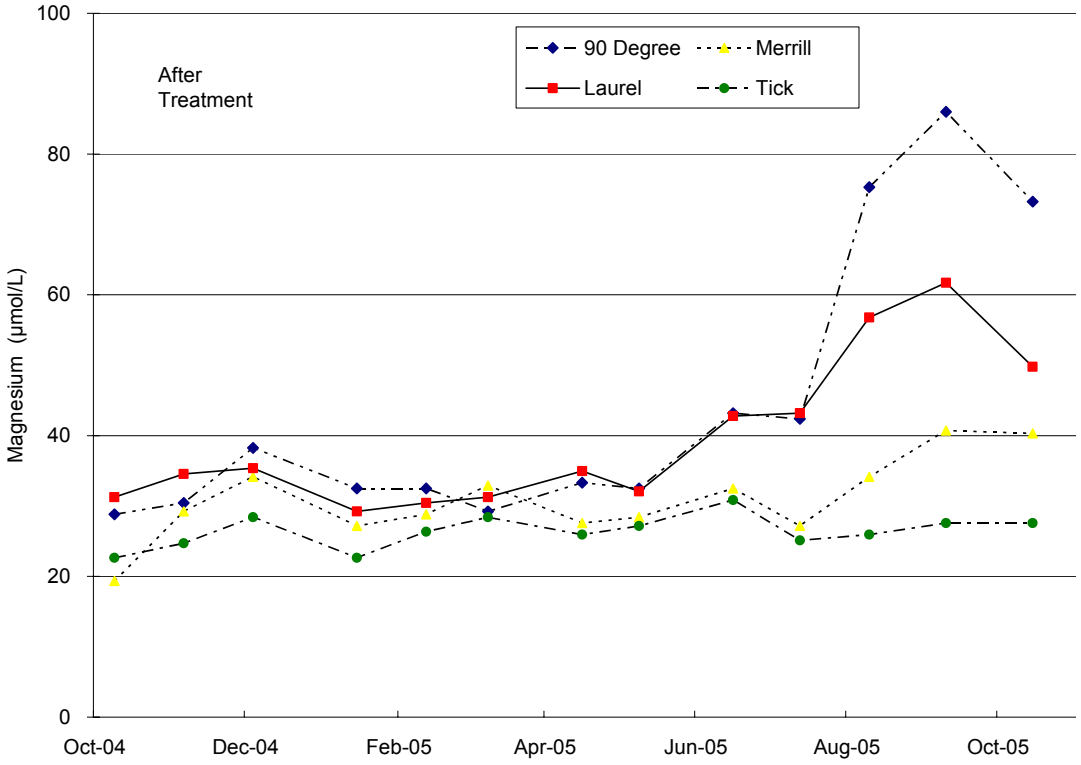

Figure 2.35. The aluminum concentration in monthly streamwater at the Mosquito Creek watersheds during the study period (July 2003-October 2005).

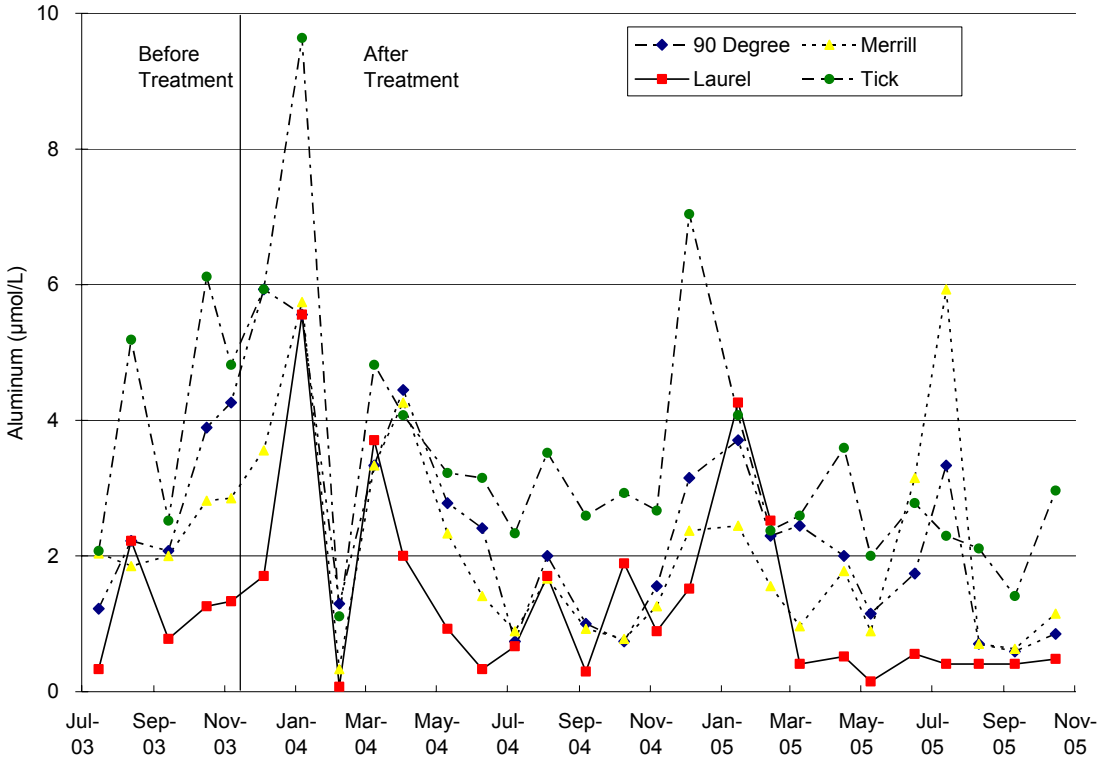

Figure 2.36. The conductivity in monthly streamwater at the Mosquito Creek watersheds during the study period (July 2003-October 2005).

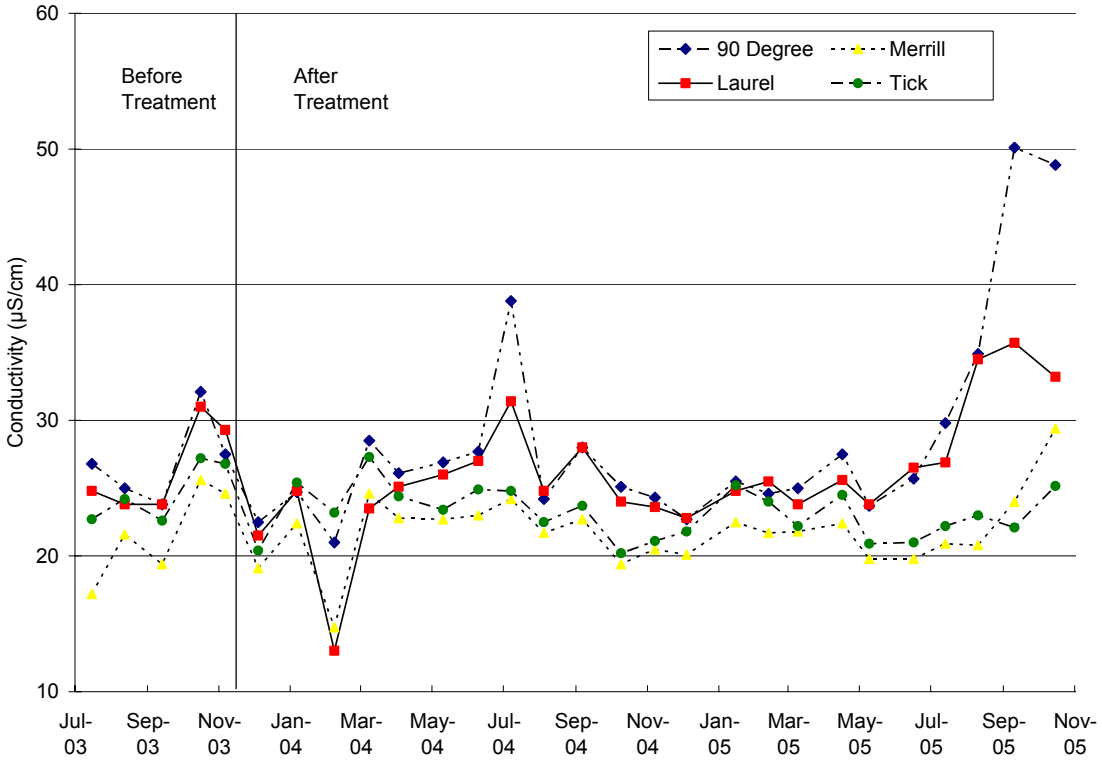

Figure 2.37. The acid neutralizing capacity in monthly streamwater at the Mosquito Creek watersheds during the study period (July 2003-October 2005).

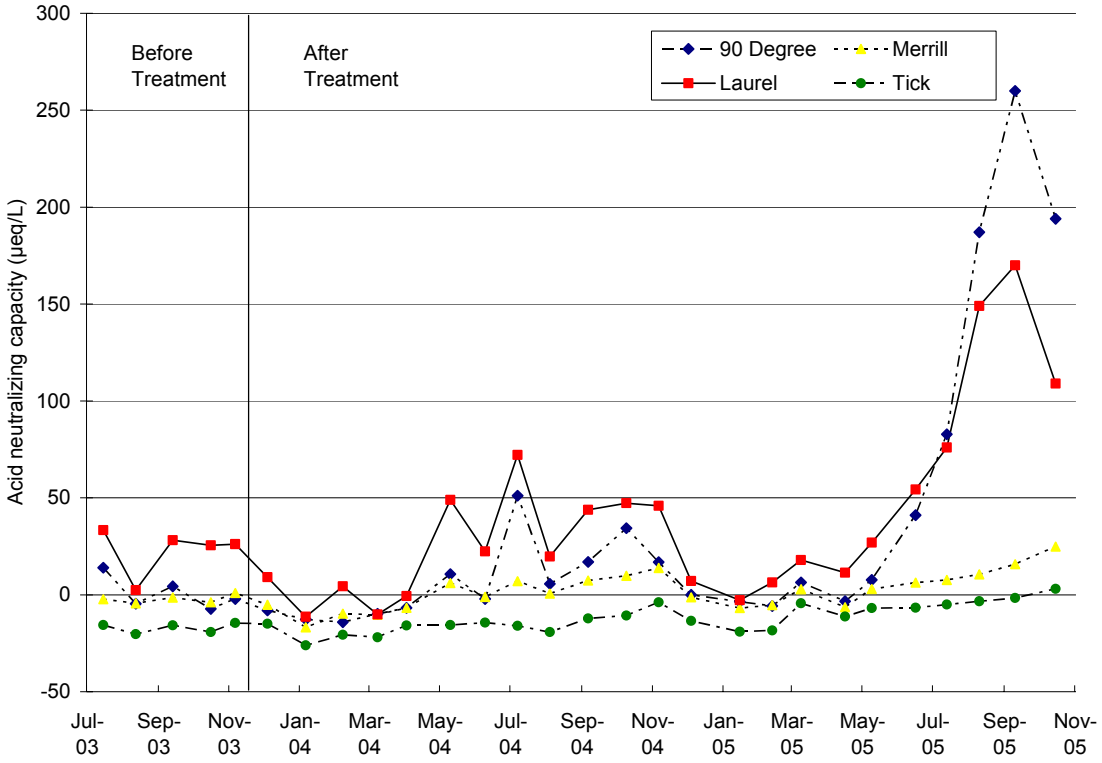

Chapter 3. Estimation of Mean Water Residence Times Using ^{18}O in Two Adjacent Appalachian Forested Watersheds

ABSTRACT

The temporal variations of $\delta^{18}O$ compositions in precipitation, soil water, and streamwater during the period January 2002 to October 2005 were used to estimate the mean residence time of water in two adjacent forested watersheds (Laurel and 90 Degree) in northcentral Pennsylvania, USA. As forest liming experiments, Laurel and 90 Degree watersheds were treated with coarse-grained dolomitic limestone sand at a rate of 5 t ha^{-1}. Precipitation had seasonal $\delta^{18}O$ variations that could be fit with a sine-wave regression model and used to simply estimate mean residence time to the water in the watersheds. The estimated mean residence time of water using the simple sine-wave regression model was similar to the estimates from response function models based on a lumped parameter approach. Best-fits between measured and computed $\delta^{18}O$ variations in soil water collected from tension lysimeters were obtained with the linear-piston flow model. The mean residence time for soil water varied from about 2 to 4 months, depending on soil characteristics and sampling depth and location. On the catchment scale, the best-fit curves in streamwater were obtained using either the dispersion model or the exponential-piston flow model. The estimated mean residence times for streamwater at the Laurel and 90 Degree watersheds were about 14 to 17 months and about 11 to 12 months, respectively. Piston-flow appeared to be responsible for a slightly larger volume of streamwater on the Laurel watershed than did the 90 Degree watershed. Based on the water chemistry results, forest liming treatment effects on soil water and streamwater occurred within 4 months and 18months after limestone sand application. The estimated mean residence time of soil water and streamwater in these watersheds was in general agreement with the water quality

results.

3.1. Introduction

As constituents of water molecules, the stable isotopes oxygen-18 (^{18}O), deuterium (^{2}H), and tritium (^{3}H) have been widely used to understand storm runoff generation in watersheds including the validation of results from hydrometric studies of flow pathways (McDonnell, 1990), and from sources of storm runoff using hydrograph separation techniques (Sklash et al., 1976; Rodhe, 1981; DeWalle et al., 1988).

With changes in the isotopic signatures of waters, stable isotopes can also provide information about mean residence time of water, defined as the average time water takes to leave a system, either a specified soil depth or a stream, in the watershed (McGuire et al., 2002). The understanding of mean residence time of water in the watershed is especially valuable for the investigation of contaminant transport and the prediction of land use change effects on future water quality. Viville et al. (2006) suggested that knowledge of the mean residence time of water will be important in determining whether liming effects will take place, and when they will do so in an acidified watershed.

The purpose of this study is to determine the mean residence time of soil water and streamwater in the two small watersheds for the 2002-2005 observation period using sine-wave regression models and lumped parameter models. The study took place in two mountainous acidified watersheds in northcentral Pennsylvania, USA. In order to improve soil nutrient conditions and drainage water quality, coarse-grained dolomitic limestone was applied at a rate of 5 t ha^{-1} over the watersheds in fall 2003 and 2004 and six soil plots (15.2

meter by 9.1 meter) in summer 2005. Determining the mean water residence time at these watersheds could help in predicting land use changes.

3.2. Methods

3.2.1. Study Area

The Mosquito Creek basin has a drainage area of 230 km^2 that forms a tributary of the West Branch of the Susquehanna River. This basin has been studied for effectiveness of forest liming in remediating streamwater acidity as a consequence of acid deposition. Within the Mosquito Creek basin, adjacent, two small watersheds (Laurel and 90 Degree) were selected to investigate the mean residence time of soil water and streamwater (Figure 3.1). The drainage areas for the Laurel and 90 Degree watersheds are 1.76 km^2 and 1.36 km^2, respectively. The Laurel and 90 Degree watersheds are entirely covered by northern hardwood forest and share similar physiographic characteristics. Elevation of the two watersheds ranged from 536 m to 674 m. Both watersheds are dominated by sandstone, conglomerate, and shale from the Pottsville Formation of Pennsylvanian age and the Burgoon Sandstone of Mississippian age. The climate is temperate mountainous; mean annual precipitation is 1056 mm, monitored at the Clarence, PA weather station (9.4 km from the Mosquito Creek basin's outlet).

3.2.2. Data Collection

All samples for the oxygen-18 isotope analysis were collected in 25 ml Nalgene® bottles. Precipitation samples were collected on a weekly basis beginning January 2002 at

the Hills Creek State Park (Pennsylvania Atmospheric Deposition Monitoring Station), located at an elevation of 476 m (41º48′16″ / 77º11′25″) and terminated with the final collection of samples in October 2005. Due to budgetary constraints, a volume-weighted composite was made monthly from the weekly precipitation samples. The $\delta^{18}O$ (‰) precipitation values at the study watersheds were adjusted for altitude effect (-0.325‰/100 m).

At study watersheds, soil water samples were collected with tension lysimeters for 10 storm events from April to October 2005. Tension lysimeters were evacuated to 60 k Pa prior to anticipated rainfall events. There were three soil plots (15.2 meter by 9.1 meter) on each watershed (a total of 6 soil plots). At each of the soil plots, soil water samples were collected at both 30 cm and 80 cm soil depths. A composite soil water sample from the three sampling sites on each watershed was made for each soil depth for each storm event. Streamwater samples were obtained monthly by grab sampling at the Laurel and 90 Degree gauging stations beginning July 2003 and terminating with collections in October 2005.

3.2.3. Data Analysis

3.2.3.1. Laboratory analysis

Oxygen-18 (^{18}O) compositions of all water samples (161 samples in total) were analyzed by a micromass optima dual inlet mass spectrometer at the Stable Isotope Laboratory (Institute of Arctic and Alpine Research, University of Colorado at Boulder) according to the standard CO_2 equilibration method (Epstein & Mayeda, 1953). The ^{18}O composition of water samples is reported as relative deviations from the Vienna Standard

Mean Ocean Water (V-SMOW) in per mil (‰) and calculated by:

$$\delta^{18}O_s = (\frac{R_x - R_s}{R_s}) * 1000 \quad (1)$$

where $\delta^{18}O_s$ is the sample ^{18}O concentration in ‰; R_x is the ratio of the heavy to light isotope ($^{18}O/^{16}O$) for the sample; and R_s is the ratio of $^{18}O/^{16}O$ for the V-SMOW. The analytical precision of the $\delta^{18}O$ measurement was ± 0.07‰ at the laboratory, based on the average standard deviation (1-σ). However, the standard deviation of the $\delta^{18}O$ measurements was 0.12‰, based on 6 submitted duplicate samples.

3.2.3.2. Estimation of mean residence time

Two methods were used to determine the mean residence times of soil water and streamwater at the two study watersheds. One method used the simple sine-wave regression model, and the other used the FLOWPC program (version 3.2, 2000) based on the lumped parameter approach.

Sine-wave regression model

The sine-wave regression model provides preliminary information regarding the mean residence time of soil water and streamwater with little effort and cost. Periodic regression analysis was used to fit sine-wave regression models to $\delta^{18}O$ variations in precipitation, soil water, and streamwater during the study periods (DeWalle et al., 1997). The seasonal sine-wave model to fit $\delta^{18}O$ variation was computed as follows:

$$\delta^{18}O = X + A[\cos(ct - \theta)] \quad (2)$$

where $\delta^{18}O$ is the modelled ^{18}O in ‰; X is the annual average $\delta^{18}O$ in ‰; A is the measured ^{18}O annual amplitude in ‰; c is the angular frequency of annual variations in radians or 0.01724 radian per day; t is the time in days after the start of the sampling period (1 January 2002); and θ is the phase lag or time of annual peak $\delta^{18}O$ in radians.

The sine-wave regression models fitted to $\delta^{18}O$ variations in input (precipitation) and output (soil water and streamwater) were used to estimate mean residence time in soil water and streamwater. The water was assumed to be well-mixed and to have a steady state, and an exponential distribution of residence times (Maloszewski et al., 1983; Stewart and McDonnell, 1991; DeWalle et al., 1997); thus, the mean residence time of water leaving the system was calculated as:

$$T = \frac{1}{c}\left[\left(\frac{A_{z1}}{A_{z2}}\right)^2 - 1\right]^{1/2} \quad (3)$$

where T is the mean residence time of water in days; c is the angular frequency of variations in radians as defined in equation (2); A_{z1} is the annual amplitude of input (precipitation) in ‰; and A_{z2} is the annual amplitude of the output (streamwater or soil water at the defined soil depth) in ‰.

Isotopic damping depth is defined as the soil depth required to reduce the amplitude of $\delta^{18}O$ variations in soil water and/or streamwater to 1/e (DeWalle et al., 1997). Isotopic damping depth was calculated from the amplitude change as follows:

$$d_h = \frac{(Z_2 - Z_1)}{\ln(A_{z2} / A_{z1})} \quad (4)$$

where d_h is the isotopic damping depth in cm; Z_2 is sampling depth for the soil water and/or

average soil depth for the streamwater; Z_1 is the depth at the surface = 0; and A_{z1} and A_{z2} are defined as in equation (3). Average soil depth of 100 cm at two watersheds was assumed for the streamwater, based on the field visit.

Lumped parameter models using FLOWPC program

Lumped parameter models, so-called black-box models, assume flow pattern within the system is constant and consider the system as a whole (Maloszewski and Zuber, 1996). The isotopic signature of input is converted into output through the black-box, which contains the system response function of calculations. These models do not require any physical knowledge of the watershed before interpreting results; however, the system response function does provide information about the physical structure of the system (Maloszewski and Zuber, 1982). A brief summary of the theory of the lumped-parameter approach used in the FLOWPC program (version 3.2, December 2000) is given next.

For a system with a hydrologic steady state, the output ^{18}O values in the soil water or streamwater were estimated from the transformed input ^{18}O value in precipitation through a convolution integral (Maloszewski and Zuber, 1982) as follows:

$$\delta_{out}(t) = \int_0^\infty \delta_{in}(t-t')g(t')\exp(-\lambda t')dt' \qquad (5)$$

where δ_{out} (t) and δ_{in} (t) are the output and input of ^{18}O compositions, respectively; t is the calendar time; t′ is the integration variable that describes the exit time of tracer leaving the system; g(t′) is the system response function that describes the distribution of the residence times, t′; and λ is radioactive decay constant. For stable isotopes, such as δ^2H and $\delta^{18}O$, λ is

equal to 0.

The input of ^{18}O compositions (^{18}O values in precipitation) for equation (5) is computed according to Zuber and Maloszewski (2000) as:

$$\delta_{in}(t) = \overline{\delta} + \left[\alpha_i P_i \left(\delta_i - \overline{\delta}\right)\right] / \left(\sum_{i=1}^{n} \alpha_i P_i / n\right) \quad (6)$$

where $\overline{\delta}$ is the mean input of $\delta^{18}O$ values that must be equal to the mean output of $\delta^{18}O$ values; and n is the number of months for which the observations are available. The value of α is defined as an infiltration coefficient calculated according to Grabczak et al. (1984) is as follows:

$$\alpha = \left[\left(\overline{\delta P_w} - \delta G\right) \times \left(\sum_{i=10}^{3} P_i\right)_w\right] \Big/ \left[\left(\delta G - \overline{\delta P_s}\right) \times \left(\sum_{i=4}^{9} P_i\right)_s\right] \quad (7)$$

where $\overline{\delta P_w}$ and $\overline{\delta P_s}$ are the long-term weighted mean precipitation $\delta^{18}O$ values for the winter and summer months, respectively; and δG is the mean $\delta^{18}O$ value of the local groundwater resulting from recent precipitation (Grabczak et al., 1984). The winter months are considered to be October through March (from the tenth month to the third month of the next calendar year), and the summer months are April through September (from the fourth month to the ninth month of the calendar year).

The types of residence time distribution of the tracer (g(t′)), which defines the lumped parameter model, are 1) piston flow model, 2) exponential model, 3) exponential-piston flow model, 4) dispersion model, 5) linear model, and 6) linear-piston flow model. The response functions of these models are thoroughly described by Maloszewski and Zuber (1982, 1996) and briefly summarized here:

1) Piston flow model

The piston flow model assumes that the tracer is only transported by advection and moves at the same velocity on the same flow line so that all flow lines have the same residence time. Because it ignores the hydrodynamic dispersion and molecular diffusion within flow systems, this model is considered to have limited practical use. However, in confined aquifers where water has been detached and isolated since the recharge time, the piston flow model is suitable for estimating mean residence time (Maloszewski and Zuber, 1982). The piston flow model is defined by the following system response function, g(t′), as:

$$g(t') = \delta(t' - t_t) \quad (8)$$

where $\delta(t'-t_t)$ is the Dirac delta function; t′ is a time variable; and t_t is the mean residence time of water (mean transit time of water) in the system, the only fitting parameter of this model.

2) Exponential model

The exponential model assumes 1) all flow lines have exponential distribution of transit times without exchange and mixing of tracer between the flow lines; and 2) mixing of tracer only occurs at the output sampling site (Maloszewski and Zuber, 1996). This model derivation assumes the response function of a well-mixed system to be as follows:

$$g(t') = t_t^{-1} \exp(-t'/t_t) \quad (9)$$

where t_t, mean residence time of water in the system, is the only fitting parameter of this

model.

3) Exponential-piston flow model

The exponential-piston flow model measures the residence time distribution of the tracer in the system by connecting the exponential model with the piston flow model. Because it allows for a delay of the shortest flow paths, this model is more realistic than the exponential model (Zuber and Maloszewski, 2000). The weighting function of the exponential-piston flow model is defined as:

$$g(t') = (\eta / t_t)\exp(-\eta t' / t_t + \eta - 1), \quad \text{if} \quad t' \geq t_t(1-\eta^{-1}) \tag{10}$$

$$g(t') = 0, \quad \text{if} \quad t' < t_t(1-\eta^{-1})$$

where η is the ratio of the total volume to the volume with exponential distribution of residence times. The η is equal to 1 for the exponential flow model so that if the value of η is closer to infinity (∞), the output system has piston flow distributions of residence times (Maloszewski and Zuber, 1982). This model has two fitting parameters: η and t_t.

4) Dispersion model

The dispersion model is applicable to flow in a dispersive system. The dispersion model assumes that flow paths are affected by hydrodynamic dispersion or geomorphologic dispersion. Tracers can spread by heterogeneity of flow path. The dispersion model is defined by the following weighting function (Maloszewski and Zuber, 1982) as:

$$g(t') = t'^{-1} * (\frac{4\pi P_D t'}{t_t})^{-1/2} * \exp\left[-\frac{t_t}{4P_D t'}(1-\frac{t'}{t_t})^2 \right] \tag{11}$$

where P_D is the dispersion parameter and equal to $D/vx=1/P_e$ (D is the coefficient of dispersion (m^2/sec); v is the mean flow velocity in the system (m/sec); x is the length of the flow lines (m); and P_e is the Peclet number that measures the ratio of advection to dispersion. For example, a small dispersion parameter (or a large Peclet number) indicates characteristics of an advective system. The response function of this model has two fitting parameters: t_t and P_D.

5) Linear model

The linear model assumes that the residence time distribution of tracer is constant and that mixing between the flow lines does not occur (Maloszewski and Zuber, 1996). The weighting function of linear model is defined as:

$$g(t') = 1/(2t_t), \quad \text{if } t' \le 2t_t \qquad (12)$$

$$g(t') = 0, \quad \text{if } t' > 2t_t$$

The linear model has one fitting parameter: t_t. Maloszewski and Zuber (1982) have questioned the practical applicability of the linear model because no reports have been published that estimate mean residence time using this model.

6) Linear-piston flow model

The linear-piston flow model is a combination of the linear model and the piston flow model. Therefore, it describes a system using a connected linear flow reservoir in a series with a piston flow reservoir (Maloszewski and Zuber, 1996). The weighting function of the linear-piston flow model is defined as:

$$g(t') = \eta/(2t_t), \qquad t_t - (t_t/\eta) \le t' \le t_t + (t_t/\eta) \tag{13}$$

$$g(t') = 0, \qquad t' < t_t\,(1 - 1/\eta)$$

$$g(t') = 0, \qquad t' > t_t\,(1 - 1/\eta)$$

where η is the ratio of the total volume to the volume with the linear distribution of transit times. The value of η = 1 indicates that the system is dominated by the linear flow model. For $\eta \to \infty$, the output system approaches the piston flow distribution of residence time. Similar to the exponential-piston flow model, the weighting function of this model has two fitting parameters: t_t and η.

3.2.3.3. Statistical analysis

Goodness of fit for the sine-wave regression model

Goodness of fit for the sine-wave regression model to the observed isotopic measurements was evaluated using the coefficient of determination and the root mean square error and described as follows:

The coefficient of determination (R^2) is defined as the ratio of the explained variation by the sine-wave regression to the total variation of the observed data. The R^2 measures how well the sine-wave regression line represents the isotopic compositions of the observed data. The statistic for R^2 is computed as follows:

$$R^2 = \frac{\left(\sum Cc_i Cm_i - \frac{(\sum Cc_i)(\sum Cm_i)}{n}\right)^2}{\left(\sum Cc_i^{\,2} - \frac{(\sum Cc_i)^2}{n}\right)\left(\sum Cm_i^{\,2} - \frac{(\sum Cm_i)^2}{n}\right)} \tag{14}$$

where Cc_i is the i-th calculated (fitted to the sine-wave regression) isotopic composition;

Cm_i is the i-th measured isotopic composition; and n is the number of observations. The value of R^2 ranges from 0 to 1. When the value of R^2 =1.0, the sine-wave regression line perfectly fits all the observed data points; 100% of the variation in measured isotopic compositions is explained by the fitted sine-wave regression and all residuals are zero.

The root mean square error (RMSE), is the same as the square root of the mean square error (MSE), and it measures the average mismatch between each measured isotopic composition of the data and the fitted isotopic composition data by the sine-wave regression. The statistic for the RMSE is calculated as:

$$\text{RMSE } (‰) = \sqrt{\frac{1}{n}\sum_{i=1}^{n}\left(Cm_i - Cc_i\right)^2} \qquad (15)$$

where Cc_i, Cm_i, and n are defined in the above equation (14). The smaller the value of the RMSE, the better the fit of the sine-wave regression model to the observed data.

Goodness of fit for the lumped parameter models

Among different types of lumped parameter models, the best-fit model was determined by the goodness of fit criteria between the observed and simulated output data. Types of goodness of fit for the lumped parameter models to the observed output measurements are SIGMA, model efficiency, and Pearson's correlation coefficient. These formulas are described next.

As a goodness of fit measurement, a value of SIGMA is provided by the FLOWPC program and computed as follows:

$$\text{SIGMA} = \left[\sum_{i=1}^{n}\left(Cm_i - Cc_i\right)^2\right]^{1/2} / n \qquad (16)$$

where Cm_i is the i-th measured isotopic composition; Cc_i is the i-th calculated (fitted) isotopic composition; and n is the number of observations. The value of SIGMA = 0 indicates a perfectly fitted model to the measured data, with an indication of better fit for a smaller value of the SIGMA.

As a goodness of fit, the model efficiency (ME) is introduced in Hornberger et al. (1992) and provided by the FLOWPC program. The formula for the estimate is as follows:

$$\text{ME} = 1 - \frac{\sum_{i=1}^{n}\left(Cc_i - Cm_i\right)^2}{\sum_{i=1}^{n}\left(Cc_i - C_{mean}\right)^2} \qquad (17)$$

where Cc_i and Cm_i are defined in equation (16) and C_{mean} is the mean of the measured isotopic compositions. A model efficiency ME=1.0 indicates a perfect fit of the model to the measured data, while ME = 0.0 indicates that the model's fit to the measured data is very poor. In the latter cases, the fit is nothing better than a horizontal line through the mean of the measured isotopic compositions.

Pearson's correlation coefficient (r) measures the strength and direction of a linear relationship between the observed and calculated isotopic compositions and is computed as follows:

$$r = \frac{\sum Cc_i Cm_i - \frac{(\sum Cc_i)(\sum Cm_i)}{n}}{\sqrt{\left(\sum Cc_i^{\,2} - \frac{\left(\sum Cc_i\right)^2}{n}\right)\left(\sum Cm_i^{\,2} - \frac{\left(\sum Cm_i\right)^2}{n}\right)}} \qquad (18)$$

where Cc_i, Cm_i, and n are defined as in equation (16). The value of r ranges from -1 to 1. A value of r=-1 indicates a perfectly negative linear relationship; a calculated isotopic composition value increases as a measured isotopic composition value decreases. A value of r=0 indicates no linear relationship between the variables. A value of r=1 indicates a perfectly positive linear relationship; a calculated isotopic composition value increases with increases in the measured isotopic composition value.

3.3. Results

3.3.1. Temporal Variation of Isotopic Measurements

3.3.1.1. Precipitation $\delta^{18}O$

The study covered the period from January 2002 to October 2005. Temporal variations in monthly total precipitation, mean air temperature, oxygen isotopic composition ($\delta^{18}O$) in precipitation during the study period are shown in Figure 3.2, and notations for their graphs are summarized in Table 3.1. Total monthly precipitation and monthly mean air temperature were monitored at the Clarence climate station (elevation 423.7m, 41°03'N / 77°57'W). Total annual precipitation was about 1292 mm, and monthly mean air temperature ranged from -4.4 °C to 20.7 °C, with an annual average of 7.6 °C, over a four-year period. Monthly variation of the $\delta^{18}O$ (‰) in precipitation follows more or less similar patterns as the monthly mean air temperature. The monthly mean air temperatures are plotted against monthly $\delta^{18}O$ compositions in precipitation in Figure 3.3. Results from the linear regression analysis showed more or less strong positive correlations: $\delta^{18}O$ in precipitation = (0.38* monthly mean air temperature)-13.6; R^2=70.9%; adjusted

R^2=70.3%; P-value=0.000. These correlations effect seasonal variations of $\delta^{18}O$ in precipitation input to the watershed, and they indicate the possibility of a rough estimate of $\delta^{18}O$ variations in precipitation from mean air temperature in future research. The $\delta^{18}O$ of precipitation ranged from -20.17‰ (January 2002) to -3.4‰ (October 2002), with an average of -10.55‰ during the entire study period (Table 3.2).

As the study site is located in the Northern Hemisphere, the $\delta^{18}O$ of precipitation during the winter months (October to March) are more depleted than the $\delta^{18}O$ of precipitation during the summer months (April to September). Based on data from the hydrologic year 2005, the mean of monthly $\delta^{18}O$ in precipitation during the winter months was -14.36‰, almost two times lower than the -7.93‰ mean in $\delta^{18}O$ precipitation for the summer months. The $\delta^{18}O$ of precipitation for the 2005 hydrologic year were more depleted and had a higher amplitude than the $\delta^{18}O$ of precipitation in the 2004 hydrologic year (Table 3.3).

3.3.1.2. Soil water $\delta^{18}O$

The average soil water $\delta^{18}O$ composition at 30 cm depth collected by tension lysimeters was more depleted at the Laurel watershed than at the 90 Degree watershed (Table 3.2). At 30 cm depth, the mean $\delta^{18}O$ in soil water at the Laurel watershed was -9.18‰, ranging from -11.11‰ to -4.78‰, whereas the mean $\delta^{18}O$ in soil water at the 90 Degree watershed was -7.84‰, ranging from -11.37‰ to -4.31‰. The amplitude of the soil water $\delta^{18}O$ variation at 30 cm depth at the Laurel watershed was 3.17‰; this was slightly lower than that measured at the 90 Degree watershed (3.53‰, Table 3.3).

At 80 cm depth, the mean $\delta^{18}O$ in soil water at the Laurel watershed was -8.40‰ and ranged from -10.6‰ to -3.83‰, whereas, the mean $\delta^{18}O$ in soil water at the 90 Degree watershed was -8.26‰ and ranged from -10.34‰ to -5.31‰ (Table 3.2). The mean $\delta^{18}O$ in soil water at 80 cm depth was also more depleted at the Laurel watershed. The amplitude of soil water $\delta^{18}O$ composition at 80 cm depth was 2.51‰ at the 90 Degree watershed, which was lower than the amplitude at the Laurel watershed (3.41‰, Table 3.3).

The isotopic damping depth in soil water at 30 cm depth on the Laurel watershed was 39.26 cm compared to the 45.78 cm on the 90 Degree watershed. Isotopic damping depth in soil water at 80 cm depth on the Laurel watershed was 115.79 cm, which was higher compared to the 80.40 cm damping depth on the 90 Degree watershed (Table 3.3).

3.3.1.3. Streamwater $\delta^{18}O$

Temporal $\delta^{18}O$ variations in streamwater both on the Laurel and 90 Degree watersheds are shown in Figure 3.4. The mean $\delta^{18}O$ composition in streamwater at the Laurel watershed was -9.56‰, and ranged from -10.65‰ to -8.71‰, whereas, the mean $\delta^{18}O$ composition in streamwater at the 90 Degree watershed was -9.28‰, and ranged from -10.59‰ to -8.39‰ (Table 3.2). All the minimum, mean, and maximum $\delta^{18}O$ compositions in streamwater at the Laurel watersheds were lower than those measured at the 90 Degree watershed.

The $\delta^{18}O$ variations in streamwater both at the Laurel and 90 Degree watersheds were comparatively damped and showed delayed peaks compared to the $\delta^{18}O$ variations in precipitation (Figure 3.4). At both watersheds, the amplitude of $\delta^{18}O$ compositions in

streamwater was significantly lower than the amplitude of those in precipitation and soil water (Table 3.3). The amplitude of $\delta^{18}O$ variations in streamwater at the Laurel and 90 Degree watersheds were 0.76‰ and 0.97‰, respectively.

Isotopic damping depth in streamwater at the Laurel watershed calculated from the amplitude change was 45.68 cm, slightly lower than the 51.32 cm streamwater isotopic damping depth at the 90 Degree watershed (Table 3.3). Isotopic damping depth in streamwater was about 6 cm higher than that in soil water at 30 cm depth in both watersheds.

3.3.2. Mean Residence Time Estimated by the Sine-Wave Regression Model

3.3.2.1. Sine-wave regression models with ^{18}O measurements

All measurements of $\delta^{18}O$ in precipitation, soil water, and streamwater fitted well with their respective sine-wave regression models for both the Laurel and 90 Degree watersheds, with the exception of soil water at 80 cm depth on the 90 Degree watershed (p-value=0.166, Table 3.4).

Temporal variation in precipitation $\delta^{18}O$ and its fitted values with the sine-wave regression model are shown in Figure 3.5. Oxygen isotopic compositions in precipitation data were used for three consecutive hydrologic years 2003, 2004, and 2005. As an input to the watershed, about 63% of the total variation in the $\delta^{18}O$ of precipitation can be explained by the sine-wave regression model (significant at $\alpha \leq 0.05$, Table 3.4, Figure 3.5). The root mean square error (RMSE) measures the average mismatch between each measured data point and the sine-wave regression model so that the smaller the value of the RMSE, the

better the fit to the sine-wave regression model. The sine-wave regression model for the $\delta^{18}O$ variation in precipitation had higher mismatch values with measured $\delta^{18}O$; a value of the RMSE in precipitation was 2.57‰. This value is higher than the RMSE of the fitted models for soil water and streamwater.

Temporal variations of $\delta^{18}O$ in soil water and its fitted values with sine-wave regression models at the Laurel watershed and 90 Degree watershed are shown in Figures 3.6 and 3.7, respectively. Temporal variation in soil water $\delta^{18}O$ at the Laurel watershed fit the sine-wave regression model better than that in soil water at the 90 Degree watershed (Table 3.4). The $\delta^{18}O$ variation in soil water at 30 cm depth on the Laurel watershed was well fitted with the sine-wave regression model (R^2=0.85, adjusted R^2=0.822, P-value=0.001, and RMSE=0.854‰). However, the $\delta^{18}O$ variations in soil water at 80 cm depth at the 90 Degree watershed were poorly fitted with the sine-wave regression model (R^2=0.225, adjusted R^2=0.129, P-value=0.166, and RMSE=1.543‰).

Temporal variation in streamwater $\delta^{18}O$ at the Laurel watershed were fitted with a sine-wave regression model better than that fitted in streamwater $\delta^{18}O$ at the 90 Degree watershed, and had lower R^2 and RMSE values (Table 3.4 and Figure 3.8). About 79% of the total $\delta^{18}O$ variation in streamwater at the Laurel watershed could be explained by a sine-wave regression model, whereas about 56% of the total $\delta^{18}O$ variation in streamwater at the 90 Degree watershed could be explained by a sine-wave regression model.

3.3.2.2. Mean residence time for soil water and streamwater

The estimated mean residence time for soil water was about 3 to 4 months on both

watersheds using the sine-wave regression model (Table 3.4). At 30 cm depth, the mean residence time for soil water on the Laurel watershed was 95 days (3.2 months), which was higher than the 81-day (2.7 months) transit time for the 90 Degree watershed. However, at 80 cm depth the mean residence time for soil water on the 90 Degree watershed was higher than the Laurel watershed. The estimated mean residence time for soil water at 30 cm depth was slightly higher than that at 80 cm depth (a 9-day difference) on the Laurel watershed, whereas, the mean residence time for soil water at 30 cm depth was notably lower than that at 80 cm depth (a 47-day difference) for the 90 Degree watershed.

The mean residence time for streamwater on the Laurel watershed was higher than that estimated for streamwater on the 90 Degree watershed (Table 3.4). The mean residence times for streamwater on the Laurel and 90 Degree watersheds were 516 days (17.2 months) and 346 days (11.5 months), respectively.

3.3.3. Mean Residence Time Estimated by the FLOWPC Program

3.3.3.1. Input function

The infiltration coefficient was calculated using data for the amount of precipitation and $\delta^{18}O$ compositions in precipitation for three consecutive hydrologic years (2003, 2004, and 2005). The infiltration coefficients, estimated from equation (7), for the Laurel and 90 Degree watersheds were 1.88 and 2.41, respectively. The higher values over 1 estimated for infiltration coefficients might be caused by much lower long-term weighted-mean precipitation $\delta^{18}O$ value of -13.84‰ for the winter and much higher long-term weighted-mean precipitation $\delta^{18}O$ value of -7.80‰ for the summer than the mean $\delta^{18}O$

streamwater for the Laurel (-9.54‰) and 90 Degree (-9.25‰) watersheds. It is not possible to have an infiltration coefficient higher than 1. The Zuber and Maloszewski (2000) reported that the infiltration coefficient is generally within a range of 0.4-0.8 for moderate climates. They note that if mean residence time is 10-20 years, modeling accuracy within this range is only affected slightly by the assumed infiltration coefficient. In addition, Maloszewski and Zuber (1996) suggested that the infiltration coefficient could be assumed by the modeller, where an input function was unavailable. They recommended using a value of 0.5 to 0.7 for the infiltration coefficient, if mean isotopic composition in precipitation was similar to that in groundwater. The assumed infiltration coefficients used for the Laurel and 90 Degree watersheds were 0.59 and 0.67, respectively. Input functions for the two watersheds were obtained from the equation (6) with the assumed infiltration coefficients.

3.3.3.2. Mean residence time for soil water

The estimated mean residence times for soil water and streamwater, as determined by the models, and their respective parameters and goodness of fits are summarized in Table 3.5. The mean residence times for soil water at both 30 cm and 80 cm depths were obtained using the linear-piston flow model (LPM). At the Laurel watershed, the estimated mean residence time and its parameters for soil water using LPM were quite similar between the two different soil depths. For soil water at the Laurel watershed, mean residence time was estimated as 2.4 months (η=3.4) at 30 cm depth, and 2.6 months (η=3.5) at 80 cm depth (Table 3.5, Figures 3.9 and 3.10). However, the model parameters for soil

water at the 90 Degree watershed were not determined to have similar values. At the 90 Degree watershed, the mean residence time for soil water at 30 cm depth was 2.6 months with η=3.5, more than a month shorter than the 3.9 months mean residence time for soil water with η=5.2 at 80 cm depth (Table 3.5, Figures 3.11 and 312).

At 30 cm depth, estimated mean residence times for soil water were similar between the two watersheds; 2.4 months at the Laurel watershed and 2.6 months at the 90 Degree watershed (Table 3.5, Figures 3.9 and 3.11). However, at 80 cm depth, the mean residence time for soil water was 2.6 months for the Laurel watershed, more than a month shorter than the 3.9-month mean residence time estimated for the 90 Degree watershed (Table 3.5, Figures 3.10 and 3.12).

3.3.3.3. Mean residence time for streamwater

The best-fit curve between measured and simulated $\delta^{18}O$ compositions in streamwater at the Laurel watershed is shown in Figure 3.13 (exponential-piston flow model (EPM) with mean residence time=14 months, η=1.15 and dispersion model (DM) with mean residence time= 15 months, P_D=0.67). The simulated $\delta^{18}O$ compositions in streamwater using EPM or DM underestimated, compared to the measured $\delta^{18}O$ compositions in streamwater at the Laurel watershed. Based on SIGMA criterion as goodness of fit, EPM fits better than DM to the measured $\delta^{18}O$ compositions in streamwater at the Laurel watershed (∑=0.117 and ∑=0.119, respectively, Table 3.5). However, based on the ME and r criterion, DM fits better than EPM to the measured $\delta^{18}O$ compositions in streamwater at the Laurel watershed; higher ME and r values with DM.

For streamwater at the 90 Degree watershed, measured and simulated $\delta^{18}O$ compositions are shown in Figure 3.14. Mean residence time for streamwater at the 90 Degree watershed was 11.5 months using EPM with η=1.09, and 10.5 months using DM with P_D =0.66 (Table 3.5 and Figure 3.14). Results were the same with simulated $\delta^{18}O$ in Laurel streamwater. The simulated $\delta^{18}O$ compositions in streamwater using EPM or DM were lower than measured $\delta^{18}O$ compositions in streamwater at the 90 Degree watershed. Mean residence time for streamwater at the 90 Degree watershed was lower than that estimated at the Laurel watershed (a 3.5-month difference with the EPM and a 4.5-month difference with the DM). Based on the results of SIGMA and r criterion, the variation in $\delta^{18}O$ streamwater at the 90 Degree watershed with EPM is a slightly better fit than that with DM, whereas DM fits better than EPM based on the ME criterion (Table 3.5).

3.4. Discussion

3.4.1. Precipitation Input

Precipitation is a major input to the watershed, therefore, understanding the precipitation cycles in $\delta^{18}O$ variations is important. Other studies have found that $\delta^{18}O$ variations in precipitation did not fit strongly with the sine-wave regression model (DeWalle et al., 1997; Burns and McDonnell, 1998; McGuire et al., 2002) due to lack of seasonal variation. In the present study, the $\delta^{18}O$ variations in precipitation were somewhat well fitted with sine-wave regression model (R^2=63%, Table 3.4) and directly influence seasonal variations in the water of interest (soil water and streamwater) at the watershed. The strong correlation between the monthly $\delta^{18}O$ composition in precipitation and the

monthly mean air temperature indicates that the $\delta^{18}O$ variations in precipitation can be easily obtained with a known air temperature.

The average amplitude of the $\delta^{18}O$ variations in precipitation was 6.06‰ during the three consecutive hydrologic years (2003, 2004, and 2005). This value was markedly higher than precipitation amplitudes reported by other studies of regions with similar climates. DeWalle et al. (1997) and McGuire et al. (2002) reported 3.15‰ and 1.84‰ amplitudes in precipitation, respectively, which resulted in unclear seasonality.

3.4.2. Soil Water Mean Residence Time

Mean residence time for soil water based on other isotope studies in forested watersheds are summarized in Table 3.6. In the Method category of Table 3.6, sine-wave regression assumes precipitation as an input and soil water as an output from a steady state, well-mixed reservoir. The exponential distribution of residence times was also assumed. However, in this study, exponential flow, dispersion flow, and exponential-piston flow models appeared to be the best residence time distributions as determined by goodness of fit.

In the current study, the mean residence time for soil water at 30 cm depth using the sine-wave regression model was 81 days to 95 days, a quite similar result to that reported by Burns and McDonnell (1998) using zero-tension lysimeters and to DeWalle et al. (1997) using tension lysimeters at the same soil depth with same method. Estimated mean residence time for soil water at 80 cm depth using the sine-wave regression model was 86 days to 128 days for the present study. This is similar to the results reported by

Stewart and McDonnell (1991) using zero-tension lysimeters. At the Maimai headwater catchment in New Zealand, Stewart and McDonnell used the same residence time calculation method to estimate the 12- to more than 100-day mean residence time of soil water at soil depths ranging from 20 cm to 80 cm.

Based on response function models in the system, the best fits between measured and computed $\delta^{18}O$ variations in soil water in the current study were obtained with the linear-piston flow model (LPM), which has characteristics of both the linear flow and the piston flow system; the linear flow reservoir is serially connected with the piston flow reservoir (Bayari, 2002). The LPM has seldom been used to estimate the mean residence time of water in the watershed. However, McGuire et al. (2002) investigated the mean residence time of subsurface water in the same climate region and estimated the mean residence time for soil water using the dispersion model with a value of P_D=0.1. McGuire et al. (2002) inferred the piston-flow response in soil water based on a derived lower value of the dispersion parameter. Kreft and Zuber (1978) demonstrated that a dispersion model with a value of $P_D = 0$ represented piston flow conditions in a system. In the current study, the derived values of the fitting parameter (η) for LPM were quite large, ranging from 3.4 to 5.2, depending on soil characteristics and sampling depth and location on the two watersheds.

Mean residence time for soil water at 30 cm depth estimated by LPM was 72 days to 78 days; this was slightly shorter than that estimated by the sine-wave regression model in the present study, and more than 30 days longer than that estimated by the exponential model (Asano et al., 2002) and by the dispersion model (Stewart and McDonnell, 1991) at

40 cm depth (Table 3.6). Asano et al. (2002) determined mean residence time for soil water collected from zero-tension lysimeters. Soil water collected in this way can be expected to have a shorter residence time due to the collection of rapidly percolating gravitational soil water. Swistock et al. (1990) compared the soil leachate chemistry from tension lysimeters with that from zero-tension lysimeters and observed that zero tension lysimeters collected more macropore soil water, whereas tension lysimeters collected longer residence time on micropore soil water.

In the current study, mean residence time of soil water at 80 cm depth was 78-117 days using LPM, somewhat longer than that found by other studies using the dispersion model (Stewart and McDonnell, 1991; McGuire et al., 2002); mean residence time for soil water was reported as 63 days at 80 cm depth (Stewart and McDonnell, 1991), and 48 days at 100 cm depth (McGuire et al., 2002). In the present study, the mean residence time for soil water estimated by the simple sine-wave regression model provides quite similar results to those obtained by the response function model in a system using the FLOWPC program with goodness of fit.

Based on the results from response of soil water chemistry to liming at the 90 Degree watershed, pH, conductivity, and concentrations of calcium, magnesium, and acid neutralizing capacity in soil water at 30 cm depth increased significantly within four months after limestone sand application ($\alpha \leq 0.05$). The Ca/Al molar ratio of soil water at 80 cm depth also greatly increased within four months after liming. In general, the mean residence time of soil water, estimated by ^{18}O as a tracer for the water source was in accord with the timing of responses of soil water chemistry to liming.

3.4.3. Streamwater Mean Residence Time

The mean residence time for streamwater at the Laurel watershed estimated using the simple sine-wave regression model was 17.2 months (1.43 years), about 2 to 3 months shorter than estimates from both the dispersion model (DM) and the exponential-piston flow model (EPM). Based on water quality results, the streamwater at the Laurel watershed showed a pattern of increase in concentrations of Ca and Mg and in values of conductivity and acid neutralizing capacity within 1.5 years after liming.

The estimated mean residence time for streamwater at the 90 Degree watershed using the sine-wave regression model was 11.5 months (0.96 years), quite similar to the values determined from the response function models (DM -10.5 months; EPM -11.5 months). The sine-wave regression method seems to provide reasonable estimates of mean residence times for streamwater. Based on the results from response of water chemistry to limestone sand application, the streamwater at the 90 Degree watershed had a pattern of increase in concentrations of Ca and Mg and in values of conductivity acid neutralizing capacity about 16 months after liming. An additional four months were required in order to have limestone treatment effects on streamwater than the mean residence time of streamwater at the 90 Degree watershed. In general, the mean residence time of streamwater in these watersheds agreed with results from the streamwater chemistry response to liming application to some extent.

Table 3.7 summarizes the estimated mean residence times for streamwater using stable isotopes in forested watersheds based on other research. Depending on weather and

watershed characteristics, the mean residence time for streamwater in the other studies was quite varied; 0.25 years to more than 5 years estimated using the sine-wave regression model, and 0.4 years to 3.38 years estimated using the response function models with the lumped parameter approach. The estimated mean residence time for streamwater in the current study was within the range of results obtained from previous studies.

The η parameter for the EPM is defined as the ratio of the total volume to the exponential flow model volume. The closer to η=1, the larger the portion of the residence time distribution is from the exponential model. The best-fit curve in streamwater at the Laurel watershed was obtained using EPM with a value of η=1.15; this indicated that 13% of the volume was derived from the piston flow model, and 87% of the volume from the exponential model. Similarly, the mean residence time of streamwater at the 90 Degree watershed was estimated using the EPM with a value of η=1.09; this indicated that 8.3% of the volume derived from the piston flow model, and the rest of volume derived from the exponential flow model. The Laurel watershed had more piston flow volume in proportion to the total streamwater than did the 90 Degree watershed.

The best-fit curve in streamwater using the dispersion model was obtained with values of P_D=0.66 for the Laurel watershed and P_D=0.67 for the 90 Degree watershed. The determined dispersion parameters (P_D) for the two watersheds were quite similar and had somewhat higher values, indicating higher variations in the length of flow pathways in the watersheds. The dispersion parameters found in other residence time studies on forested watersheds were 0.15 (Maloszewski et al., 1983), 0.31 (McGuire et al., 2002), and 0.87 (Viville et al., 2006) using a dispersion model as a best-fit response function model in the

system. Although the values of the dispersion parameters found in the current study were rather high, they were still within the range of other studies conducted on forested watersheds.

3.5. Summary and Conclusion

The mean residence times of water on two small forested watersheds (Laurel and 90 Degree) in central Pennsylvania, USA, was investigated using the sine-wave regression and response function models based on the lumped parameter approach. A strong correlation between monthly mean air temperature and monthly $\delta^{18}O$ composition in precipitation indicated that air temperature may be used to predict the $\delta^{18}O$ variations in precipitation.

The mean residence time of water estimated by the simple sine-wave regression method provided similar results to those obtained by the response function model; this similarity indicated that the simple sine-wave regression method was adequate to estimate the mean residence time of water in these watersheds. The mean residence time of soil water collected from tension lysimeters was about 2 to 4 months, depending on soil characteristics and sampling depth and location. The estimated mean residence time of soil water agreed well with the chemical effects of liming treatment on soil water. At the watershed scale, the estimated mean residence time for streamwater was about 14 to 17 months at the Laurel watershed, and 11 to 12 months at the 90 Degree watershed, depending on the determined model type. The chemical effects of limestone sand applied to the watersheds would likely be manifested in streamwater within 1.5 years of application. The estimated mean residence time of streamwater in these watersheds was in general

agreement with the water quality results.

Based on lumped parameter models, the determined model type using goodness of fit provided the flow characteristics of the system. At the watershed scale, the mean residence time for streamwater estimated using the exponential-piston flow model indicated that 13% and 8.3% of total streamwater was derived from the piston flow model at the Laurel and 90 Degree watersheds, respectively.

3.6. References

Asano, Y., Uchida, T., Nobuhito, O., 2002. Residence times and flow paths of water in steep unchannelled catchment, Tanakami, Japan. Journal of Hydrology 261, 173-192.

Bayari, S., 2002. TRACER: an EXCEL workbook to calculate mean residence time in groundwater by use of tracers CFC-11, CFC-12 and tritium. Computers and Geosciences 28, 621-630.

Burns, D.A., McDonnell, J.J., 1998. Effects of a beaver pond on runoff processes: comparison of two headwater catchments. Journal of Hydrology 205, 248-264.

DeWalle, D.R., Edwards, P.J., Swistock, B.R., Aravena, R., Drimmie, R.J., 1997. Seasonal isotope hydrology of three Appalachian forest catchments, Hydrological Processes 11, 1895-1906.

DeWalle, D.R., Swistock, B.R. and Sharpe, W.E., 1988. Three component tracer model for stormflow on a small Appalachian forested catchment. Journal of Hydrology 104, 301-310.

Epstein, S., Mayeda, T., 1953. Variation of ^{18}O content of water from natural sources. Geochimica Cosmochimica Acta 4, 213-224.

Grabczak, J., Maloszewski, P., Rózanski, K., Zuber, A., 1984. Estimation of the tritium input function with the aid of stable isotopes. Catena 11, 105-114.

Hornberger, G.M., Mills, A.L., Herman, J.S., 1992. Bacterial transport in porous media: evaluation of a model using laboratory observations. Water Resources Research 28, 915-938.

Kreft, A., Zuber, A., 1978. On the physical meaning of the dispersion equation and its waters for different initial and boundary conditions. Chemical Engineering Science 33, 1471-1480.

Maloszewski, P., Zuber, A., 1982. Determining the turnover time of groundwater systems with the aid of environmental tracers. 1. Models and their applicability. Journal of Hydrology 57, 207-231.

Maloszewski, P., Rauert, W., Stichler, W., Herrmann, A., 1983. Application of flow models in an alpine catchment area using tritium and deuterium data. Journal of Hydrology 66, 319-330.

Maloszewski, P., Zuber, A., 1996. Lumped parameter models for the interpretation of environmental tracer data, Manual on Mathematical Models in Isotope Hydrogeology. IAEA-TECDOC-910, International Atomic Energy Agency, Vienna, Austria pp. 9-58.

McDonnell, J.J., 1990. A rational for old water discharge through macropores in a steep, humid catchment. Water Resources Research 26, 2821-2832.

McGuire, K.J., DeWalle, D.R., Gburek, W.J., 2002. Evaluation of mean residence time in subsurface waters using oxygen-18 fluctuations during drought conditions in the mid-Appalachians. Journal of Hydrology 261, 132-149.

Rodgers, P., Soulsby, C., Waldron, S., Tetzlaff, D., 2005. Using stable isotope tracers to assess hydrological flow paths, residence times and landscape influences in a nested mesoscale catchment. Hydrology and Earth System Sciences 9, 139-155.

Rodhe, A., 1981. Spring flood: meltwater or groundwater? Nordic Hydrology 12, 21-30.

Sklash, M.G., Farvolden, R.N., Fritz, P., 1976. A conceptual model of watershed response to rainfall, developed through the use of oxygen-18 as a natural tracer. Canadian Journal of Earth Science 13, 271-283.

Soulsby, C., Malcolm, R., Helliwell, R., Ferrier, R.C., and Jenkins, A., 2000. Isotope hydrology of the Allt a'Mharcaidh catchment, Cairngorms, Scotland: implications for hydrological pathways and residence times. Hydrological Processes 14, 747-762.

Stewart, M.K., McDonnell, J.J., 1991. Modeling base flow soil water residence times from deuterium concentrations. Water Resources Research 27, 2681-2693.

Swistock, B.R., Yamona, J.J., DeWalle, D.R., Sharpe, W.E., 1990. Comparison of soil water chemistry and sample size requirements for pan vs. tension lysimeters. Water, Air, and Soil Pollution 50, 387-396.

Viville, D., Ladouche, B., Bariac, T., 2006. Isotope hydrological study of mean transit time in the granitic Strengbach catchment (Vosges massif, France): application of the FlowPC model with modified input function. Hydrological Processes 20, 1737-1751.

Zuber, A., Maloszewski P., 2000. Lumped parameter models, Environmental Isotopes in the Hydrological Cycle, Volume VI. Modelling. IAEA/UNESCO, Paris, Technical Documents in Hydrology 39, 5-35.

Table 3.1. Notations for sampling locations.

Symbol	Definition
PR	Precipitation
LA-30	Soil water at 30 cm depth at the Laurel watershed
LA-80	Soil water at 80 cm depth at the Laurel watershed
LA-ST	Streamwater at the Laurel watershed
90-30	Soil water at 30 cm depth at the 90 Degree watershed
90-80	Soil water at 80 cm depth at the 90 Degree watershed
90-ST	Streamwater at the 90 Degree watershed

Table 3.2. Summaries of the characteristics of isotopic compositions ($\delta^{18}O$) in precipitation, soil water, and streamwater for the Laurel and 90 Degree watersheds during the study period (2002-2005).

Sampling locations	Symbol	n	$\delta^{18}O$ composition			
			Minimum (‰)	Mean (‰)	Maximum (‰)	Standard deviation
Precipitation	PR	46	-20.17	-10.55	-3.4	4.16
Laurel watershed						
Soil water at 30 cm depth	LA-30	8	-11.11	-9.18	-4.78	2.23
Soil water at 80 cm depth	LA-80	9	-10.60	-8.40	-3.83	2.42
Streamwater	LA-ST	28	-10.65	-9.56	-8.71	0.48
90 Degree watershed						
Soil water at 30 cm depth	90-30	10	-11.37	-7.84	-4.31	2.33
Soil water at 80 cm depth	90-80	10	-10.34	-8.26	-5.31	1.87
Streamwater	90-ST	28	-10.59	-9.28	-8.39	0.61

Table 3.3. Summaries of the means and amplitudes of $\delta^{18}O$ compositions and isotopic damping depths in precipitation, soil water, and streamwater for the Laurel and 90 Degree watersheds during the hydrologic years 2004 and 2005.

Sampling locations	Symbol	Hydrologic year 2004			Hydrologic year 2005		
		$\delta^{18}O$ composition (‰)		Damping depth (cm)	$\delta^{18}O$ composition (‰)		Damping depth (cm)
		Mean	Amplitude		Mean	Amplitude	
Precipitation	PR	-10.17	5.36		-11.15	6.80	-
Laurel watershed							
Soil water at 30 cm depth	LA-30	-	-	-	-9.18	3.17	39.26
Soil water at 80 cm depth	LA-80	-	-	-	-8.40	3.41	115.79
Streamwater	LA-ST	-9.48	0.60	45.66	-9.54	0.76	45.68
90 Degree watershed							
Soil water at 30 cm depth	90-30	-	-	-	-7.85	3.53	45.78
Soil water at 80 cm depth	90-80	-	-	-	-8.26	2.51	80.40
Streamwater	90-ST	-9.27	1.05	61.26	-9.25	0.97	51.32

Table 3.4. Summaries of mean residence times for soil water and streamwater at the Laurel and 90 Degree watersheds using sine-wave regression models during two hydrologic years (October 2003-September 2005).

Sampling locations	**Symbol**	**Goodness of fit**			**Mean residence time (MRT)**	
		Coefficient of determination		**RMSE** (‰)		
		R^2	***p*-value**		**(days)**	**(months)**
Precipitation	PR	0.626	0.000	2.570		
Laurel watershed						
Soil water at 30 cm depth	LA-30	0.847	0.001	0.854	95	3.2
Soil water at 80 cm depth	LA-80	0.577	0.018	1.355	86	2.9
Streamwater	LA-ST	0.786	0.000	0.071	516	17.2
90 Degree watershed						
Soil water at 30 cm depth	90-30	0.623	0.007	1.513	81	2.7
Soil water at 80 cm depth	90-80	0.225	0.166	1.543	128	4.3
Streamwater	90-ST	0.555	0.000	0.494	346	11.5

Table 3.5. Summaries of estimated mean residence times (t_t) of soil water and streamwater at the Laurel and 90 Degree watersheds using the FlowPC program.

Sampling locations	Symbol	Model	Model parameters		Goodness of fit			
			η or P_D	t_t	SIGMA	ME	Pearson's correlation coefficient	
			(dimensionless)	(months)			r	*p*-value
Laurel watershed								
Soil water at 30 cm depth	LA-30	LPM	3.4	2.4	0.2724	0.8737	0.909	0.002
Soil water at 80 cm depth	LA-80	LPM	3.5	2.6	0.3635	0.7775	0.894	0.001
Streamwater	LA-ST	DM	0.67	15.0	0.1189	0.4296	0.859	0.000
Streamwater	LA-ST	EPM	1.15	14.0	0.1171	0.3613	0.834	0.000
90 Degree watershed								
Soil water at 30 cm depth	90-30	LPM	3.5	2.6	0.3462	0.7877	0.915	0.000
Soil water at 80 cm depth	90-80	LPM	5.2	3.9	0.3658	0.6068	0.818	0.004
Streamwater	90-ST	DM	0.66	10.5	0.1849	0.3478	0.828	0.000
Streamwater	90-ST	EPM	1.09	11.5	0.1707	0.2456	0.828	0.000

Table 3.6. Estimated mean residence time for soil water based on other isotope studies in forested areas.

Reference	Place	Soil depth (cm)	MRT (days)	Method
Stewart and McDonnell (1991)	New Zealand	20-80	12- to more than 100	sine-wave regression
		20	13	dispersion model
		40	42	dispersion model
		80	63	dispersion model
DeWalle et al. (1997)	PA, USA	30	73	sine-wave regression
Burns and McDonnell (1998)	New York, USA	8-12	63	sine-wave regression
		30	80	sine-wave regression
Soulsby et al. (2000)	Scotland	Not defined*	73-219	sine-wave regression
Asano et al. (2002)	Japan	10	0-12	exponential model
		10	6-12	exponential-piston flow model
		40	9-27	exponential model
McGuire et al. (2002)	PA, USA	100	48	dispersion model

An asterisk indicated that soil water was estimated by a hydrograph separation technique from streamwater at high flow conditions.

Table 3.7. Estimated mean residence time for streamwater based on other isotope studies in forested areas.

Reference	Place	Area (km^2)	MRT (years)	Method
DeWalle et al. (1997)	PA, USA	11.34	> 5.0	sine-wave regression
	WV, USA	0.34	1.6	sine-wave regression
		0.39	1.4	sine-wave regression
Burns and McDonnell (1998)	NY, USA	0.41	0.28	sine-wave regression
		0.61	0.28	sine-wave regression
Soulsby et al. (2000)	Scotland	10.00	> 5.0	sine-wave regression
		1.69	3.6	sine-wave regression
		2.96	> 5.0	sine-wave regression
Asano et al. (2002)	Japan	0.0010	> 1.0	exponential model
		0.0018	1.01	exponential model
			1.06	exponential-piston flow model
McGuire et al. (2002)	PA, USA	1.23	0.4	exponential-piston flow model
			0.43	dispersion model
Rodgers et al. (2005)	Scotland	1.3	0.25	sine-wave regression
		30	0.94	sine-wave regression
		42	0.54	sine-wave regression
		61	1.14	sine-wave regression
		91	0.53	sine-wave regression
		233	0.57	sine-wave regression
Viville et al. (2006)	France	0.80	3.38	exponential piston-flow model
			3.33	exponential model
			2.38	dispersion model

Figure 3.1. Location of two study watersheds, Laurel and 90 Degree, and sampling sites.

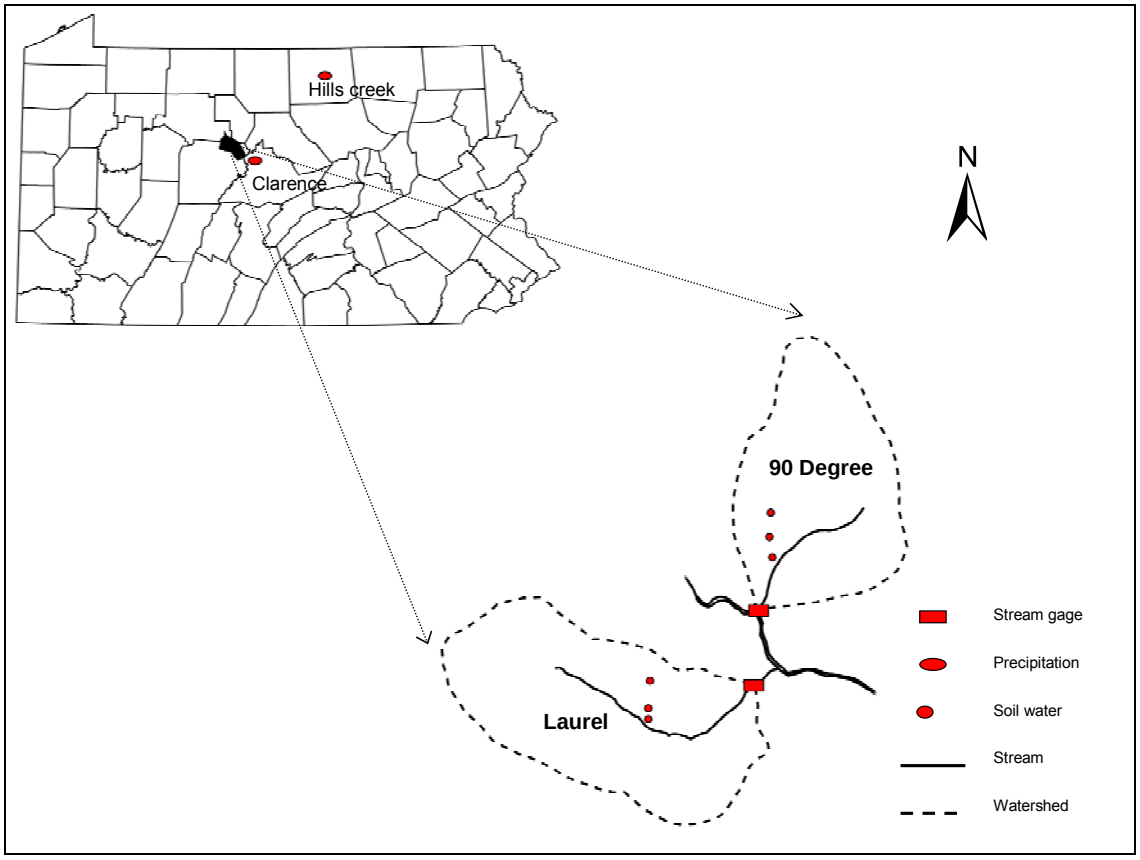

Figure 3.2. Temporal variations in monthly total precipitation and mean air temperature (upper) and $\delta^{18}O$ compositions in precipitation (lower) during the study period (2002-2005). Precipitation and temperature were monitored at the Clarence climate station (elevation 423.7m, 41°03'N / 77°57'W) and precipitation samples for ^{18}O analysis were collected at Hills Creek State Park (elevation 476 m, 41º48′16″ / 77º11′25″).

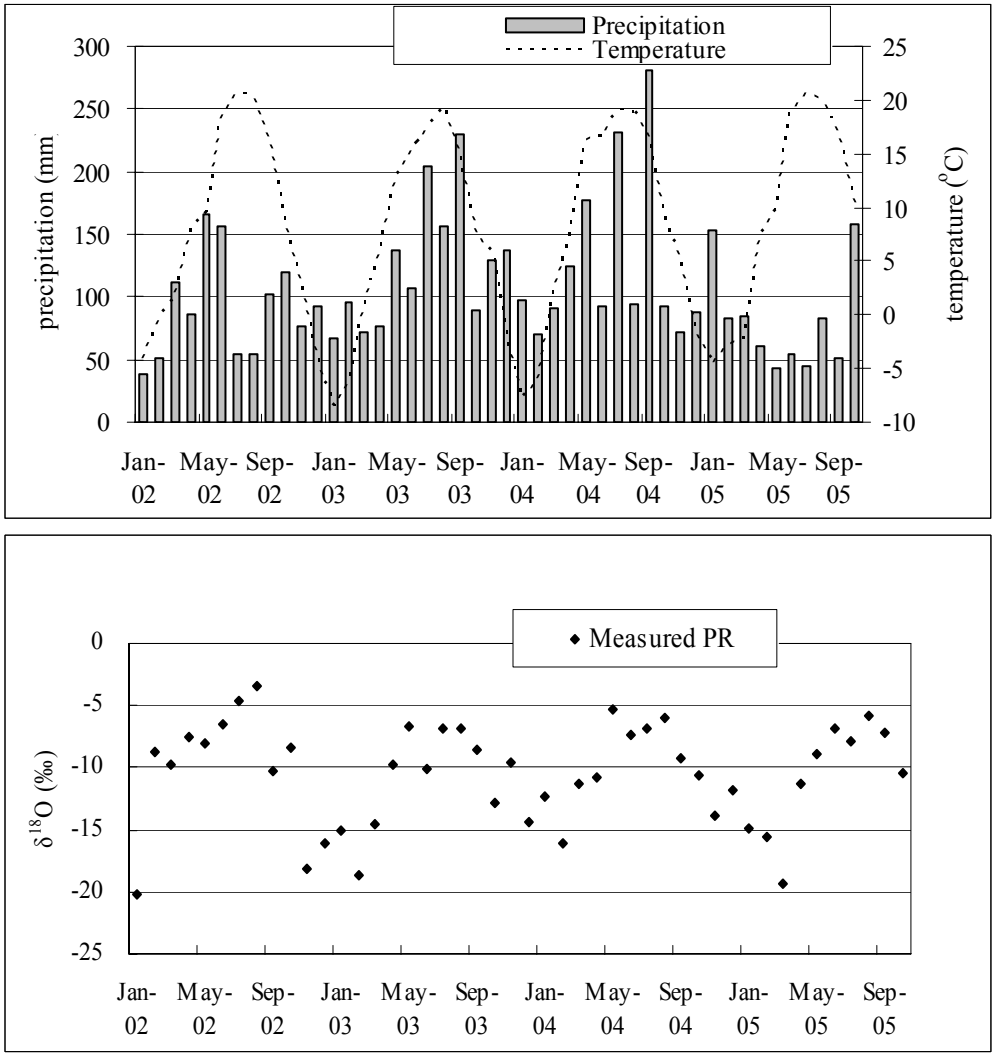

Figure 3.3. Relationship between monthly $\delta^{18}O$ of precipitation and mean monthly air temperature during the study period (2002-2005).

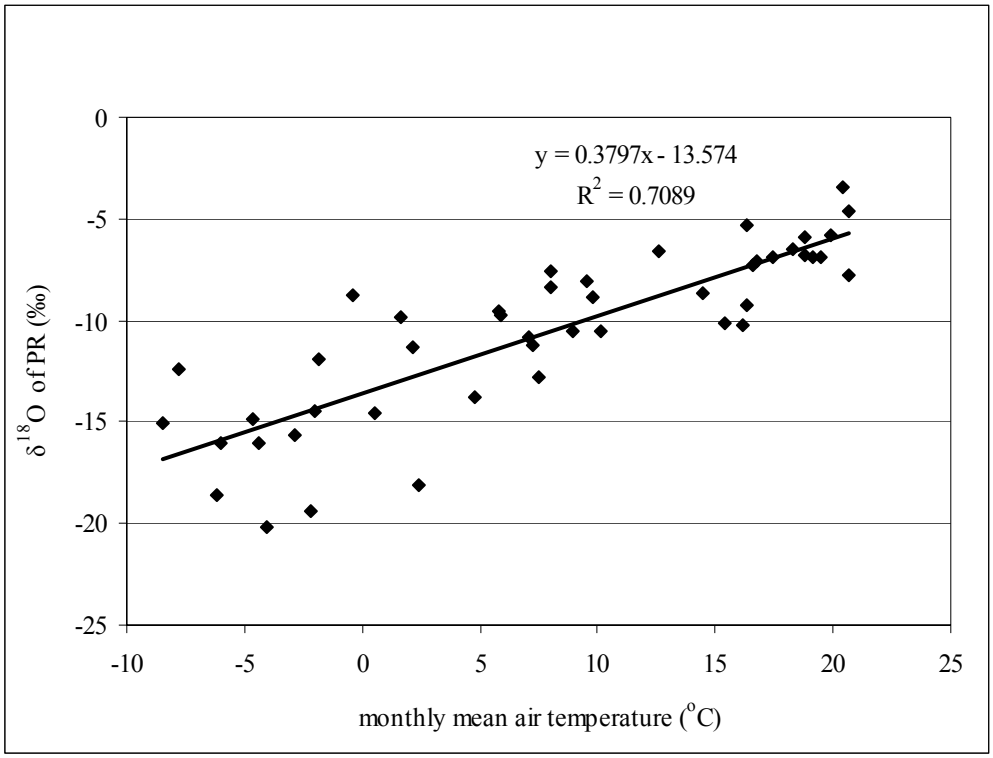

Figure 3.4. Temporal variations of $\delta^{18}O$ composition in precipitation and streamwater at the Laurel and 90 Degree watersheds (July 2003-October 2005).

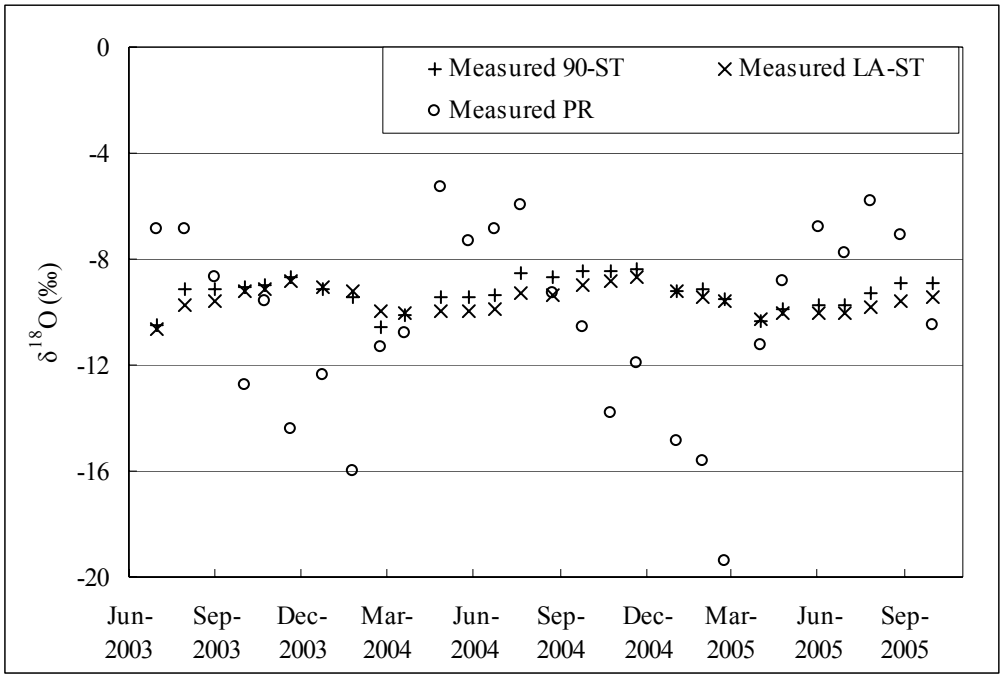

Figure 3.5. A fitted sine-wave regression model to $\delta^{18}O$ composition in precipitation during the study period (January 2002-October 2005).

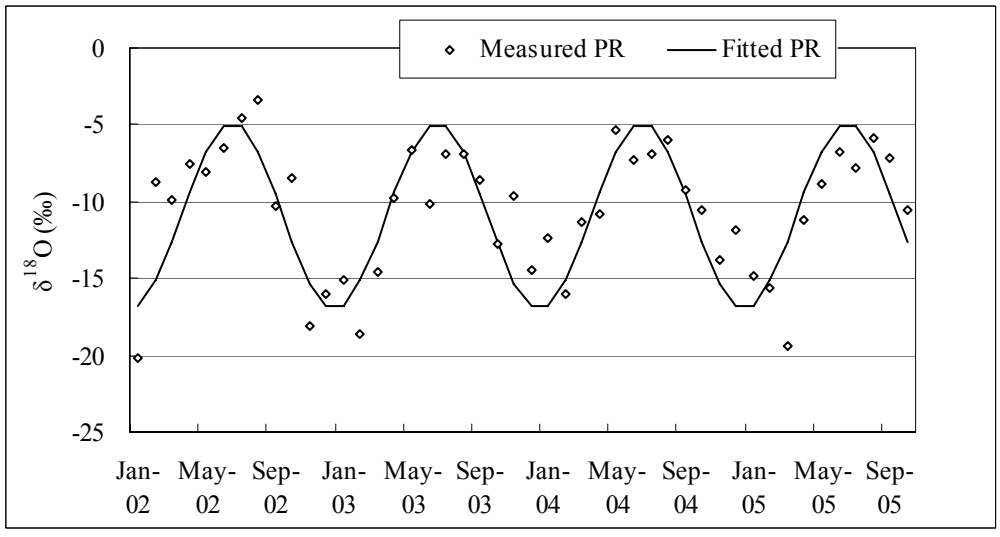

Figure 3.6. Temporal variations of $\delta^{18}O$ composition in soil water at 30 cm depth and 80 cm depth, and fitted sine-wave regression models to soil water at the Laurel watershed (April to October 2005).

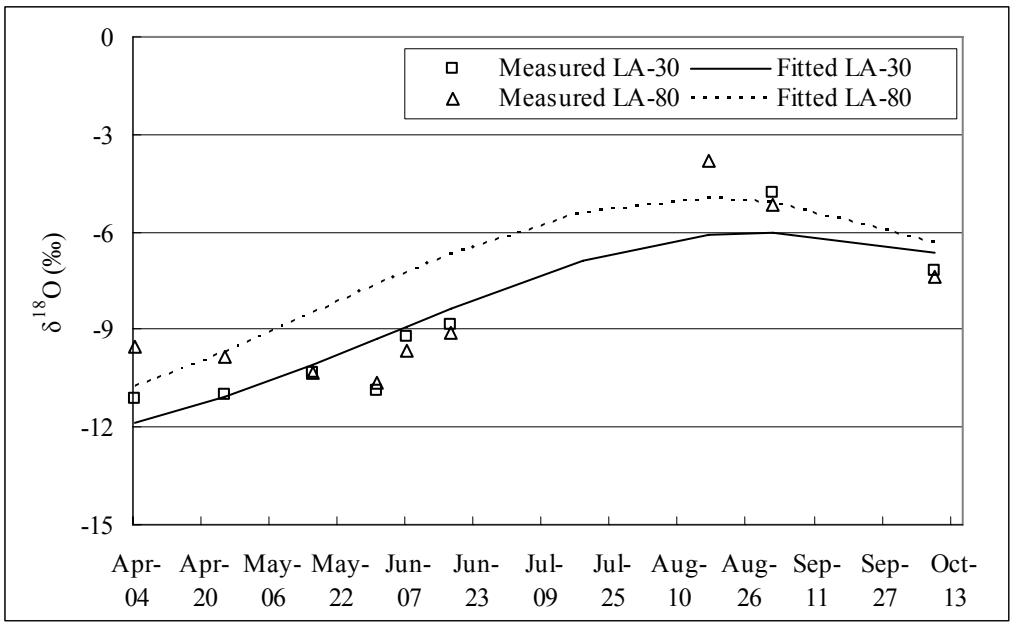

Figure 3.7. Temporal variations of $\delta^{18}O$ composition in soil water at 30 cm depth and 80 cm depth, and fitted sine-wave regression models for soil water at the 90 Degree watershed (April to October 2005).

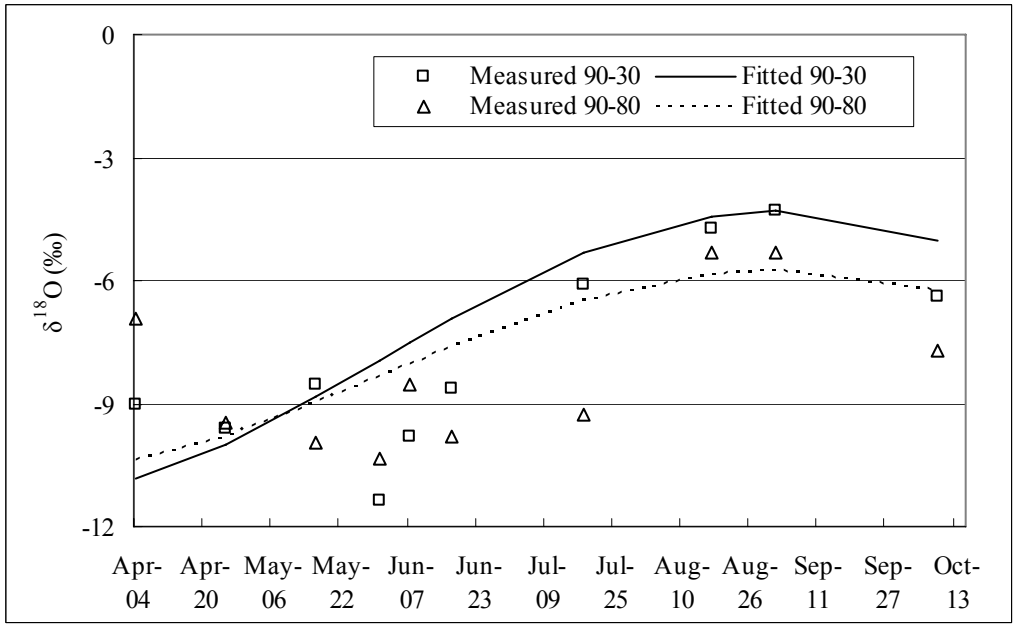

Figure 3.8. Temporal variations of monthly $\delta^{18}O$ composition in streamwater, and fitted sine-wave regression models for streamwater at the Laurel and 90 Degree watersheds (July 2003-October 2005).

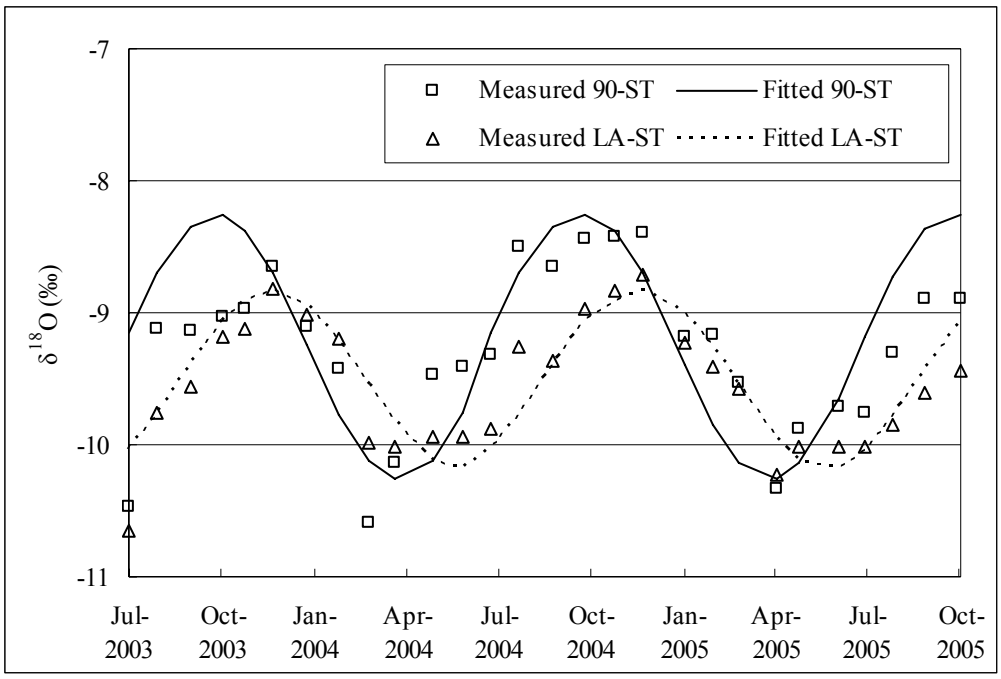

Figure 3.9. Fitted and measured $\delta^{18}O$ composition in soil water at 30 cm depth for the Laurel watershed in 2005 (LPM, linear-piston flow model).

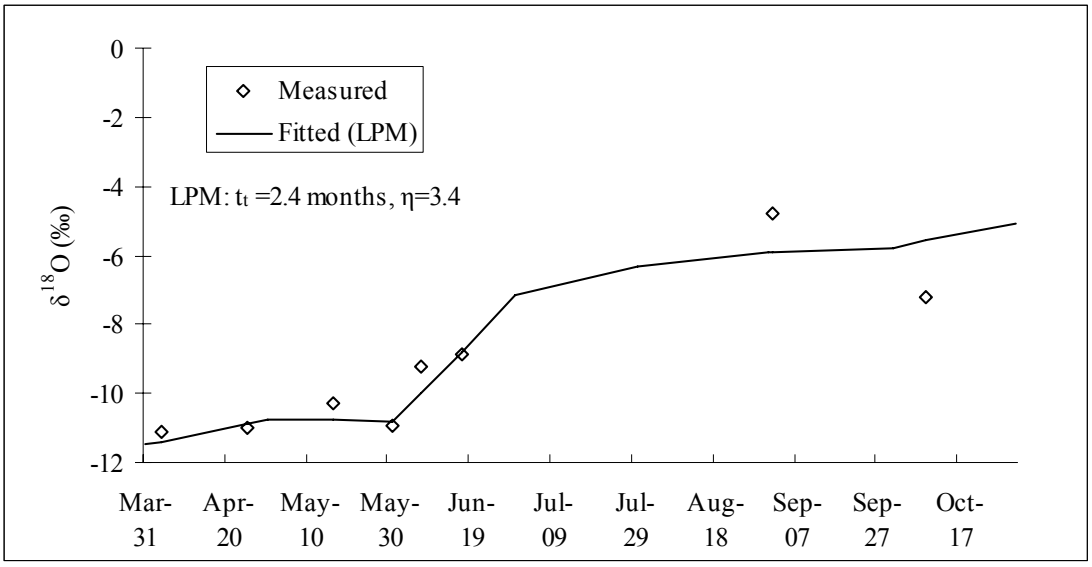

Figure 3.10. Fitted and measured $\delta^{18}O$ composition in soil water at 80 cm depth for the Laurel watershed in 2005 (LPM, linear-piston flow model).

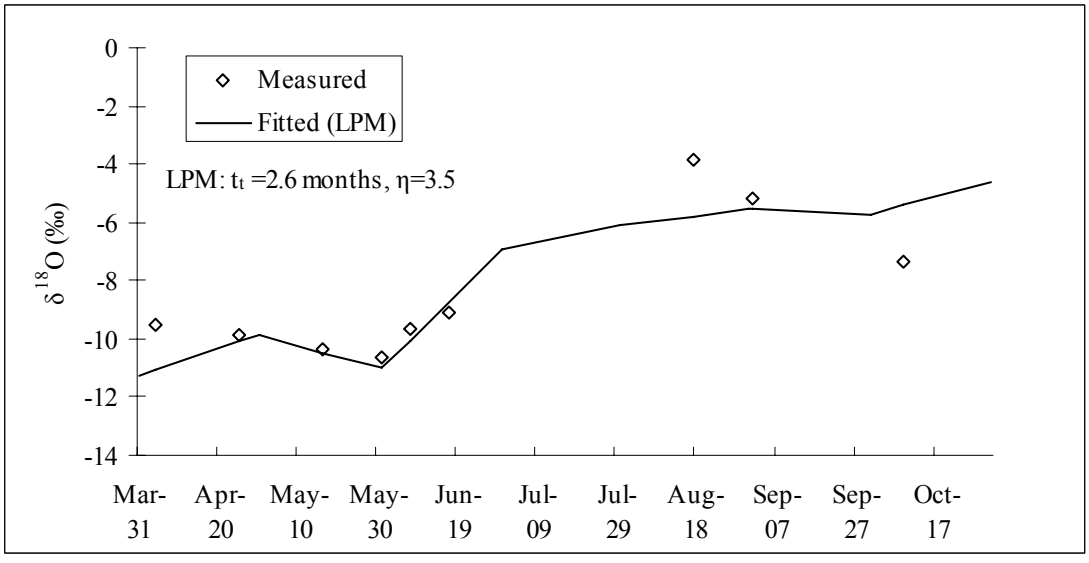

Figure 3.11. Fitted and measured $\delta^{18}O$ composition in soil water at 30 cm depth for the 90 Degree watershed in 2005 (LPM, linear-piston flow model).

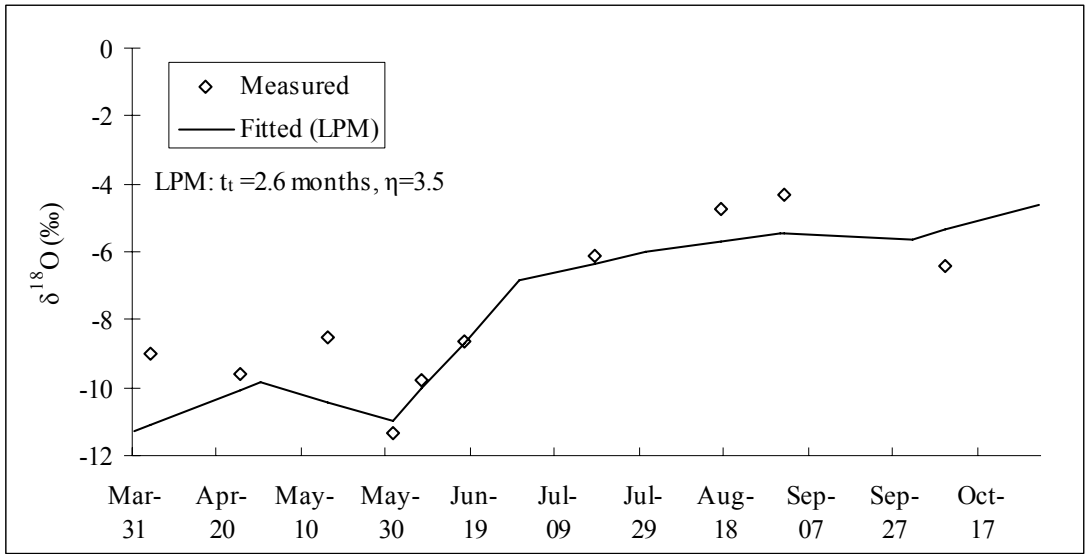

Figure 3.12. Fitted and measured $\delta^{18}O$ composition in soil water at 80 cm depth for the 90 Degree watershed in 2005 (LPM, linear-piston flow model).

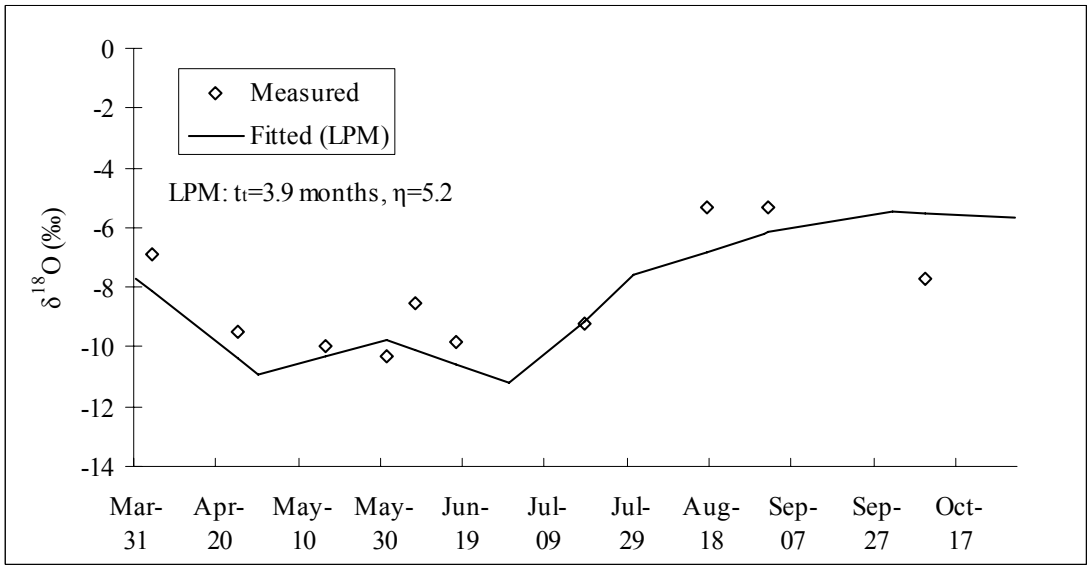

Figure 3.13. Fitted and measured $\delta^{18}O$ composition in streamwater at the Laurel watershed (July 2003-October 2005). The residence time distributions of the dispersion model (DM) and the exponential-piston flow model (EPM) are shown inset top right.

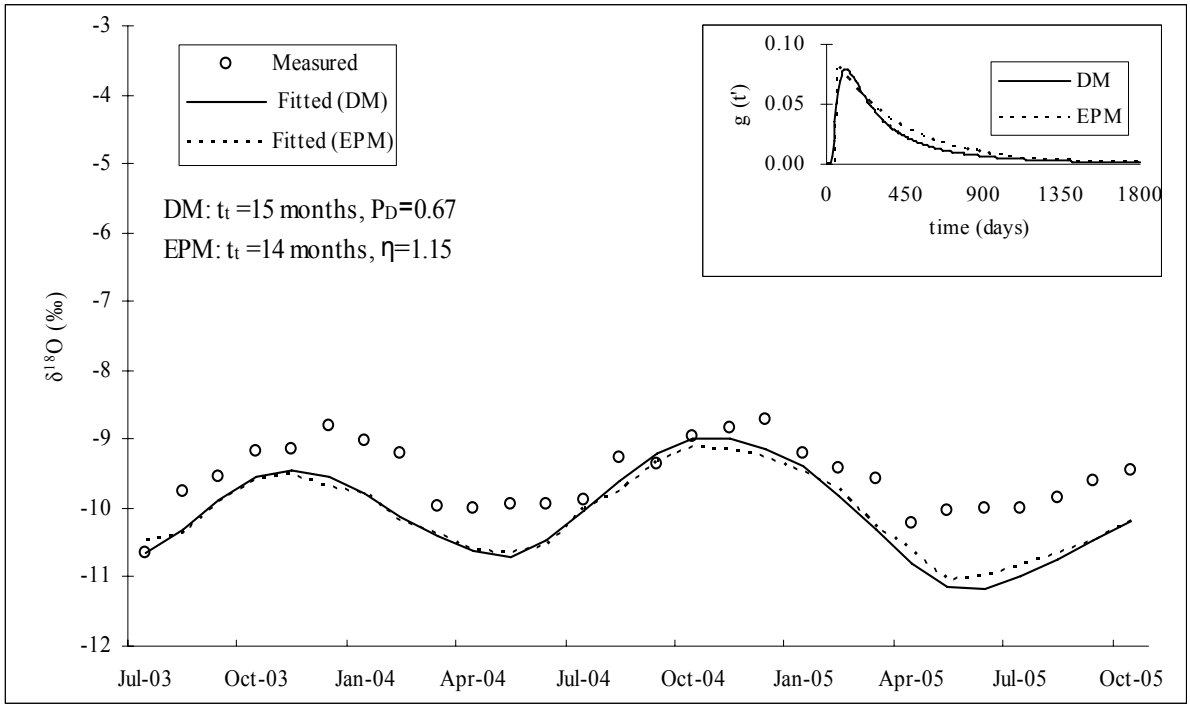

Figure 3.14. Fitted and measured $\delta^{18}O$ composition in streamwater at the 90 Degree watershed (July 2003-October 2005). The residence time distributions of the dispersion model (DM) and the exponential-piston flow model (EPM) are shown inset top right.

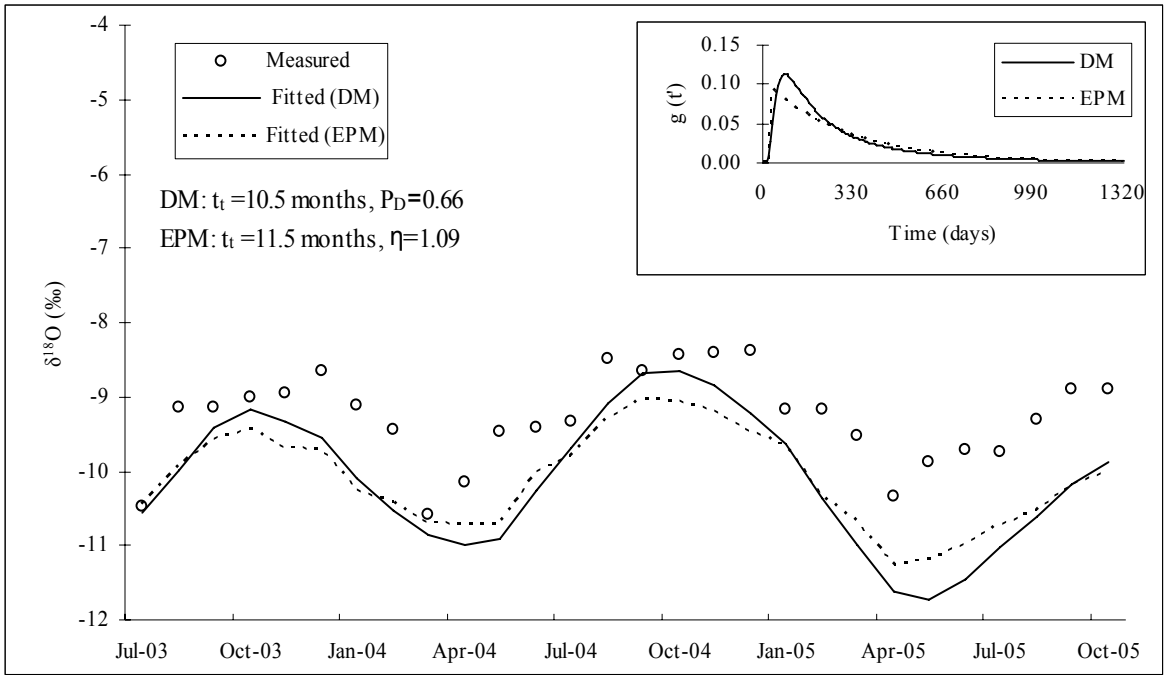

Chapter 4. Changes in Ca/Sr, Mg/Sr, and $^{87}Sr/^{86}Sr$ Ratios in Soil Water and Streamwater: Effects of Liming on an Acidified Watershed

ABSTRACT

In order to study liming treatment effects on soil water and streamwater, element concentrations (Ca, Mg, Sr) and $^{87}Sr/^{86}Sr$ ratios were measured in precipitation, throughfall, soil water, and streamwater in a small (1.36 km^2) acidified watershed (90 Degree) located in northcentral Pennsylvania, USA. Limestone sand was applied at a rate of 5 t ha^{-1}over 76 percent of the watershed in fall 2003 and three soil plots (15.2 meter by 9.1 meter) within the watershed in summer 2005. At the soil plot scale, there were increasing trends in soil water Ca/Sr and Mg/Sr ratios two months after liming. At the watershed scale, streamwater treatment effects were observed about 16 months after liming in the form of increasing concentrations of Ca, Mg, Sr and Ca/Sr and Mg/Sr ratios along with decreased $^{87}Sr/^{86}Sr$ ratios. In this study, limestone sand treatment rapidly improved nutrients in soil water and $^{87}Sr/^{86}Sr$ ratio was very useful as a solute tracer to confirm treatment effects in streamwater.

4.1. Introduction

Strontium has four naturally occurring stable isotopes with the following abundances ^{84}Sr (0.6%), ^{86}Sr (9.9%), ^{87}Sr (7.0%), and ^{88}Sr (82.5%). The isotopic abundances of ^{84}Sr, ^{86}Sr, and ^{88}Sr are constant in all earth materials, whereas the abundance of ^{87}Sr varies — an effect produced by the radioactive decay of ^{87}Rb (half-life=$48.8*10^9$ years). The $^{87}Sr/^{86}Sr$ ratio expresses the relative isotopic abundance of ^{87}Sr. Strontium (Sr) is one of the group 2 elements in the periodic table, with beryllium (Be), magnesium (Mg), calcium (Ca), barium (Ba), and radium (Ra).

Strontium has a relatively high atomic mass of 87.62 such that biological and geological processes modify a very small amount of its isotopic ratio compared to that in low atomic mass isotopes, such as H and O (Capo et al., 1998). Elemental concentrations are affected by physical (temperature and salinity) and biological factors (growth and maturation), whereas, the relative abundance of Sr isotopes is not influenced by these factors (Fowler et al., 1995; Friedland et al., 1998; Kennedy et al., 2000). Thus, the measured Sr isotopes provide more clearer results as environmental tracers than do element concentrations (Gunn et al., 1992; Fowler et al., 1995). Natural and analytical fractionation of the $^{87}Sr/^{86}Sr$ ratio is corrected in the mass spectrometer by normalizing to the stable isotope $^{86}Sr/^{88}Sr$ ratio of 0.1194 (Stewart et al., 2001). As a result, because the measured $^{87}Sr/^{86}Sr$ ratios reflecting only the relative contributions of Sr from isotopically distinct sources a greater degree of precision is achieved (Capo et al., 1998).

Because Sr and Ca manifest similar behavior due to their chemical similarities (ex, same valence and similar ionic radius), $^{87}Sr/^{86}Sr$ ratio has been used as a tracer of calcium sources, transportation, and cycling in forest ecosystems (Gosz et al., 1983; Graustein and Armstrong, 1983; Åberg et al., 1990; Åberg, 1995; Bailey et al., 1996; Blum and Erel, 1997; Clow et al., 1997; Kennedy et al., 1998).

The purpose of this study was to understand the effects of dolomitic limestone sand application over an acidified watershed using strontium isotopes as a solute tracer. Analyses of strontium isotopes in soil water and streamwater were used to confirm the presence of treatment effects in the drainage water of the treated watershed.

4.2. Methods

4.2.1. Study Area

The study site was the 90 Degree watershed, located within the Moshannon State Forest, Pennsylvania (Figure 4.1). The 90 Degree watershed has an area of 1.36 km^2 and is drained by a first-order stream within the Mosquito Creek basin. The elevation in the watershed ranges from 536 m to 674 m. Located within the Allegheny Plateau physiographic province, the watershed is mainly covered by northern hardwood forest. Soils are acidic with very stony loam in the Clymer, Cookport, and Hazleton series. The soils overlaying the Pottsville and Burgoon Sandstone formations are sandstone, conglomerate, and shale. The watershed receives an average precipitation of 1056 mm, annually.

4.2.2. Data Collection

A total of 10 rainfall events, 5 events before limestone sand application and 5 events after limestone sand application, were monitored from April 4 to October 9, 2005. Precipitation, throughfall, and soil water were collected for each event. Precipitation was collected at the Pennsylvania State University, University Park, and throughfall was sampled at the study site (Figure 4.1). Precipitation and throughfall samples were collected using a polypropylene funnel and bottle connected by plastic tubing, looped to prevent evaporation. A cheese cloth filter was placed in the funnel to prevent leaves and insects from clogging the tubing. Both precipitation and throughfall were sampled on an event basis and composited bimonthly from April to October 2005.

Soil water was collected at each of the three soil plots (15.2 meter by 9.1 meter), located at the lower, middle, upper elevations of the 90 Degree watershed. In each soil plot, soil water samples were collected at both 30 cm and 80 cm depths using tension lysimeters. A -60 k Pa vacuum was applied to each lysimeter within 36 hours before the start of a rainfall event and the lysimeters were evacuated within 36 hours after rainfall ended. For the Sr isotope analysis, soil water sampled at the specified depths (30 cm and 80 cm), was composited from the three soil plots.

Monthly streamwater was collected in a Nalgene® polyethylene bottle from July 2003 to October 2005. All water samples were placed in a cooler with ice pack immediately after sample collection, returned to the laboratory, and stored in a refrigerator at 4 ^{o}C until analysis could be conducted.

4.2.3. Limestone Sand Application

The limestone sand was purchased from the New Enterprise Stone and Lime Co. in Tyrone, PA. The limestone sand was coarse-grained with particle size distributions as follows: 41% (above 2 mm); 37% (between 500 μm and 2 mm); and 22% (below 500 μm). An analysis of the dolomitic limestone used for watershed and soil plot applications is included in Table 4.1.

4.2.3.1. Watershed application

For the watershed study, a total of 507 t of dolomitic limestone sand was applied to the 90 Degree watershed with a specially modified log skidder (Penn State Regenerator) at

a rate of 5 t ha^{-1} between October 16 and November 10, 2003. Approximately, 76% of the watershed was treated with the remainder inaccessible due to steep slopes.

4.2.3.2. Soil plot application

Results from soil chemistry analysis in fall 2004 indicated that the three soil plots (15.2 meter by 9.1 meter) located within the 90 Degree watershed did not receive limestone sand treatment, requiring additional liming to evaluate the response of soil and soil water to liming. A total of 0.21 t of the same limestone material was applied by hand at a rate of 5 t ha^{-1} on three plots on June 8, 2005.

4.2.4. Data Analysis

The chemical contents of limestone sand were analyzed using a Leeman Labs PS3000UV Inductively Coupled Plasma Emission Spectrophotometer at the Materials Characterization Laboratory (Materials Research Institute, The Pennsylvania State University at University Park, Pennsylvania).

Major elements (Ca and Mg) and a trace element (Sr) in the water samples were analyzed at the Penn State Institutes of the Environment Laboratory at The Pennsylvania State University, University Park. All water samples were filtered through a 0.45 μm pore size filter prior to analysis. Calcium and magnesium were analyzed with a Perkin-Elmer 5100 flame atomic absorption spectrometer. Total strontium was measured with a Perkin-Elmer 5100 graphite furnace with a detection limit of 0.006 μmol/L.

Strontium isotopic ratios of water samples were analyzed with the Finnigan MAT

262 multicollector thermal ionization mass spectrometer (TIMS) at the University of Pittsburgh, Pennsylvania. The $^{87}Sr/^{86}Sr$ ratios were normalized to $^{88}Sr/^{86}Sr=0.1194$ to correct for mass dependent fractionation. The mean $^{87}Sr/^{86}Sr$ ratio measured in accordance with the National Institute of Standards and Technology (NIST) standard SRM-987 was 0.71025 during the present study, which equates to a value of 0.70918 for seawater. The measured strontium isotopic composition of samples is reported both as $^{87}Sr/^{86}Sr$ ratio and as $\delta^{87}Sr$, as follows:

$$\delta^{87}Sr = 1000\left(\frac{{}^{87}Sr/{}^{86}Sr_{sample} - {}^{87}Sr/{}^{86}Sr_{seawater}}{{}^{87}Sr/{}^{86}Sr_{seawater}}\right) \quad (1)$$

The total analysis uncertainties for the $^{87}Sr/^{86}Sr$ ratio and $\delta^{87}Sr$ measurements of samples were 2σ and applied to the last decimal place.

4.3. Results

4.3.1. $^{87}Sr/^{86}Sr$ Ratios and Sr Concentrations of Precipitation and Throughfall

The $^{87}Sr/^{86}Sr$ ratios, $\delta^{87}Sr$ values, and Sr concentrations of precipitation and throughfall from April to October 2005 are shown in Table 4.2. Strontium isotope ratios of precipitation and throughfall were more radiogenic (relating to or caused by radioactivity) with time from April to October. The $^{87}Sr/^{86}Sr$ ratios of precipitation and throughfall varied between 0.7085 and 0.7137 ($\delta^{87}Sr \approx$ -0.89 to 6.39), and between 0.7118 and 0.7137 ($\delta^{87}Sr \approx$ 3.74 to 6.36), respectively. The concentrations of Sr in precipitation and throughfall were quite low; half the samples did not have a Sr concentration that met the detection threshold. Strontium concentrations varied between <0.0057 (μmol/L) and 0.0457 (μmol/L) in

precipitation, and between <0.0057 (μmol/L) and 0.0114 (μmol/L) in throughfall, respectively. During the April-May and June-July collection periods, the concentrations of Sr in precipitation were higher than those in throughfall.

4.3.2. Chemical and Isotopic Composition of Soil Water

Temporal variations of $^{87}Sr/^{86}Sr$ ratio in soil water at 30 cm and 80 cm depths from April to October 2005 are shown in Figure 4.2. A vertical bar in Figure 4.2 indicated the date of limestone sand application (June 8, 2005). The dolomitic limestone sand applied to the soil plots by hand had a $^{87}Sr/^{86}Sr$ ratio of 0.709080 ± 0.000024 ($\delta^{87}Sr \approx -0.14\pm 0.03$), which was lower than the $^{87}Sr/^{86}Sr$ ratio of seawater (=0.70918). The $^{87}Sr/^{86}Sr$ ratios in deeper soils were more radiogenic than those in shallower soils. The $^{87}Sr/^{86}Sr$ ratios in soil water at 30 cm depth vary widely both before and after limestone sand treatments during the short study period, ranging from 0.7128 ($\delta^{87}Sr \approx 5.16$) to 0.7150 ($\delta^{87}Sr \approx 8.25$). Soil water at 80 cm depth had relatively homogeneous $^{87}Sr/^{86}Sr$ ratios, compared to $^{87}Sr/^{86}Sr$ ratios in soil water at 30 cm depth. The $^{87}Sr/^{86}Sr$ ratios in soil water at 80 cm depth ranged from 0.7142 ($\delta^{87}Sr \approx 7.14$) to 0.7154 ($\delta^{87}Sr \approx 8.80$). It appeared that the $^{87}Sr/^{86}Sr$ isotope ratios in soil water did not change significantly with the addition of limestone sand.

The $^{87}Sr/^{86}Sr$ ratio vs the Sr concentration in soil water at 30 cm and 80 cm depths are shown in Figures 4.3 and 4.4. Before limestone sand treatment, the $^{87}Sr/^{86}Sr$ ratio in soil water at 30 cm depth showed a negative correlation with the Sr concentration (Pearson's correlation coefficient (r) = -0.913, p=0.030). After liming, this negative relationship did not exist (r= -0.055, p=0.965). At 30 cm soil depth, the $^{87}Sr/^{86}Sr$ ratios in soil water before

treatment were more variable than those after liming; The $^{87}Sr/^{86}Sr$ ratios in soil water were 0.7128-0.7150 ($\delta^{87}Sr \approx 5.16$-$8.25$) before liming and 0.7133-0.7145 ($\delta^{87}Sr \approx 5.81$-$7.48$) after liming. Like the results recorded for soil water at 30 cm depth, variations in $^{87}Sr/^{86}Sr$ ratios of soil water at 80 cm depth before liming were higher than that after liming (Figure 4.4). The $^{87}Sr/^{86}Sr$ ratios in soil water were 0.7142-0.7154 ($\delta^{87}Sr \approx 5.16$-$8.25$) before liming and 0.7144-0.7152 ($\delta^{87}Sr \approx 5.81$-$7.48$) after liming. There was no correlation between the $^{87}Sr/^{86}Sr$ ratios and Sr concentration in soil water at 80 cm depth before liming at the 0.1 significance level ($r= 0.765$ with a $p= 0.235$). However, after liming the $^{87}Sr/^{86}Sr$ ratios and Sr concentration correlation was significant at $\alpha \leq 0.1$ and the correlation coefficient was quite high ($r=0.915$, $p= 0.085$). It appeared that relationships between the $^{87}Sr/^{86}Sr$ ratios and Sr concentrations in soil water were changed with the addition of limestone sand.

The $^{87}Sr/^{86}Sr$ ratios vs Ca concentrations in soil water at 30 cm and 80 cm depths are plotted in Figures 4.5 and 4.6, respectively. With the addition of limestone sand, the $^{87}Sr/^{86}Sr$ ratio in soil water at 30 cm depth had a significant negative correlation with the Ca concentration ($r=-0.956$, $p=0.044$). There were no significant correlations between the $^{87}Sr/^{86}Sr$ ratio and Ca concentration in soil water at 80 cm depth before or after liming. It seemed that relationships between the $^{87}Sr/^{86}Sr$ ratios and Ca concentrations in soil water at 30 cm depth were changed due to limestone sand application

The $^{87}Sr/^{86}Sr$ ratio vs Mg concentration in soil water at 30 cm and 80 cm depths at the 90 Degree watershed are shown in Figures 4.7 and 4.8, respectively. There was no clear relationship between the $^{87}Sr/^{86}Sr$ ratio and Mg concentration in soil water at 30 cm either before or after liming application. The $^{87}Sr/^{86}Sr$ ratios in soil water at 80 cm depth were

negatively correlated with Mg concentration before liming (r=-0.994, p=0.006). With the addition of limestone sand, the $^{87}Sr/^{86}Sr$ ratio had a strong positive correlation (r=0.774, p=0.124) that was close to significance at $\alpha \leq 0.1$. It appeared as though the addition of limestone sand changed the relationship of the Sr isotope ratio with Sr, Ca, and Mg.

The relationships between Ca/Sr and Mg/Sr molar ratios in soil water are shown in Figure 4.9. In soil water at 30 cm depth, the Ca/Sr molar ratios showed a strong positive correlation with Mg/Sr molar ratios (r=0.986 with a p=0.000). With the removal of one outlier (Ca/Sr=251 and Mg/Sr=660), the Ca/Sr molar ratios in soil water at 80 cm depth also had a strong positive correlation with Mg/Sr molar ratios (r=0.865 with a p=0.005).

In order to avoid variations from dilution and concentration effects, element ratios (Ca/Sr, Mg/Sr) rather than absolute concentrations (Ca, Mg, Sr) have been used as tracers (Blum et al., 2000; Land et al., 2000; Dogramaci and Herczeg, 2002). Temporal variations in the Ca/Sr ratio of soil water at 30 cm and 80 cm depths are shown in Figure 4.10. With the addition of limestone sand, Ca/Sr molar ratios increased significantly with time. The Ca/Sr molar ratios in soil water appeared more or less consistent prior to liming, ranging from 180 (mol/mol) to 404 (mol/mol) at 30 cm depth and from 165 (mol/mol) to 279 (mol/mol) at 80 cm depth. After liming, the Ca/Sr molar ratios in soil water at 30 cm depth increased significantly from 378 (mol/mol) to 1290 (mol/mol) by the end of the study. There was no significant increase in Ca/Sr ratios in soil water at 80 cm depth after liming, except in a sample collected right after liming application (Ca/Sr ratio of 402 (mol/mol)).

The temporal variations in the Mg/Sr ratio of soil water at 30 cm and 80 cm depths during the study period are shown in Figure 4.11. Prior to liming, the Mg/Sr molar ratios in

soil water at 30 cm and 80 cm depths were relatively homogeneous, ranging from 171 (mol/mol) to 283 (mol/mol) and 174 (mol/mol) to 242 (mol/mol), respectively. After liming, the Mg/Sr molar ratios in soil water at 30 cm depth increased significantly from 302 (mol/mol) right after liming to 1915 (mol/mol) by the end of the study. After liming, the Mg/Sr molar ratios in soil water at 80 cm depth also increased to some extent, ranging from 247 (mol/mol) to 660 (mol/mol). At the end of monitoring, the Mg/Sr ratio in soil water at 80 cm depth had reached its maximum value of 660 (mol/mol).

4.3.3. Chemical and Isotopic Composition of Streamwater

Temporal variations of $^{87}Sr/^{86}Sr$ ratios and $\delta^{18}O$ compositions in monthly streamwater at the 90 Degree watershed during the study period (July 2003-October 2005) are shown in Figure 4.12. The $\delta^{18}O$ compositions in streamwater had a seasonal variation, ranging from -10.59‰ to -8.38‰. During periods of soil water recharge, the $\delta^{18}O$ composition of streamwater was low and the maximum $\delta^{18}O$ value was obtained in summer. However, $^{87}Sr/^{86}Sr$ ratios in streamwater did not show seasonal variation (Figure 4.12).

With the overlaying of soils on to the sandstone and conglomerate bedrock in the watershed, streamwater showed higher radiogenic ^{87}Sr values than did precipitation or throughfall. The dolomitic limestone sand applied over the watershed had lower isotope values of 0.7091 ($\delta^{87}Sr \approx -0.14$). Prior to limestone application, the $^{87}Sr/^{86}Sr$ ratios in streamwater ranged from 0.7151 ($\delta^{87}Sr \approx 8.33$) to 0.7153 ($\delta^{87}Sr \approx 8.60$). After liming, the $^{87}Sr/^{86}Sr$ ratios in monthly streamwater began a pattern of decreases, and reached a minimum value at the termination of the study. The $^{87}Sr/^{86}Sr$ ratios in streamwater changed

from 0.715282 ± 0.000019 (± 0.03) to a less radiogenic value of 0.714302 ± 0.000020 ($\delta^{87}Sr \approx 7.22 \pm 0.03$) during the post-treatment period.

To understand limestone sand treatment effects on streamwater, changes in elemental concentrations in streamwater were monitored. Absolute concentrations of elements have been widely used as chemical tracers because their analysis is simple and less costly. The concentrations of Ca, Mg, and Sr in streamwater at the 90 Degree watershed from July 2003 to October 2005 are plotted in Figure 4.13. The Mg concentration in streamwater was measured beginning in October 2004. Temporal variations in concentrations of Ca, Mg, and Sr in streamwater were more or less consistent until May 2005 when they began to increase. The Ca and Mg concentrations peaked in September 2005 with maximum values twice those before liming for Ca and the initial sample for Mg. Sr concentration in streamwater also reached a maximum of 0.23 μmol/L in September 2005.

$^{87}Sr/^{86}Sr$ ratios in streamwater were significantly negative correlated with Ca concentration (r=-0.939, p=0.000) and Mg concentration (r= -0.950, p=0.000) in Figure 4.14 and with the Sr concentration (r=-0.854, p=0.000) in Figure 4.15. The relationship between Ca/Sr and Mg/Sr molar ratios in streamwater is shown in Figure 4.16. Similar to the soil water results, streamwater Ca/Sr ratios had a positive correlation with Mg/Sr ratios (r=0.969, p=0.000). Temporal variations of $^{87}Sr/^{86}Sr$ and element ratios (Ca/Sr and Mg/Sr) in monthly streamwater both before and after liming are shown in Figure 4.17. The Ca/Sr and Mg/Sr ratios in streamwater began to increase in March 2005; whereas, $^{87}Sr/^{86}Sr$ ratios in streamwater began to decrease in February 2005 and continued until the end of

observations.

4.4. Discussion

4.4.1. Precipitation and Throughfall

The $^{87}Sr/^{86}Sr$ ratios in precipitation collected bimonthly at the Pennsylvania State University showed similar values for a sample in April-May ($^{87}Sr/^{86}Sr$ =0.7085, $\delta^{87}Sr \approx$ -0.89) and a sample in June-July ($^{87}Sr/^{86}Sr$ =0.7093, $\delta^{87}Sr \approx 0.23$); the August-September sample showed the highest radiogenic value of 0.7137 ($\delta^{87}Sr \approx 6.39$). The $^{87}Sr/^{86}Sr$ ratio in precipitation was somewhat constant during the summer and increased in fall. Négrel and Roy (1998) measured $^{87}Sr/^{86}Sr$ ratios in rainfall collected during one year in France and obtained results similar to those of the current study. They reported a relatively constant $^{87}Sr/^{86}Sr$ ratio of 0.7092-0.7094 in rainfall during the summer and the highest rainfall $^{87}Sr/^{86}Sr$ ratio (=0.7131) at the beginning of the fall. In addition, Graustein and Armstrong (1983) reported a small range in $^{87}Sr/^{86}Sr$ ratio (0.7100-0.7104) in rainfall during the summer in New Mexico; whereas, Andersson et al. (1990) measured a large range in $^{87}Sr/^{86}Sr$ ratio (0.7098-0.7194) in snow in central Sweden and Norway.

Limestone sand was not applied to the throughfall collection site so that $^{87}Sr/^{86}Sr$ ratios in throughfall were not influenced by limestone particles. Nakano et al. (1993 and 2001) reported that the $^{87}Sr/^{86}Sr$ ratios of stemflow and throughfall during the summer period were generally similar to those of plant material due to leaching from bark and foliage. A possible deduction from these results is that, the $^{87}Sr/^{86}Sr$ ratios of plants at the study site could be closer to the range of $^{87}Sr/^{86}Sr$ ratios in throughfall (=0.7118-0.7137;

$\delta^{87}Sr \approx 3.74\text{-}6.36$) during the summer.

Nakano et al. (2001) reported that Sr concentration in throughfall was higher than that in precipitation due to canopy leaching. However, in the present study the Sr concentrations in throughfall were somewhat lower than that in precipitation, although the absolute amount of Sr in both were quite low (half the samples were below the detection threshold). Both Sr concentrations in precipitation and throughfall were quite varied; more than one order of magnitude from <0.0057 μmol/L to 0.0457 μmol/L for precipitation and from <0.0057 μmol/L to 0.0114 μmol/L for throughfall. Bullen et al.(1996) also observed quite low Sr concentrations in summer precipitation in northcentral Wisconsin. The range of Sr throughfall concentrations in the Bullen et al study was 0.007-0.012 μmol/L. Lower Sr concentrations in precipitation during summer were also observed in Japan and averaged 0.02 μmol/L during a nine-year period (Nakano and Tanaka, 1997).

4.4.2. Limestone Treatment Effects in Soil Water

The dolomitic limestone sand used in this project had a very low $^{87}Sr/^{86}Sr$ ratio value (=0.7091, $\delta^{87}Sr \approx -0.14$), lower than the $^{87}Sr/^{86}Sr$ ratio of seawater (=0.70918). Although the present study did not measure the Sr content of limestone, Faure (1986) reported a very high concentration of Sr in limestone (=610 ppm). River water draining carbonate rocks had large quantities of Sr with lower $^{87}Sr/^{86}Sr$ ratios (Curtis and Stueber, 1973; Steele and Pushkar, 1973; Négrel and Roy, 1998). The dolomitic limestone also had higher concentrations of Ca and Mg. This suggests that the dolomitic limestone treatment should increase the concentrations of Sr, Ca, and Mg and decrease the $^{87}Sr/^{86}Sr$ ratios in soil

water and streamwater.

In the present study, the $^{87}Sr/^{86}Sr$ ratios in soil water were different depending on the sampling depth. In addition, the $^{87}Sr/^{86}Sr$ ratios in soil water at 30 cm depth were quite varied, but $^{87}Sr/^{86}Sr$ ratios in soil water at 80 cm depth were relatively constant during the study period. Nakano et al. (1993) observed relatively constant $^{87}Sr/^{86}Sr$ ratios in soil water regardless of sampling depth and season at a Japanese larch site. Before liming, the average $^{87}Sr/^{86}Sr$ ratio in soil water at 80 cm depth (=0.714936, $\delta^{87}Sr \approx 8.29$) was more radiogenic than that in soil water at 30 cm depth (=0.713951, $\delta^{87}Sr \approx 6.73$). The increase in $^{87}Sr/^{86}Sr$ ratio in soil water with depth may be caused by capillary action from the groundwater to the soil. An average $^{87}Sr/^{86}Sr$ ratio in streamwater before liming was 0.7152 ($\delta^{87}Sr \approx 8.46$) and an average soil depth of 100 cm in this watershed was assumed by field visit. Although $^{87}Sr/^{86}Sr$ ratios in bedrock were not measured, 90 Degree watershed was covered by sandstone and conglomerate bedrock, which, according to Sultan (2003) has higher $^{87}Sr/^{86}Sr$ ratio (0.71659±0.00088) and lower Sr concentrations (31±11 ppm). Nakano et al. (1993) reported decreased $^{87}Sr/^{86}Sr$ ratios at 70 cm soil depth due to capillary flow of Sr from groundwater with lower $^{87}Sr/^{86}Sr$ ratio.

After liming, the $^{87}Sr/^{86}Sr$ ratio in soil water did not have a negative relationship with Sr, Ca, and Mg concentrations; decreases in the $^{87}Sr/^{86}Sr$ ratio corresponded with increases in element concentrations. The limestone sand application might play a role in changing the relationship of the $^{87}Sr/^{86}Sr$ ratio with Ca, Mg, and Sr concentrations. However, the small number of samples could not make clear confirmation of treatment effects on soil water.

There are several possible reasons why $^{87}Sr/^{86}Sr$ ratios in soil water did not appear to respond to limestone sand treatment. First, soil water samples were collected on an event-basis rather than a fixed-schedule basis. Event-basis soil water samples collect percolating soil water rather than soil water held under tension between rainfall events. Consequently, throughfall might play a major role in event-basis soil water samples. As a treatment effect, the tendency to decrease in $^{87}Sr/^{86}Sr$ ratios of soil water by limestone sand ($^{87}Sr/^{86}Sr = 0.7091$) may be negated by the $^{87}Sr/^{86}Sr$ ratio of throughfall (0.7118-7137). Second, more time may be required to deliver by-product of limestone sand from the soil surface to the specified soil sampling depth. The results of the ^{18}O isotope studies (Chapter 3) showed the mean residence time of soil water at 30 cm and 80 cm depths as about 3 months and 4 months, respectively. The $^{87}Sr/^{86}Sr$ ratio in soil water was measured during the first four months after limestone sand application. As a constituent of water molecules, ^{18}O isotope traces only the water source so mean residence time of soil water is defined as average time it takes for water to be delivered from soil surface to a defined soil depth. On the other hand, the Sr isotope only traces the solute source so that the $^{87}Sr/^{86}Sr$ ratio in soil water represents minerals contributing to the soil water chemistry from the soil surface to the soil sampling depth (Kendall and McDonnell, 1998). As only the water source traced by ^{18}O, the mean residence time of soil water does not truly reflect changes in the Sr isotope under a limestone application.

Third, after liming, the $^{87}Sr/^{86}Sr$ ratio in soil water can be determined by three components of input: 1) the atmospheric deposition (dry and wet deposition), 2) the product of natural weathering, and 3) the anthropogenic input (dolomitic limestone sand).

Complicated mixing from these three inputs could lead to higher variations in the $^{87}Sr/^{86}Sr$ ratio in soil water; this would make it difficult to determine the treatment effects of Sr isotopes on soil water. Fourth, the composite soil water at the specified soil depth, collected from the three soil plots might not truly represent $^{87}Sr/^{86}Sr$ ratio in soil water due to a large degree of spatial variation. In addition, before liming the $^{87}Sr/^{86}Sr$ ratios in soil water were not isotopically homogeneous, exhibiting higher temporal variations in $^{87}Sr/^{86}Sr$ ratio. This makes it hard to determine a distinct $^{87}Sr/^{86}Sr$ ratio value prior to liming. Fifth, a higher dose of smaller particle size dolomitic limestone sand might produce a more rapid response. In the current study, limestone sand applied at a rate of 5 t ha^{-1} over soil plots was quite coarse grained (about 43% >2 mm).

The element ratios (i.e., Ca/Sr and Mg/Sr) rather than absolute concentrations (Ca, Mg, and Sr) can eliminate variations by concentration and dilution effects (Land et al., 2000; Négrel and Pauwels, 2004; Négrel and Petelet-Giraud, 2005), so that Ca/Sr and Mg/Sr ratios as chemical tracers can be useful for estimating liming treatment effects on soil water. Temporal variations in the monthly Ca/Sr and Mg/Sr ratios of soil water indicated that treatment effects occurred in the soil. Two months after liming, the Ca/Sr and Mg/Sr ratios of soil water at 30 cm depth had increased significantly. Mg/Sr soil water ratios at 80 cm depth were generally consistent during the two-month period immediately following liming, after which they increased. The Ca/Sr ratios in soil water at 80 cm depth did not increase significantly during the observation period.

4.4.3. Limestone Treatment Effects in Streamwater

There were apparent seasonal variations in the $\delta^{18}O$ compositions in streamwater (the enrichment of $\delta^{18}O$ in summer streamwater by evaporation), whereas there were no indications of seasonal variations in $^{87}Sr/^{86}Sr$ ratio measurements. Other research has also reported similar results, reporting streamwater $^{87}Sr/^{86}Sr$ ratios as generally homogeneous. Land et al. (2000) found no clear seasonal variation in the $^{87}Sr/^{86}Sr$ ratios in streamwater in northern Sweden, except for slight increases during snowmelt periods. Based on four years of observations, Kennedy et al. (2000) reported very constant $^{87}Sr/^{86}Sr$ ratios in streamwater across seasons and years in the White and West rivers in Vermont, U.S.A. Nakano et al. (2001) observed temporal and spatial homogeneity of the $^{87}Sr/^{86}Sr$ ratio in streamwater at the Kawakami watershed in central Japan.

Strontium isotopes are not fractionated by biological, physical, geological factors, and natural and analytical fractionation of ratios can be corrected. The $^{87}Sr/^{86}Sr$ ratio helps to interpret absolute concentrations (Ca, Mg, and Sr) and element ratios (Ca/Sr, Mg/Sr). For these reasons, the $^{87}Sr/^{86}Sr$ ratio was used as a tracer for solute sources, such as limestone sand, in streamwater. The mean residence time of streamwater is defined as the average time water takes to leave the flow system until it reaches a watershed outlet (McGuire et al., 2002). The estimated mean residence time of streamwater at the 90 Degree watershed was about 12 months using ^{18}O isotope in water (see Chapter 3). The absolute concentrations (Ca, Mg, and Sr) and element ratios (Ca/Sr and Mg/Sr) in streamwater began to increase about 16 months after liming on the 90 Degree watershed. Streamwater exhibited a pattern of decrease in $^{87}Sr/^{86}Sr$ ratios sixteen months after watershed liming and had reached its

least radiogenic ^{87}Sr values at the termination of the study. Considering dolomitic limestone has higher concentrations of Ca, Mg, and Sr with lower $^{87}Sr/^{86}Sr$ ratio, increasing patterns of absolute concentrations (Ca, Mg, and Sr) and element ratios (Ca/Sr and Mg/Sr) and decreasing trends in $^{87}Sr/^{86}Sr$ ratios in streamwater were a sign of limestone sand treatment effects. It appeared that limestone interaction times of water transported through the 90 Degree watershed to the streamwater estimated by the strontium isotope signature was about four months longer than the estimated mean residence time of streamwater (12 months). This observation supports the conclusion of Bain and Bacon (1994) that the strontium isotope ratio in streamwater provides a very sensitive indicator of environmental change.

4.5. Summary and Conclusion

Previously limestone sand treatment effects on soil water and streamwater chemistry at the 90 Degree watershed were tested using element concentrations as chemical tracers. Results from the ^{18}O study showed that mean residence time of soil water and streamwater at the 90 Degree watershed was about 3 to 4 months and about 12 months, respectively. Because the strontium isotope is not fractionated by biological, physical, and geological factors, and because analytical fractionation can be corrected, the strontium isotope as an isotopic tracer for the solute source was used to confirm watershed level limestone sand treatment effects and to help interpret absolute concentrations (Ca, Mg, and Sr) and element ratios (Ca/Sr, Mg/Sr).

The limestone sand used in this project had higher concentrations of Ca, Mg, and

Sr, and a lower $^{87}Sr/^{86}Sr$ ratio. Approximately 16 months after liming, treatment effects appeared in streamwater in the form of increased Ca, Mg, and Sr concentrations and a decrease in $^{87}Sr/^{86}Sr$ ratio. This was four months longer than the retention time estimated by ^{18}O isotope analyses.

$^{87}Sr/^{86}Sr$ ratios in soil water did not appear to respond to limestone sand treatment. Temporal and spatial variations in the $^{87}Sr/^{86}Sr$ ratios of soil water coupled with only a short-term monitoring period made the determination of treatment effects on soil water difficult. However, ratios of Ca/Sr and Mg/Sr in soil water increased about two months after liming. Overall, Sr isotopes proved useful in confirming watershed level limestone sand treatment effects.

4.6. References

Åberg, G., Jacks, G., Wickman, T., Hamilton, P.J., 1990. Strontium isotopes in trees as an indicator for calcium availability. Catena 17, 1-11.

Åberg, G., 1995. The use of natural strontium isotopes as tracers in environmental studies. Water, Air, and Soil Pollution 79, 309-322.

Andersson, P., Löfvendahl, R., Åberg, G., 1990. Major element chemistry, δ^2H, $\delta^{18}O$ and $^{87}Sr/^{86}Sr$ in a snow profile across Central Scandinavia. Atmospheric Environment 24A, 2601-2608.

Bailey, S.W., Hornbeck, J.W., Driscoll, C.T., Gaudette, H.E., 1996. Calcium inputs and transport in a base-poor forest ecosystem as interpreted by Sr isotopes. Water Resources Research 32, 707–719.

Bain, D.C., Bacon, J.R., 1994. Strontium isotopes as indicators of mineral weathering in catchments. Catena 22, 201-214.

Blum, J.D., Erel, Y., 1997. Rb-Sr isotope systematics of a granitic soil chronosequence: The importance of biotite weathering. Geochimica et Cosmochimica Acta 61, 3193–3204.

Blum, J.D., Taliaferro, E.H., Weisse, M.T., Holmes, R.T., 2000. Changes in Sr/Ca, Ba/Ca and $^{87}Sr/^{86}Sr$ ratios between trophic levels in two forest ecosystems in the northeastern U.S.A. Biogeochemistry 49, 87-101.

Bullen, T.D., Krabbenhoft, D.P., Kendall, C., 1996. Kinetic and mineralogic controls on the evolution of groundwater chemistry and $^{87}Sr/^{86}Sr$ in a sandy silicate aquifer, northern Wisconsin, USA. Geochimica et Cosmochimica Acta 6, 1807-1821.

Capo, R.C., Stewart, B.W., Chadwick, O.A., 1998. Strontium isotopes as tracers of ecosystem processes: theory and method. Geoderma 82, 197-225.

Clow, D.W., Mast, M.A., Bullen, T.D., Turk, J.T., 1997. Strontium 87/strontium 86 as a tracer of mineral weathering reactions and calcium sources in an alpine/subalpine watershed, Loch Vale, Colorado. Water Resources Research 33, 1335-1351.

Curtis, J.B. Jr., Stueber, A.M., 1973. $^{87}Sr/^{86}S$ ratios and total strontium concentrations in surface waters of the Scioto River drainage basin, The Ohio Journal of Science 73, 166-175.

Dogramaci, S.S., Herczeg, A.L., 2002. Strontium and carbon isotope constraints on carbonate-solution interactions and inter-aquifer mixing in groundwaters of the semi-arid Murray Basin, Australia. Journal of Hydrology 262, 50-67.

Faure, G., 1986. Principles of Isotope Geology. 2nd edition. John Wiley & Sons, New York, 589 pp.

Fowler, A.J., Campana, S.E., Jones, C.M., Thorrold, S.R., 1995. Experimental assessment of the effect of temperature and salinity on elemental composition of otoliths using laser ablation ICPMS. Canadian Journal of Fisheries and Aquatic Sciences 52, 1431-1441.

Friedland, K.D., Reddin, D.G., Shimizu, N., Hass, R.E., Youngson, A.F., 1998. Strontium: calcium ratios in Atlantic salmon (*Salmo salar*) otoliths and observations on growth and maturation. Canadian Journal of Fisheries and Aquatic Sciences 55, 1158-1168.

Gosz, J.R., Brookins, D.G., Moore, D.I., 1983. Using Sr isotope ratios to estimate inputs to ecosystems. Bioscience 33, 3-30.

Graustein, W.C., Armstrong R.L., 1983. The use of $^{87}Sr/^{86}Sr$ ratios to measure atmospheric transport into forested watersheds. Science 219, 289-292.

Gunn, J.S., Harrowfield, I.R., Proctor, C.H., Thresher, R.E., 1992. Electron microprobe analysis of fish otoliths — evaluation of techniques for studying age and stock discrimination. Journal of Experimental Marine Biology and Ecology 158, 1-36.

Kendall, C., McDonnell, J.J. (eds.), 1998. Isotope Tracers in Catchment Hydrology Elsevier Science B.V., Amsterdam, 839 pp.

Kennedy, B.P., Blum, J.D., Folt, C.L., Nislow, K.H., 2000. Using natural strontium isotopic signatures as fish markers: methodology and application. Canadian Journal of Fisheries and Aquatic Sciences 57, 2280-2292.

Kennedy, M.J., Chadwick, O.A., Vitousek, P.M., Derry, L.A., Hendricks, D.M., 1998. Changing sources of base cations during ecosystem development, Hawaiian Islands. Geology 26, 1015-1018.

Land, M., Ingri, J., Andersson, P.S., Öhlander, B., 2000. Ba/Sr, Ca/Sr and $^{87}Sr/^{86}Sr$ ratios in soil water and groundwater: implications for relative contributions to streamwater discharge. Applied Geochemistry 15, 311-325.

McGuire, K.J., DeWalle, D.R., Gburek, W.J., 2002. Evaluation of mean residence time in subsurface waters using oxygen-18 fluctuations during drought conditions in the

mid-Appalachians. Journal of Hydrology 261, 132-149.

Nagano, T., Yokoo, Y., Yamanaka, M., 2001. Strontium isotope constraint on the provenance of basic cations in soil water and streamwater in the Kawakami volcanic watershed, central Japan. Hydrological processes 15, 1859-1875.

Nakano, T., Tanaka, T., 1997. Strontium isotope constraints on the seasonal variation of the provenance of base cations in rain water at Kawakami, central Japan. Atmospheric Environment 31, 4237-4245.

Nakano, T., Tanaka, T., Tsujimura, M., Matsutani, J., 1993. Strontium isotopes in soil-plant-atmosphere continuum (SPAC). Tracers in Hydrology (Proceedings of the Yokohama symposium, July 1993). International Association of Hydrological Sciences Publications. 215, 73-78.

Négrel, P., Roy, S., 1998. Chemistry of rainwater in the Massif Central (France): a strontium isotope and major element study. Applied Geochemistry 13, 941-952.

Négrel, Ph., Pauwels, H., 2004. Interaction between different groundwaters in Brittany catchments (France): Characterizing multiple sources through strontium- and sulphur isotope tracing. Water, Air, and Soil Pollution 151, 261-285.

Négrel, Ph., Petelet-Giraud, E., 2005. Strontium isotopes as tracers of groundwater-inducted floods: the Somme case study (France). Journal of Hydrology 305, 99-119.

Steele, J., Pushkar, P., 1973. Strontium isotope geochemistry of the Scioto River basin and the $^{87}Sr/^{86}S$ ratios of the underlying lithologies. The Ohio Journal of Science 73, 331-338.

Stewart, B.W., Capo, R.C., Chadwick, O.A., 2001. Effects of rainfall on weathering rate, base cation provenance, and Sr isotope composition of Hawaiian soils. Geochimica et Cosmochimica Acta 65, 1087-1099.

Sultan, K., 2003. Geochemical and Sr-isotopic characteristics of stream and spring waters from small-forested catchments at Seto, central Japan. Environmental Geology 44, 308-324.

Table 4.1. Results of the spectrochemical analysis of limestone sand applied over the watershed in 2003 and soil plots applied in 2005.

	Limestone sand (% total weight)	
	watershed application, year 2003	**Soil plot application, year 2005**
Loss on Ignition	41.70	40.70
CaO	26.00	27.40
MgO	16.40	18.00
SrO	< 0.005	< 0.05

Table 4.2. $^{87}Sr/^{86}Sr$ ratios, $\delta^{87}Sr$ values, and Sr concentrations of precipitation and throughfall samples collected from April to October 2005.

Samples	**Date**	**$^{87}Sr/^{86}Sr$ ±2σ**			**$\delta^{87}Sr$±2σ**			**Sr (µmol/L)**
Precipitation	Apr-May	0.708549	±	0.000021	-0.89	±	0.03	0.0342
	Jun-Jul	0.709343	±	0.000020	0.23	±	0.03	0.0457
	Aug-Sep	0.713713	±	0.000027	6.39	±	0.04	<0.0057
	October	-			-			<0.0057
Throughfall	Apr-May	0.711830	±	0.000021	3.74	±	0.03	0.0114
	Jun-Jul	0.712529	±	0.000028	4.72	±	0.04	<0.0057
	Aug-Sep	0.713640	±	0.000022	6.29	±	0.03	0.0114
	October	0.713691	±	0.000032	6.36	±	0.05	<0.0057

Figure 4.1. Location of sampling sites at the 90 Degree study watershed.

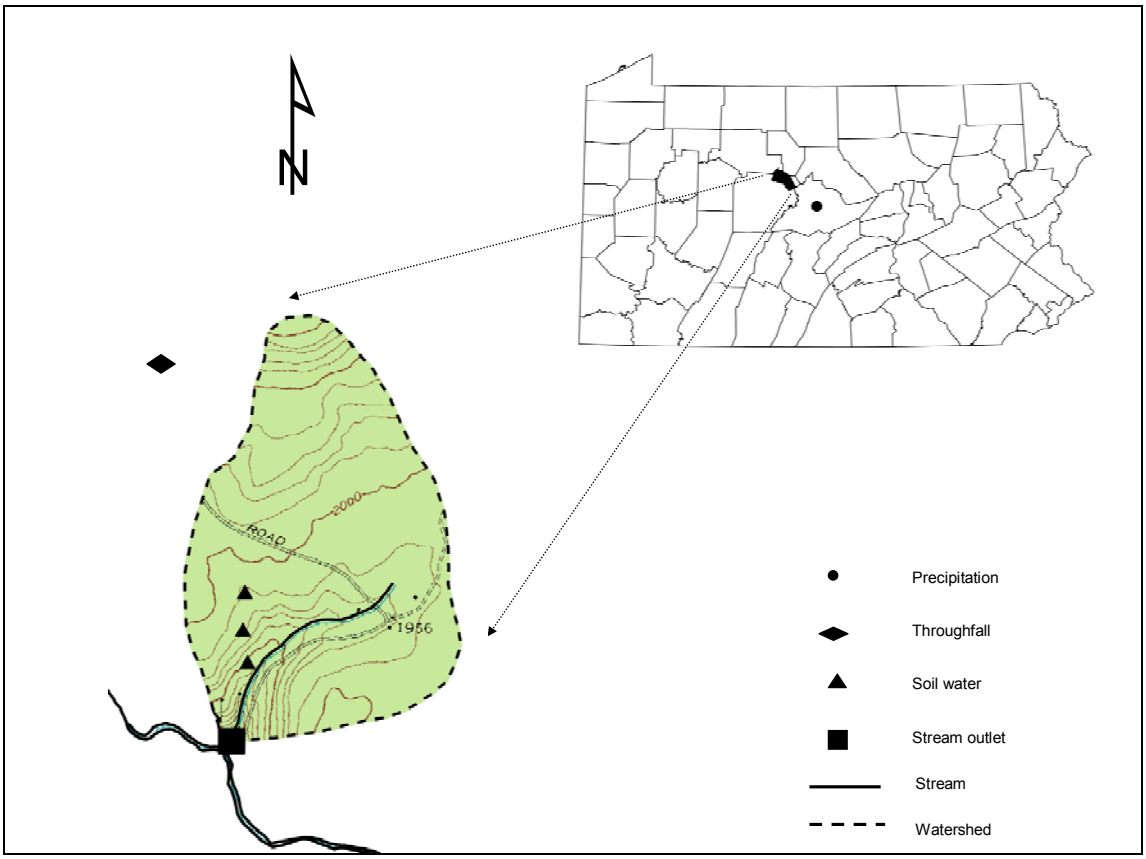

Figure 4.2. Temporal variations of $^{87}Sr/^{86}Sr$ ratio in soil water at 30 cm and 80 cm depths collected from the 90 Degree watershed (April to October 2005).

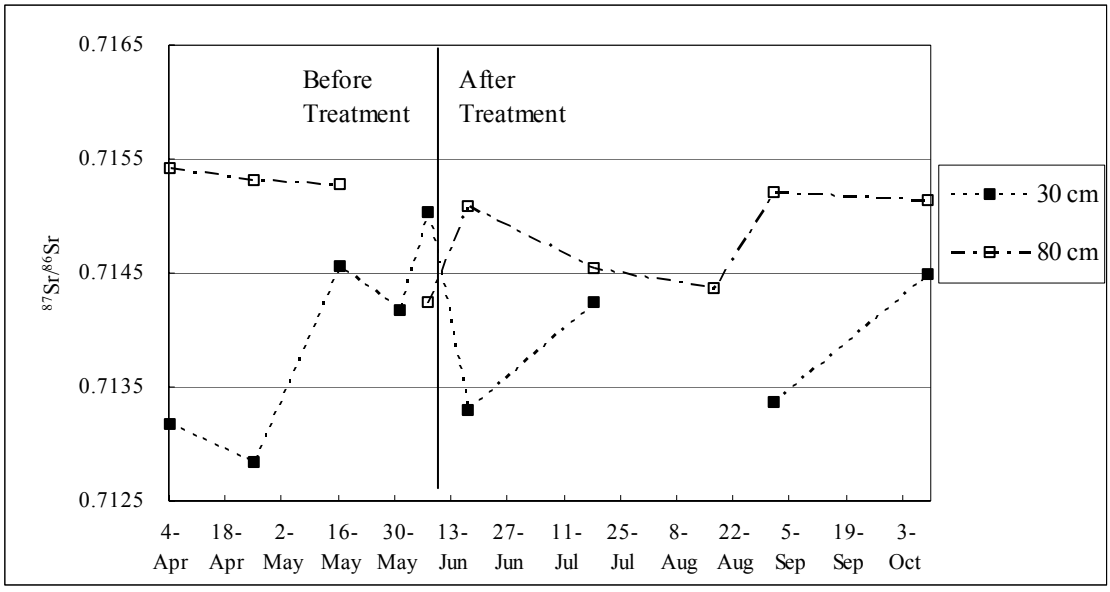

Figure 4.3. Plot of $^{87}Sr/^{86}Sr$ ratio vs Sr concentration in soil water at 30 cm depth collected from the 90 Degree watershed (April to October 2005).

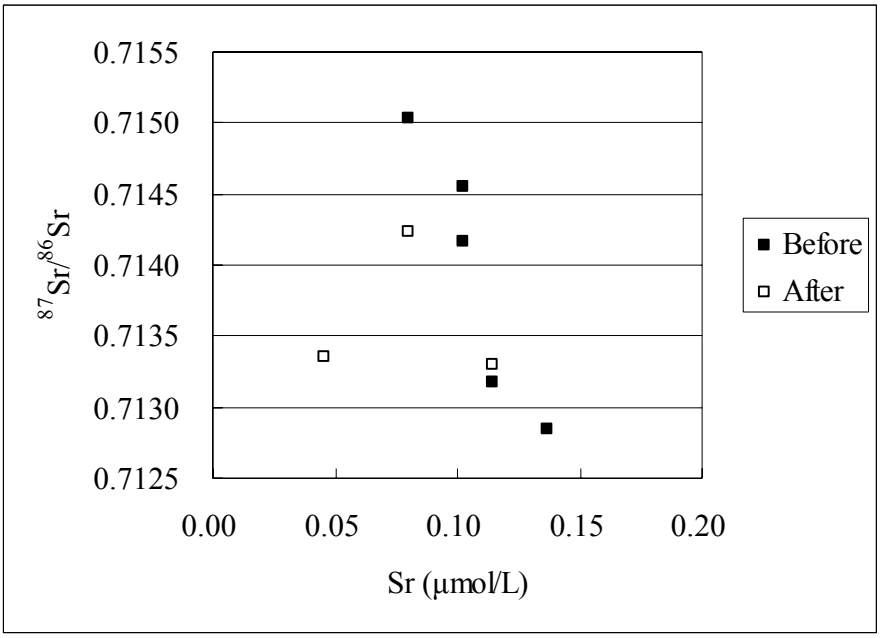

Figure 4.4. Plot of $^{87}Sr/^{86}Sr$ ratio vs Sr concentration in soil water at 80 cm depth collected from the 90 Degree watershed (April to October 2005).

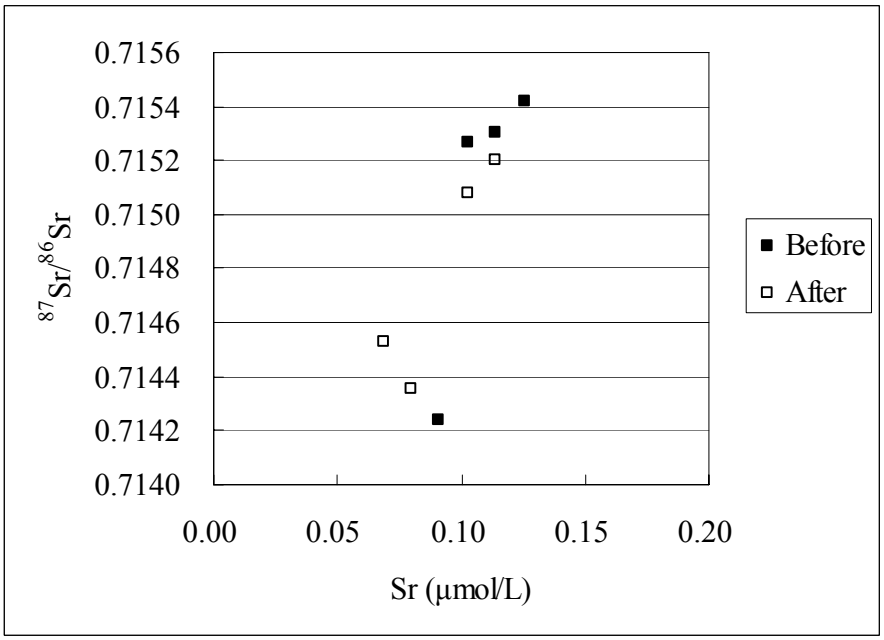

Figure 4.5. Plot of $^{87}Sr/^{86}Sr$ ratio vs Ca concentration in soil water at 30 cm depth collected from the 90 Degree watershed (April to October 2005).

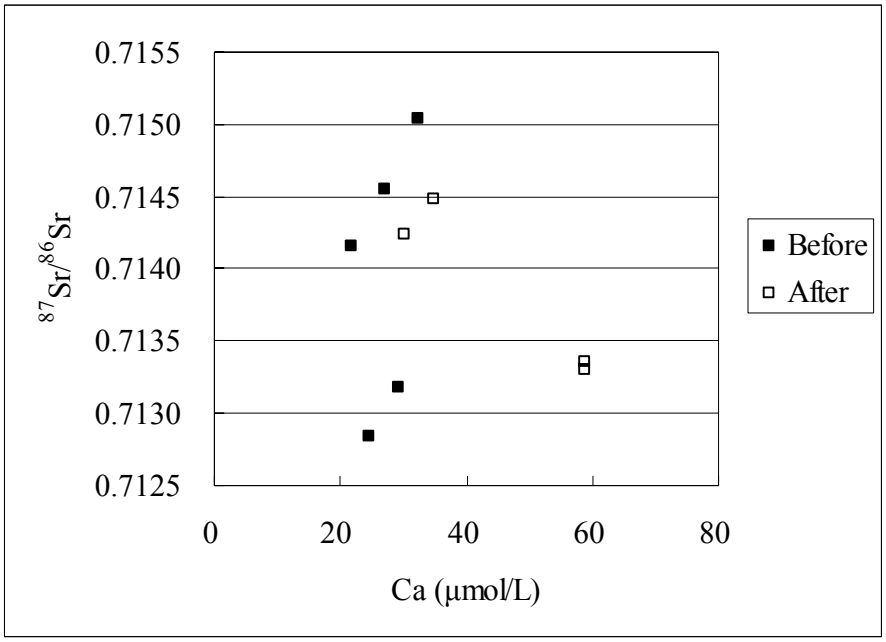

Figure 4.6. Plot of $^{87}Sr/^{86}Sr$ ratio vs Ca concentration in soil water at 80 cm depth collected from the 90 Degree watershed (April to October 2005).

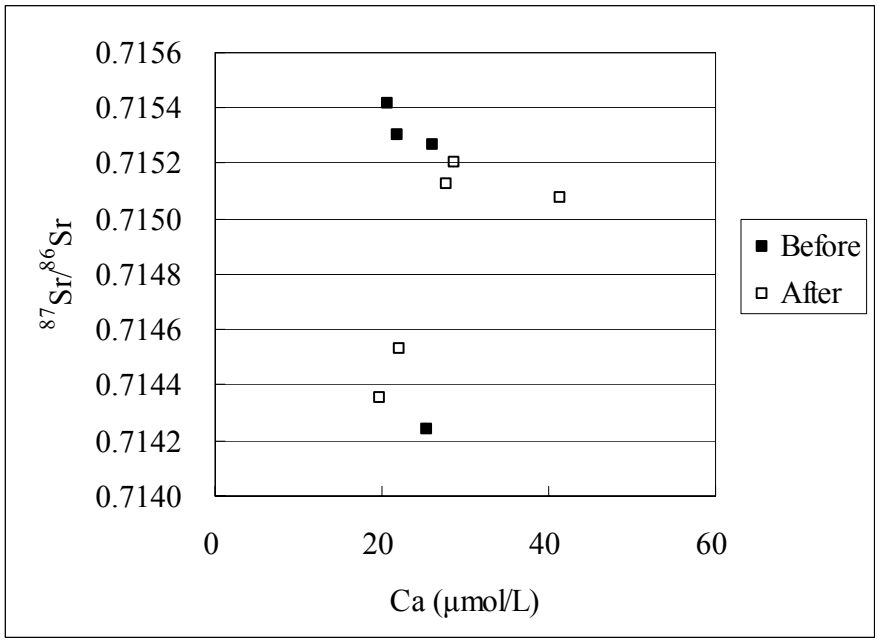

Figure 4.7. Plot of $^{87}Sr/^{86}Sr$ ratio vs Mg concentration in soil water at 30 cm depth collected from the 90 Degree watershed (April to October 2005).

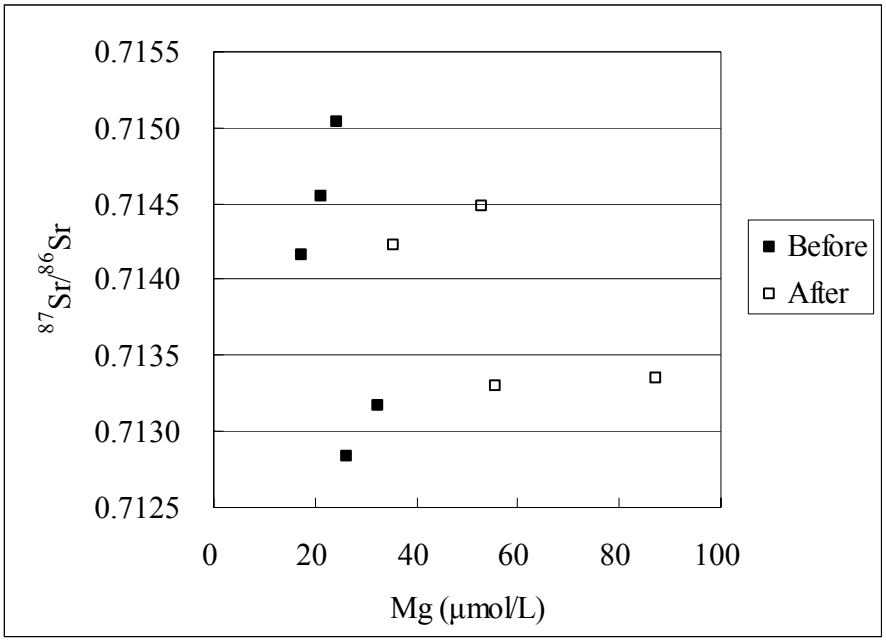

Figure 4.8. Plot of $^{87}Sr/^{86}Sr$ ratio vs Mg concentration in soil water at 80 cm depth collected from the 90 Degree watershed (April to October 2005).

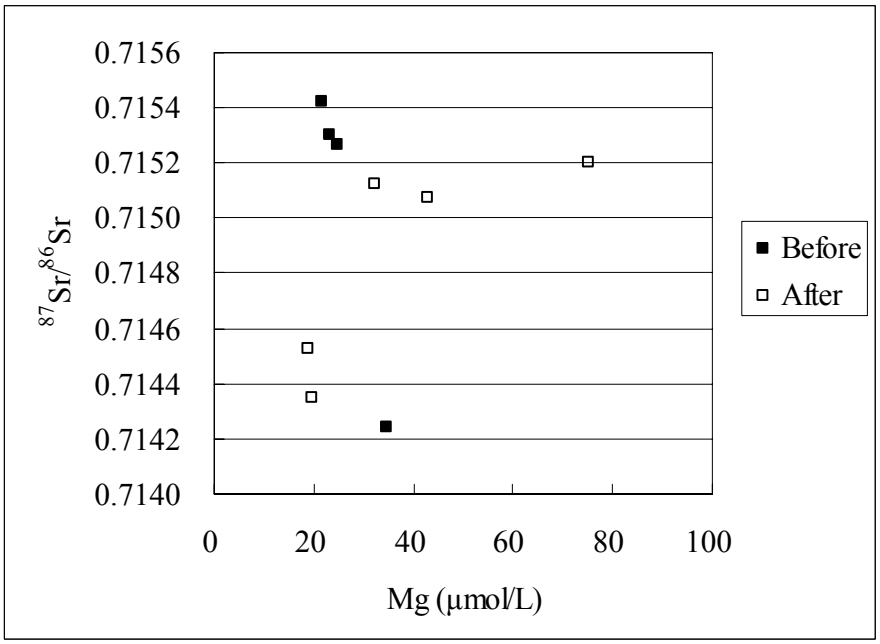

Figure 4.9. The relationships between Ca/Sr and Mg/Sr molar ratios in soil water at 30 cm and 80 cm depths from the 90 Degree watershed.

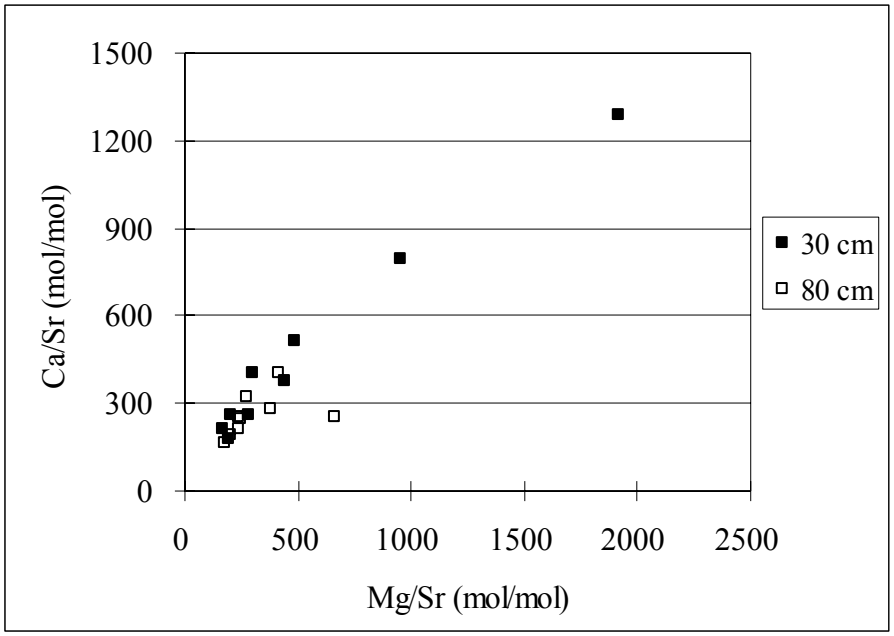

Figure 4.10. Temporal variations in Ca/Sr ratios of soil water at 30 cm and 80 cm depths from the 90 Degree watershed (April to October 2005).

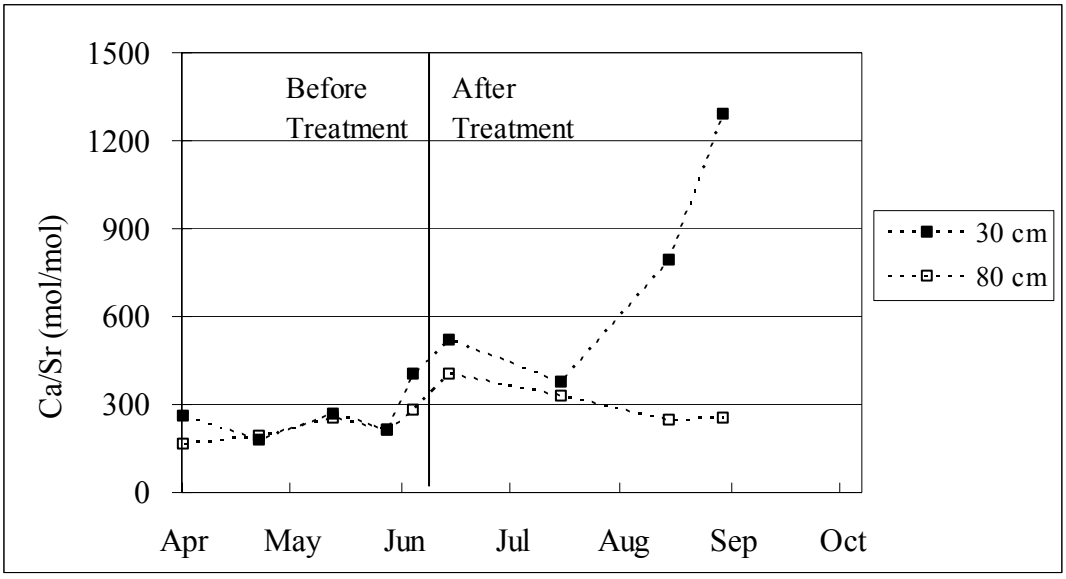

Figure 4.11. Temporal variations in Mg/Sr ratios of soil water at 30 cm and 80 cm depths from the 90 Degree watershed (April to October 2005).

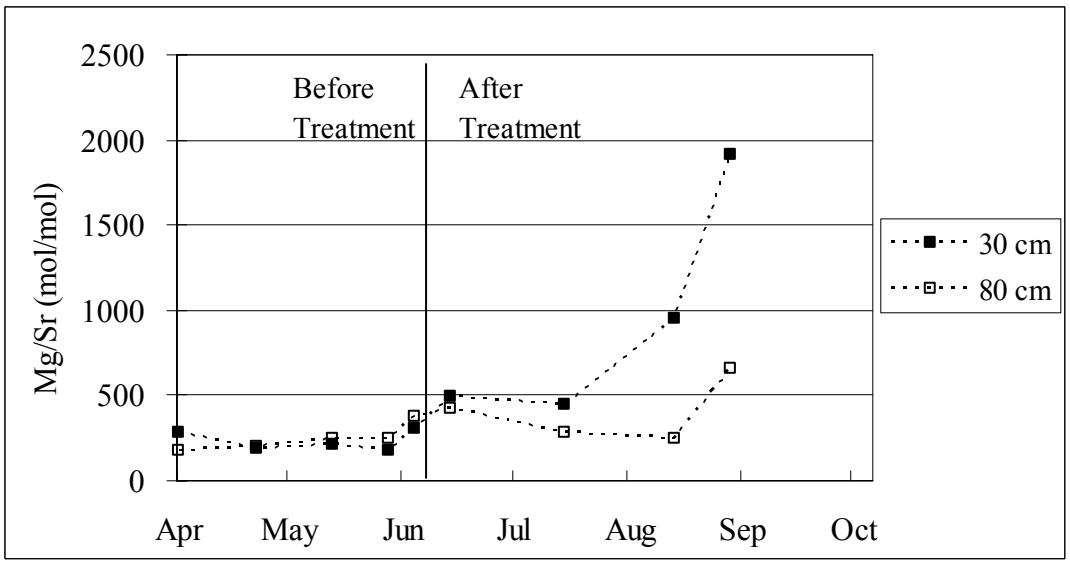

Figure 4.12. Temporal variations of $^{87}Sr/^{86}Sr$ ratios and $\delta^{18}O$ compositions in monthly streamwater at the 90 Degree watershed during the study period (July 2003-October 2005). Arrows indicate the date of limestone sand application. Error bar on $^{87}Sr/^{86}Sr$ ratio is ±2σ of measured value.

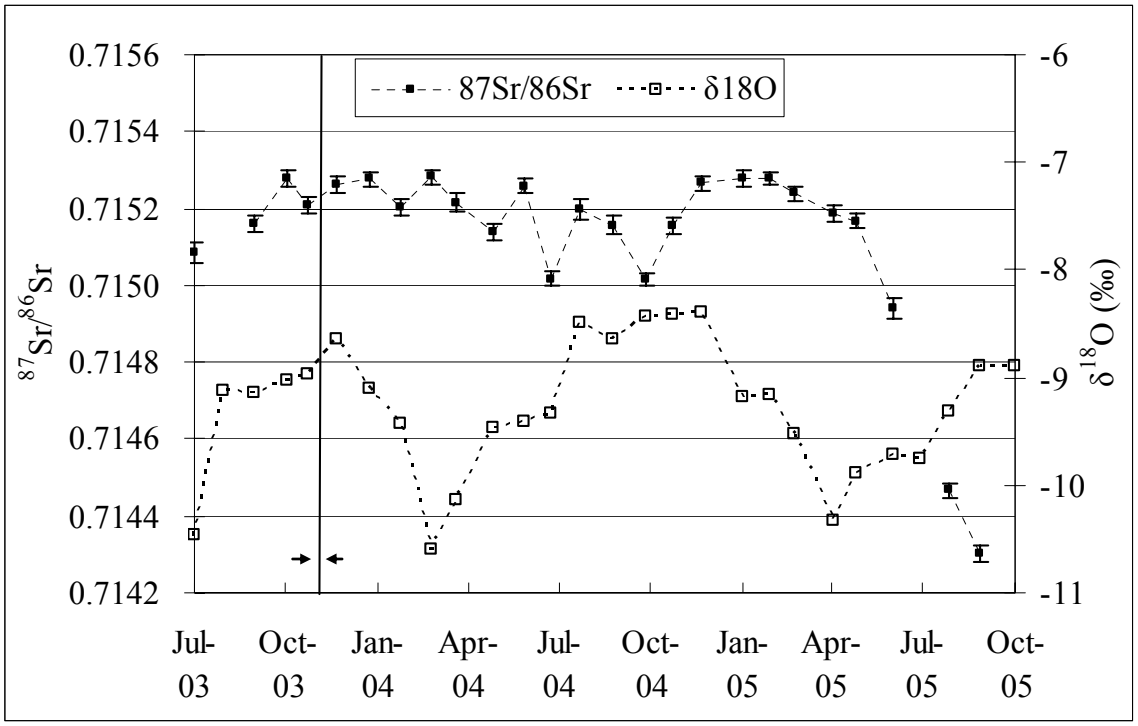

Figure 4.13. Temporal variations in concentrations of Ca, Mg, and Sr of monthly streamwater at the 90 Degree watershed during the study period (July 2003-October 2005). Arrows indicate the date of limestone sand application.

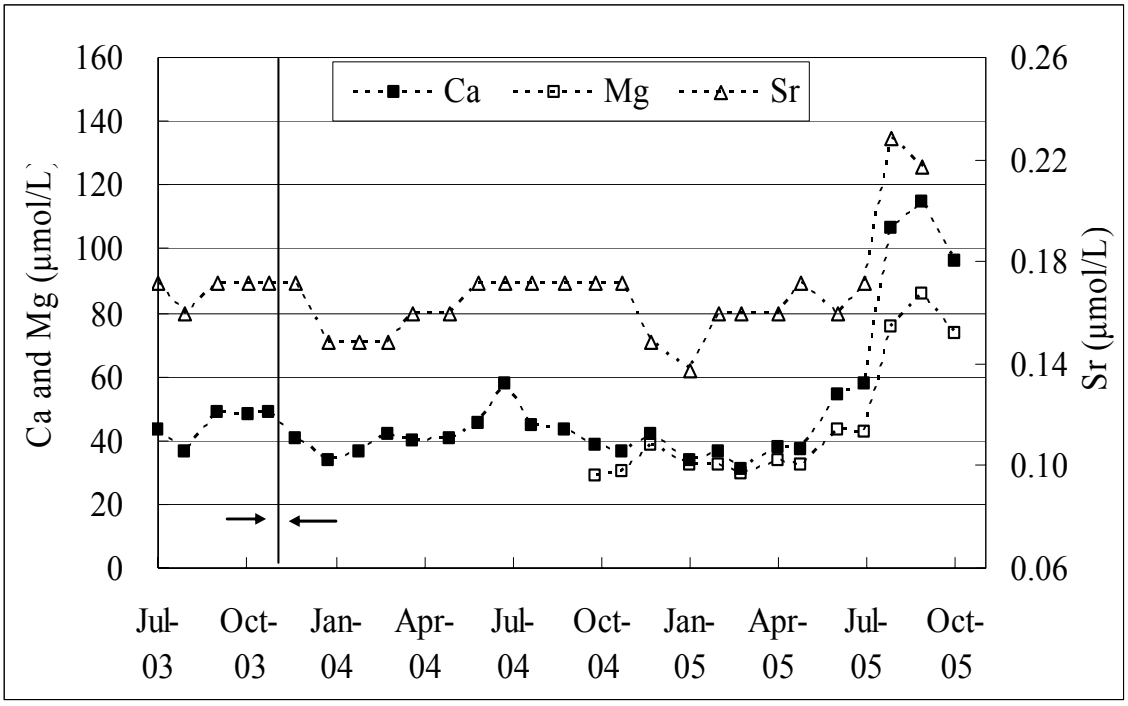

Figure 4.14. Plot of $^{87}Sr/^{86}Sr$ ratios vs Ca and Mg concentrations in streamwater at the 90 Degree watershed.

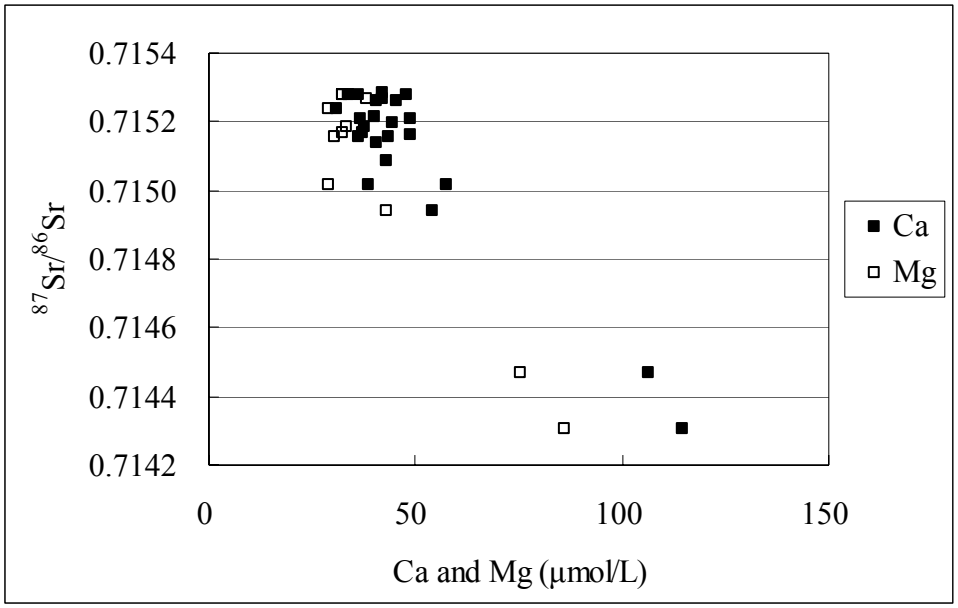

Figure 4.15. Plot of $^{87}Sr/^{86}Sr$ ratios vs Sr concentrations in streamwater at the 90 Degree watershed.

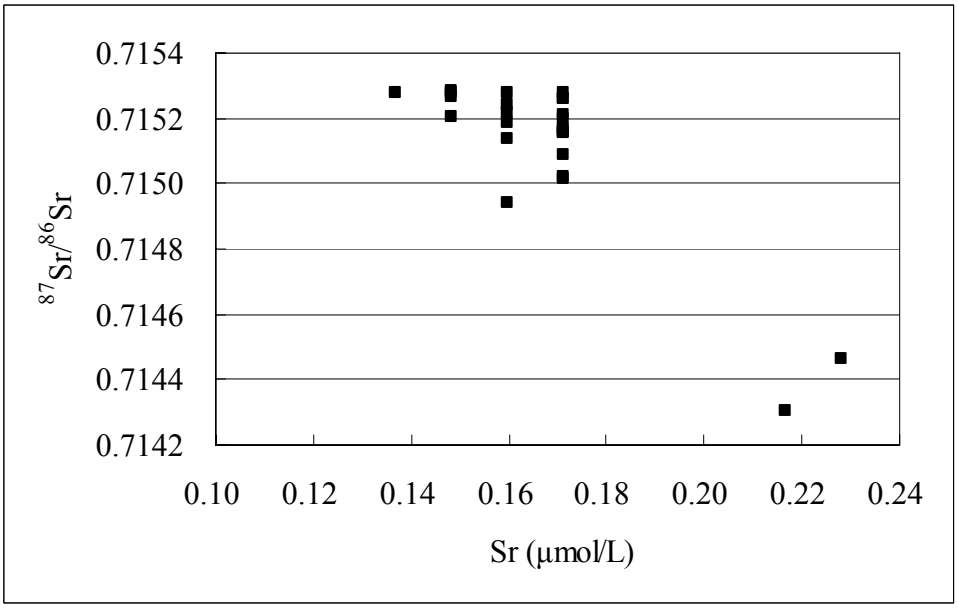

Figure 4.16. Relationship between Ca/Sr and Mg/Sr molar ratios in streamwater at the 90 Degree watershed.

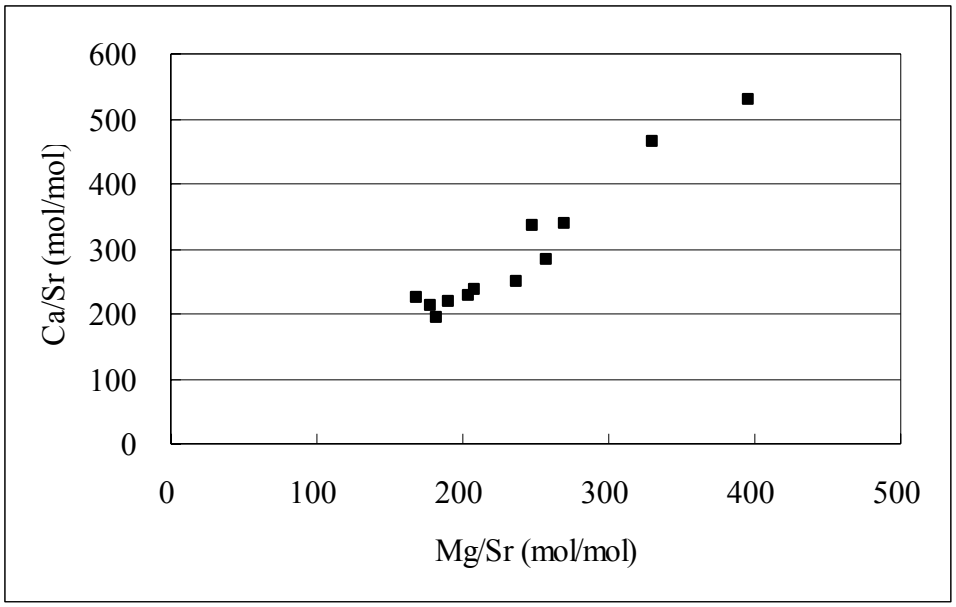

Figure 4.17. Temporal variations of $^{87}Sr/^{86}Sr$, Ca/Sr, and Mg/Sr ratios in monthly streamwater at the 90 Degree watershed during the study period. Arrows indicate the date of limestone sand application.

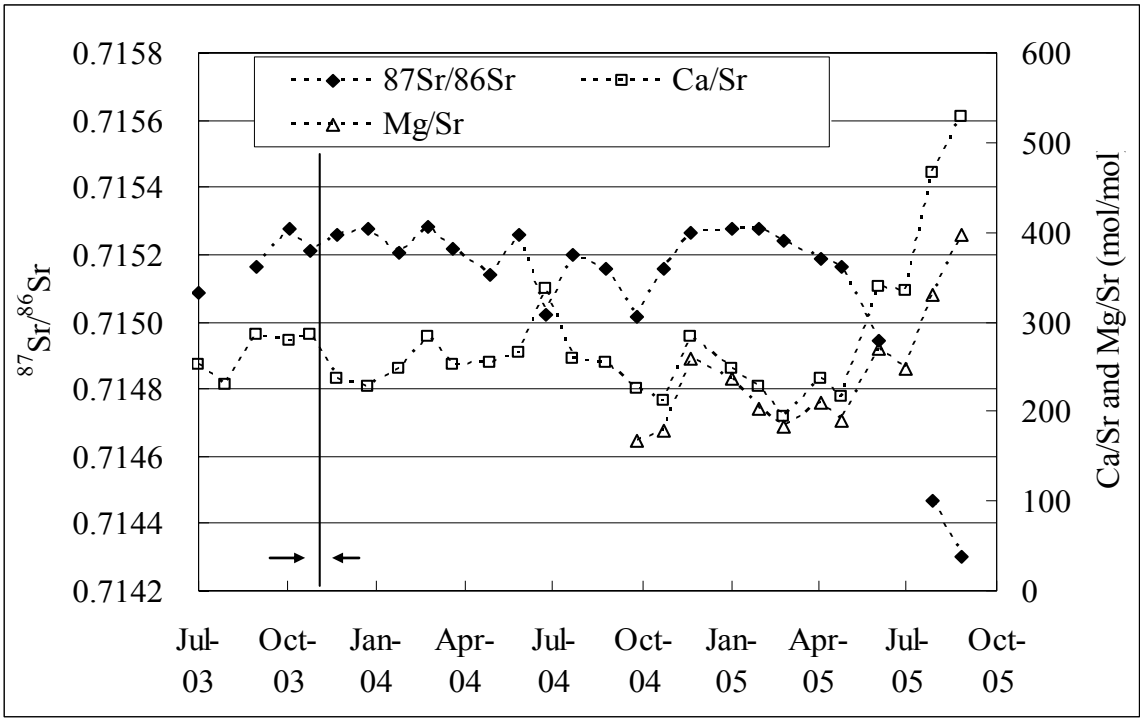

Chapter 5. Synthesis

Because Pennsylvania has received higher acid deposition when compared to adjacent states, it has suffered forest degradation and a decrease in fish populations. The state's declines in sugar maple trees and cold water fisheries are particularly detrimental given the potential economic loss they entail for the region. To make matters worse, soils in Pennsylvania are quite acidic with limited ability to neutralize strong acid deposition. As a result, steps must be taken to improve forest ecosystem health. The present research investigated short-term effects of dolomitic limestone application on acidified watersheds, using an integrated set of hydrometric, hydrochemical, and multi-isotopes.

Coarse-grained dolomitic limestone sand was applied by the Penn State Regenerator at a rate of 5 t ha^{-1} over the Laurel and 90 Degree watersheds, with hand application to soil solution sampling sites. In Chapter 2 demonstrated the chemical responses of soils, soil solution, and streamwater with the addition of limestone sand were described. Based on field visits, limestone sand remained undissolved in the near soil surface for up to four months after treatment. However, mineral A horizon soils had increased soil pH, exchangeable base cations, and base saturation after liming. pH, conductivity, calcium, magnesium, acid neutralizing capacity, and Ca/Al molar ratio increased in soil solution at 30 cm depth within four months after liming. The rapid response of soil solution at 30 cm depth to liming could be due to the hydrophobic nature of organic material in the forest floor and enhanced macropore transport of fine size limestone particles by infiltrating precipitation (Marshner et al., 1992; Geary and Driscoll, 1996). Geary and Driscoll (1996) observed greater increases in pH, calcium, and acid neutralizing

capacity in soil solution within six months after calcite application. At the watershed scale, streamwater did not have an immediate response to liming. Lag time could be partly the result of the mean residence time of streamwater. Approximately 1.5 years after liming, streamwater at the treated watersheds showed an improvement in water quality over streamwater at the control watershed. However, as presented in Chapter 2, absolute concentrations in either soil water or streamwater can have variations due to dilution and concentration effects. Therefore, isolating the exact effects of treatment was not possible.

Chapter 4 introduced Ca/Sr and Mg/Sr molar ratios and strontium isotopes as solute tracers to investigate liming treatment impact on soil water and streamwater. Elemental ratios can avoid variations from dilution and concentration effects, and strontium isotope can eliminate physical, biological, and analytical fractionations. Results obtained using elemental ratios and strontium isotopes may be more significant in interpreting the effects of liming than the results derived from absolute concentration as discussed in Chapter 2. Strontium isotopes have thusfar not been used to detect watershed level liming effects. About 16 months after liming, a pattern of decrease in $^{87}Sr/^{86}Sr$ ratios in streamwater was observed, indicating a treatment effects. However, the strontium isotopic signature showed no indication of a change in soil water with the addition of limestone sand, even though chemistry change had observed. Large variations of $^{87}Sr/^{86}Sr$ in soil water and limited sample size may have prevented observation of a isotopic treatment response. However, before liming, the variations of Ca/Sr and Mg/Sr ratios in soil water at 30 cm depth were consistent and these ratios increased in soil water at 30 cm depth two months after treatment indicating a treatment effect.

Determination of the mean water residence time at the watershed level can be helpful in estimating the timing of land use change on water quality. Chapter 3 presents the research conducted on the determination of mean water residence time using ^{18}O isotope measurements. The estimated mean residence time of soil water at 30 cm and 80 cm depths were about 2-3 months and 3-4 months, respectively. Within this range of residence time, the changes of absolute concentrations and elemental ratios in soil solution to liming only occurred at 30 cm depth as presented in Chapters 2 and 4. At the watershed scale, the mean residence time of streamwater as estimated with ^{18}O isotope techniques at the 90 Degree watershed was about 12 months. Chemical and strontium isotope ratios in streamwater did not appear to be consistent with the ^{18}O estimated residence time for 90 Degree watershed. The chemistry and strontium isotope in streamwater started to show a response 1.5 years (18 months) after treatment. Residence time estimates using ^{18}O in water appeared to underestimate time of travel for Ca and Mg delivered in baseflow from the limestone sand treatment. However, from a practical point of view, the estimated mean residence time of water presented in Chapter 3 certainly provided a reasonable estimate of time to anticipated baseflow water quality change in this application.

Overall, this dissertation demonstrates that the application of dolomitic limestone sand to forested watersheds with extremely acidic soils rapidly improved water quality. Although, the long-term effect of liming on the study watersheds is unknown, it could be expected from other work (Dalziel et al., 1994; Staaf et al., 1996; Hindar et al., 2003). In conclusion, forest liming appeared to be very effective in the remediation of acid deposition related problems in baseflow from the small forested watersheds monitored in this study.

Additional work would be required to determine liming benefits during high flows.

5.1. References

Dalziel, T.R.K., Wilson, E.J., Proctor, M.V., 1994. The effectiveness of catchment liming in restoring acid waters at Loch Fleet, Galloway, Scotland. Forest Ecology and Management 68,107-117.

Geary, R.J., Driscoll, C.T., 1996. Forest soil solutions: Acid/base chemistry and response to calcite treatment. Biogeochemistry 32, 195-220.

Hindar, A., Wright, R.F., Nilsen, P., Larssen, T., Høgberget, R., 2003. Effects on stream water chemistry and forest vitality after whole-catchment application of dolomite to a forest ecosystem in southern Norway. Forest Ecology and Management 180, 509-525.

Marshner, B., Stahr, K., Renger, M.Z., 1992. Lime effects on pine forest floor leachate chemistry and element fluxes. Journal of Environmental Quality 21, 410-419.

Staaf, H., Persson, T., Bertills, U., 1996. Skogsmarkskalkning. Resultat och slutsatser från Naturvårdsverkets försöksversamhet (Liming of forest soil. Results and conclusions of the research activity by the Swedish Environmental Protection Agency), Report 4559, 290 pp. (in Swedish).

Vita

Hyeon Jeong Kim
Penn State Institutes of Energy and the Environment
132 Land and Water Research Building
The Pennsylvania State University
University Park, PA 16802

Education

2007	Ph.D.	Forest Resources Management Watershed Stewardship Option	Pennsylvania State University, USA
2001	M.Sc.	Forest Resources Management	University of British Columbia, Canada
1996	B.A.	Forest Management	Kangwon National University, South Korea

Awards and Activities

2000	Scholarship for the Second Annual Fluid Dynamics Summer School in Edmonton, Alberta
1998	McPhee Fellowship at UBC
1993-1996	Kangwon National University outstanding grade scholarship
1998	Committee member for evaluating applicants of endowed Chair in Forest Hydrology at UBC

Publications & Major Papers

Kim, H. J., Sidle, R.C., Moore, R.D. 2005. Shallow lateral flow from a forested hillslope: influence of antecedent wetness. Catena 60, 293-306.

Kim, H. J., Sidle, R.C., Moore, R.D., Hudson, R. 2004. Throughflow variability during snowmelt in a forested mountain catchment, coastal British Columbia, Canada. Hydrological Processes 18, 1219-1236.

Henderson, S., Kim, H.J., 2002. Interior watershed assessment procedure for the Raft River Watershed. Report. Integrated Woods Services Ltd., Canada.

Henderson, S., Kim, H.J., 2002. Hydrological data analysis for Nahatlatch River. Report. Integrated Woods Services Ltd. Canada.

Henderson, S., Kim H.J., 2002. Nelson Creek and Posby Lake community watersheds reconnaissance channel assessment. Report. Integrated Woods Services Ltd., Canada.

Kim, H. J., 2001. Hydrologic contributions of subsurface flow during snowmelt and rainfall in a forest catchment, coastal British Columbia, M.Sc. Thesis, University of British Columbia, Canada, 144pp.

Kim, H. J., 1996. Relationship between Biodiversity and Forest Management, B.A. Thesis, Kangwon National University, South Korea, 40pp.